INVESTIGATION OF THE ELECTRONIC STRUCTURE AND VIBRATIONAL SPECTRUM OF C_{60} AND ITS VARIOUS COMPOUNDS

Ph.D. THESIS

in

Engineering Physics
University of Gaziantep

By
Hayriye TÜTÜNCÜLER

August 2000

Approval of the Graduate School of Natural and Applied Science.

Assoc.Prof.Dr. Ali Rıza TEKİN
Director

I certify that I have read this thesis and that in my opinion it is fully adequate, in scope and quality, as a dissertation for the degree of Doctor of Philosopy.

Assoc.Prof.Dr. Bülent GÖNÜL
Chairman of the Department

I certify that I have read this thesis and that in my opinion it is fully adequate, in scope and quality, as a dissertation for the degree of Doctor of Philosopy.

Assist.Prof.Dr. Ramazan KOÇ
Supervisor

Examining Commitee in Charge

Prof.Dr. Refik KAYALI .....

Assoc.Prof.Dr. Süleyman ÖZÇELİK .....

Assoc.Prof.Dr. Ömer BAKKALOĞLU .....

Assoc.Prof. Dr. Zihni ÖZTÜRK .....

Assist.Prof.Dr. Ramazan KOÇ .....

ABSTRACT

INVESTIGATION OF THE ELECTRONIC STRUCTURE AND VIBRATIONAL SPECTRUM OF C_{60} AND ITS VARIOUS COMPOUNDS

TÜTÜNCÜLER, Hayriye
Ph.D. in E.P., University of Gaziantep
Supervisor: Asst. Prof. Dr. Ramazan Koç
August 2000, 113 Pages

In this thesis three main properties of C_{60} molecule are investigated. These are electronic energy levels, normal modes of vibrations, and Jahn-Teller (JT) effect due to electron-vibron interaction for the ionised C_{60} molecule.

The electronic energy levels have been computed by using Hückel method as a function of bond strength between the atoms in the molecule. The effect of bond strength is investigated and it is seen that the result is satisfactory for all icosahedral complexes. In order to simplify Hückel matrices, the projection operators and molecular orbitals of icosahedral structure are constructed

Vibrational modes of C_{60} molecule were found by using the force constant model. This model includes bending force constants in addition to the bond stretching force constants and the interaction between the nearest ten neighbour atoms is taken into consideration to get accurate results.

The $H\otimes(2h\oplus g)$ Jahn-Teller problem is investigated analytically by developing a new method. It is checked that the method is applicable to all JT problems. The JT problem is then solved by breaking symmetries of icosahedral group into its

maximal little groups. It is seen that the energy surfaces are located trigonal (D_3) or pentagonal (D_5) symmetry depending on the coupling strength constant.

Several computer programs are developed to calculate electronic energy levels and to solve JT problems.

Keywords: Fullerenes, C_{60}, normal modes, Hückel method, electronic energy level, symmetry breaking, JT effect.

ÖZET

C_{60} VE ÇEŞİTLİ BİLEŞİMLERİNİN ELEKTRONİK YAPISININ VE TİTREŞİM SPEKTRUMUNUN İNCELENMESİ

TÜTÜNCÜLER, Hayriye
Ph.D. in F.M., Gaziantep Üniversitesi
Tez Yöneticisi: Y.Doç.Dr. Ramazan Koç
Ağustos 2000, 113 sayfa

Bu tezde C_{60} molekülünün üç önemli özelliği incelenmiştir. Bunlar, elektronik enerji seviyeleri, normal titreşim modları ve iyonize olmuş C_{60} molekülünde elektron-vibron etkileşmesinden kaynaklanan Jahn-Teller (JT) etkisidir.

Elektronik enerji seviyeleri bağ kuvvetlerinin fonksiyonu gözönüne alınarak Hückel metoduyla hesaplanmıştır. Bağ kuvvetlerinin etkisi incelenmiş ve sonucun tüm ikosahedral kompleksler için geçerli olduğu görülmüştür. Hückel matrislerini kolaylaştırmak için izdüşüm işlemcileri ve moleküler yörüngeler hesaplanmıştır.

C_{60} molekülünün titreşim modları kuvvet sabiti modeliyle bulunmuştur. Bu model bağ çekim sabitlerinin yanısıra bağ açı sabitlerini de içermektedir ve hassas sonuçlar elde etmek için en yakın on atomun birbiriyle etkileşmesi gözönüne alınmıştır.

$H\otimes(2h\oplus g)$ JT problem, yeni bir model geliştirilerek analitik olarak incelenmiştir. Bu modelin tüm JT sistemler için uygun olduğu test edilmiştir. Daha sonra JT problemi, ikosahedral grubu simetriyi maksimal alt gruplarına kırarak çözülmüştür. Etkileşme şiddet sabitine bağlı olarak, enerji yüzeylerinin D_3 veya D_5 simetrisine yerleştiği görülmüştür.

Elektronik enerji seviyelerini hesaplamak ve JT problemlerini çözmek için birkaç bilgisayar programı geliştirilmiştir.

Anahtar Kelimeler: Fullerene, C_{60}, normal modlar, Hückel metod, elektronik enerji seviyeleri, simetri kırma, JT etkisi.

ACKNOWLEDGEMENTS

I would like to express my sincerest gratitude and thanks to my supervisor Assist.Prof.Dr. Ramazan Koç for his guidance, suggestion, valuable critism and great help in the preparation of this study. I would say that this thesis is at least as his as mine.

My husband and sons Anıl and Berkay are also to be thanked for their patience, love and continual encouragement. This work took away a lot of the time and care of mine they deserved.

TABLE OF CONTENTS

LIST OF TABLES

LIST OF FIGURES

LIST OF SYMBOLS

J: Angular momentum quantum operator.

$J_{\pm}$:Ladder operator.

j, ℓ: Angular momentum quantum number.

χ: Real basis of matrix generators of SO(3) and characters of irreducible or reducible representation.

Γ: Irreducible or reducible representation.

S: Subgroup.

g: Order of the group.

k: Number of the elements in a class.

P: Projection operator.

n: Dimension of the irreducible representation.

R: Symmetry operator.

ϕ: Atomic orbital.

ψ: Molecular orbital.

H: Hamiltonian operator.

E: Energy eigenvalues.

β: Overlap (resonance) integral for single bond and angle bending bond force constant.

T: Kinetic energy.

m: mass of the atoms.

V: Potential energy.

L: Lagrangian operator.

q: Generalized coordinate.

ω: frequency of the vibration.

D^{j}: Irreducible representation.

A: State of 1-dimensional representation of icosahedral group.

T_1, T_2: State of 3-dimensional representation of icosahedral group.

G: State of 4-dimensional representation of icosahedral group.

H: State of 5-dimensional representation of icosahedral group.

u: Small displacement vector.

N: Number of atoms.

α: Coulumb integral and stretching bond force constant.

Φ: Dynamic matrix.

D: Matrix representations of any group.

r: Position vectors of icosahedral group.

γ: Overlap (resonance) integral for double bond.

ξ: Bond alternation constant.

Q: Nuclear coordinate.

X: Electronic coordinate.

$U_{\ell,m}(X,Q)$: Polynomial potential function.

B_m: JT interaction matrix.

Λ: Direct sum of irreducible matrix generators.

F: Coupling parameter of JT matrices

CHAPTER 1

STRUCTURE AND PROPERTIES OF THE FULLERENES: A BRIEF INTRODUCTION

Fullerenes are carbon allotropes of carbon (C_n) and built up of fused pentagons and hexagons. The smallest stable and at the same time the most abundant fullerene is the buckminsterfullerene C_{60}. Buckminsterfullerene has the shape of soccer ball. The next stable homologue is C_{70} followed by C_{76}, C_{82}, C_{90}, C_{94} and C_{96}. The building principle of the fullerenes is a consequence of Euler theorem which says that carbon cages is in the form of trivalent polyhedron with exactly 12 pentagonal and (n/2-10) hexagonal faces for the closure of each spherical network

The proposed structure for C_{60}, a "truncated icosahedron", is derived from an icosahedron by truncating or "snipping off" each of the twelve vertices (see Figure 1.1). Hence, each vertex is replaced by a five-membered ring – a pentagon. This snipping process also converts each of the twenty former triangular faces into six-membered rings hexagons.

The average nearest neighbour carbon-carbon (C-C) distance in C_{60} (1.44 Å) is almost identical to that in graphite (1.42 Å). Each carbon atom in a C_{60} molecule is identical has four valance electrons and bonds to each of the three nearest-neighbour carbon atoms. C_{60} is trigonally bonded to three other carbon atoms. Two of the bonds are located at the fusion of a hexagon and a pentagon are single bonds. The third bond is located at the fusion between two hexagons is a double bond. Since all the bonding requirements of carbon atoms are satisfied, the C_{60} molecule are expected to form Van der Waals bonded molecular solid which is an insulator (or semiconductor).

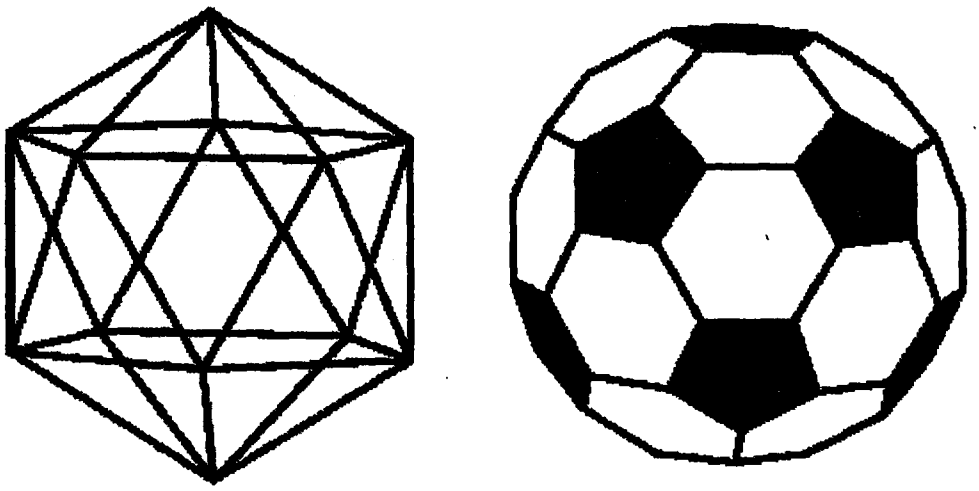

Figure 1.1. Icosahedron (left) and "truncated icosahedron" (right).

C_{60} molecules crystallize into a cubic structure with a lattice constant 14.17 $\mathring{A}$, a nearest neighbour C_{60}- C_{60} distance of 10.02 $\mathring{A}$, and density of 1.72 g/cm^3. At room temperature, the balls have rotational freedom and the ball centers are arranged on a face centered cubic(fcc) lattice with one per primitive fcc unit cell or four balls per simple unit cell. The space group of C_{60} is T_h^6 (Tetrahedral).

C_{60} and related fullerenes have attracted a great deal of interest in recent years because of their unusual properties. Fullerenes are of broadly interest to scientists in many fields: to physicists for their relatively high T_c superconductivity (33K), five fold local symmetry of icosahedral fullerenes and the quasi 1-D behaviour of fullerene-related nanotubules; to chemists for the large family of new compounds that can be prepared from fullerenes; to earth scientists because of the very old age of shungite, a mineral deposit that contains a high concentration of fullerenes and the material scientists as representing a source of monodisperse nanostructures that can be assembled in film and crystal form and whose properties can be controlled by doping and intercalation.

1.1. OUTLINE OF THE STUDY

This thesis covers three main topics related to the vibrational spectrum, electronic structure and electron (hole)-vibron coupling in the positively ionized C_{60} systems. In chapter 2, comprehensive literature survey of research on the subject is summarized. After two introductory chapters, we introduce the study for investigation of electronic energy levels using Hückel method, a model developed to compute the vibrational modes of C_{60}, and a new method to compute Jahn-Teller interaction for positively ionized C_{60} molecule (C_{60}^{+}).

In chapter 4, electronic spectrum of C_{60} has been computed. It is well known that Hückel method is applicable to compute electronic structure for large carbon systems. We have constructed Hückel Hamiltonian to find energy levels. The results are relevant with the previous results.

In Chapter 5, we focus our attention to calculate the normal modes of vibrations of atoms in C_{60}. After discovery of C_{60} molecule many authors have studied the vibrational spectrum of the molecule. Most of the recent results have been collected and a model has been constructed.

Chapter 6 is devoted to the study of the JT effect for the ionic form of C_{60} molecule. Since the icosahedral group is the largest finite group in 3D, fullerene ions are the richest and most attractive JT coupled systems. The details of $H\otimes(g\oplus 2h)$ coupling constitute the main topic of this chapter. Concept of this chapter is born with a surprise. Through years JT problems have been studied by using standard method. In this work, it is amazingly interesting that we have solved the problem by using symmetry mechanism. Our results are in agreement with the previous works. In addition to these, Jahn-Teller interaction matrices for $T\otimes h$, $G\otimes g$ and $G\otimes h$ coupling system have been obtained.

This thesis also contains some computer programs that compute projection operator, vibrational levels, and JT interaction matrices.

1.2. DISCOVERY OF THE C_{60}

Until a few years ago, there were two known forms of pure carbon, such as graphite and diamond. Then an improbable-seeming third form of carbon was discovered: a hollow cluster of 60 carbon atoms shaped like a soccer ball. Buckminsterfullerene or "buckyballs"--named for the American architect R. Buckminster Fuller, whose geodesic domes had a similar structure--is the roundest, most symmetrical large molecule known. It is exceedingly rugged and very stable, capable of surviving the temperature extremes of outer space.

At the beginning of 70^{th} century existence of the fullerene was predicted by soviet chemists D.Bochvar and E.Galpern and Japanese physicist E.Osawa independently from each other. The early theoretical suggestions for icosahedral C_{60} were not widely appreciated, and some of this literature was only rediscovered after the experimental work of Kroto and co-workers in the middle 1980's established the stability of the C_{60} molecule in the gas phase. Concurrently, astrophysicists were trying to identify some unusual IR emissions of interstellar dust from carbon stars. In these studies, a group of over 40 diffuse lines is seen, from about 1.5 to 3 eV for which the origin is unknown. A neighbouring line at 5.6 eV had been associated with graphite and so it was thought that the group at lower energy was related to finite size carbon-clusters.

In the fall of 1990, a new type of condensed matter, based on C_{60}, was synthesized for the first time by Kratschmer and co-workers who found a simple method for preparing gram quantities of C_{60} that had previously been available only in trace quantities in the gas phase. He reported that in soot produced in an optimized helium atmosphere at 100 torr and observed four infrared lines that corresponded to the allowed transitions predicted theoretically existence of C_{60}. A subsequent paper by Kratschmer et al. reported the major breakthrough that upon dissolving the soot in a non-polar solvent, such as benzene, a characteristic colour changes to dark red occurs. Upon distilling the liquid from the remaining soot, and letting evaporation occur, small crystallites form. These crystallites were analyzed by mass spectroscopy and they were found to consist mainly of C_{60} molecules. X ray diffraction studies of

these crystals, showed a close packed arrangement with a nearest neighbour distance of 10 Å.

As carbon is a basic element of a living substance structure, the discovery of its new forms has a special significance and forces to reconsider the presentations of fundamental processes, happened by the participation of carbon in alive and lifeless nature.

These carbon cages turn out to have extraordinary chemical and physical properties. They react with elements from across the periodic table and with the chemical species known as free radicals--key to the polymerization processes widely used in industry--thus opening up the fullerenes to the manipulative magic of organic chemists. When a fullerene is "doped" by inserting just the right amount of potassium or cesium into empty spaces within the crystal, it becomes a superconductor--the best organic superconductor known. More important, because C_{60} is a relatively simple system, it may help physicists master the still mysterious theory of high-temperature superconductivity.

Speculation and some hard work on potential applications began almost immediately after the discovery of buckyballs. Possible applications of interest to industry include optical devices; chemical sensors and chemical separation devices; production of diamonds and carbides as cutting tools or hardening agents; batteries and other electrochemical applications, including hydrogen storage media; drug delivery systems and other medical applications; polymers, such as new plastics; and catalysts.

Catalysts, in fact, appear to be a natural application for fullerenes, given their combination of rugged structure and high reactivity. Experiments suggest that fullerenes, which incorporate alkali metals, possess catalytic properties resembling those of platinum. The C_{60} molecule can also absorb large numbers of hydrogen atoms almost one hydrogen for each carbon without disrupting the buckyball structure. This property suggests that fullerenes may be a better storage medium for hydrogen than metal hydrides, the best current material, and hence possibly a key factor in the development of new batteries and even of non-polluting automobiles

based on fuel cells. A thin layer of the C_{70} fullerene, when deposited on a silicon chip, seems to provide a vastly improved template for growing thin films of diamond.

At the same time their application means the nearest technological revolution that the results are difficult to foresee. The fullerenes activity permits to apply them in technological processes, connected with the crystals cultivation, conducting the selective catalytic transformations and, first of all, with deriving completely new materials having artificially ordered electronic, magnetic and optical properties. This is, for example, polymeric materials, possessing the defined magnitude of conductivity or magnetic properties, new catalysts, high selective absorbents, new classes of superconductors, semiconductors, magnetics, segnetoelectrics, nonlinear optical materials. It is real to create a new material 200 times stronger than steel. Fullerenes with a special cluster size of about 10 angstroms can be used as "nanobricks" for the creation of new materials, including high-density information recording. Films obtained on the base of fullerenes, can solve a problem of clearing the polluted surfaces. Increasing the reflection of the surface covered by fullerenes during its laser exposure it allows making aeroplanes practically invisible to laser radars. There are new synthesis technologies for diamonds and diamond similar junctions of ultra-high hardness.

One from obvious direct consequences of the fullerenes usage is the decreasing of sizes, power consumption, making the diversified engineering devices and technological processes more ecologic. It will make it possible to improve performances of such devices, as: lasers, photographic films, magnetic disks and computers; to create ecologically pure current origins. The most amazing possibility of fullerenes is its purposeful cultivation by chemical methods (in a test-tube) micro bricks of sizes comparable with neurons as a fundamental base for computers. As to perspectives, it means the creation of pocket supercomputers. At the same time, the research possibilities are also increased. All this permits to forecast a stream of new discoveries and inventions in all areas, including most unexpected.

In connection with a very expensive price of fullerenes (price of 1 gram from 40 dollars for the extract of C_{60} and C_{70} up to 65 thousand dollars for C_{84}) their

industrial application in engineering is not a question of the nearest future. But the great sensations are waiting for us in the field of the fullerenes application in medicine. The most sensational result is the ability to apply the derivatives of fullerenes for treatment of virus diseases, caused by the AID-infection. Its medical investigation has already begun.

The strategic scientific importance of fullerenes is the following. Thanks to fullerenes, the connection between various natural sciences becomes much more tight. It leads to the extension of scientific outlook of scientists and to the deepening of the outlook horizon of scientific foundation as a whole.

1.3. SYMMETRY OF C_{60} MOLECULE

We review here only a few basic aspects of the physics of C_{60}. The detailed reviews have been found in references [1-15]. The molecular symmetry group of C_{60} is icosahedral (I_h) group in 3D. It contains 120 elements and it is the product group of Ixi where 'i' is the group composed by the inversion and identity element. The symmetry operations of icosahedron consists of identity operation, 12 fivefold axes through the centers of pentagonal faces, 20 threefold axes through centers of hexagonal faces and 15 twofold axes through the centers of joining two hexagons. 60 symmetry operations in I are organized in the following classes: the identity, $12C_5$, $12C_5^2$, $20C_3$ and $15C_2$.

The group I has five classes and its irreducible representations are: A (1-dimensional), T_1,T_2 (3 dimensional), G (4-dimensional), and H (5-dimensional). In I_h, the characters of inversion add a g (gerade) or u (ungerade) subscript for even or odd representations. The inversion operation leaves the degeneracies untouched. The molecular states and excitations are basis of one of the irreducible representations.

C_{60} has high symmetry, which gives rise to many degeneracies in the vibrational modes and electronic levels of C_{60}. The eigenstates of C_{60} are conveniently classified using symmetry in terms of the irreducible representations of the icosahedral point group.

1.4. VIBRATIONAL MODES AND ELECTRONIC ENERGY LEVELS OF C_{60}

The 60 carbon atoms of fullerene are arranged as a regular roughly spherical cage, of approximately 0.7 nm in diameter. There are two types of bonds between atoms: 30 of them belong to the six membered rings only; the other 60 are in common between the two kinds of rings.

The C_{60} has 174 (3N-6) vibrational degrees of freedom. Because of high symmetry most of them are degenerate. Group theoretical analysis allows the classification of the vibrational modes of C_{60}. There are 10 Raman active modes and 4 infrared-active modes.

Many approaches have been taken to the vibrational modes of C_{60}. Some of them are: tight-binding method, semi-emprical tight-binding method, the local preudoatomic orbital method, and Gaussian-basis-set method. In this study, the vibrational spectrum of C_{60} has been generated with the force constant method by adapting Keating type potential. In most of the models, the force constants have been computed by fitting the results to the Raman active A_g and H_g modes.

The simplest method to calculate the electronic energy levels of C_{60} molecule is Hückel method. Since the lowest unoccupied (LUMO) and highest occupied (HOMO) molecular orbitals (MO's) of the C_{60} molecule have primarily p_z character, where p_z is pointing radially out of the spherical molecule from the atom where it is centered, the calculations by Hückel method gives us correct result. In this work, we have examined the electronic structure.

1.5. JAHN-TELLER EFFECT

In this introductive section, we spend a few words on Jahn Teller effect and linear $H\otimes(g\oplus 2h)$, $T\otimes h$, $G\otimes g$ and $G\otimes h$ coupling systems for icosahedral group. According to the theorem by Jahn and Teller (JT) highly symmetrical molecular configurations in degenerate electronic states are subjected to distorting forces acting along certain nontotally symmetric vibrational modes. These vibrations carry the nuclei over into

distorted configurations, which are characterized by subgroup symmetries of the parent molecular point group. As it is well known, the molecular symmetry is reduced in the static JT effect with the splitting of the electronic state degeneracy. The JT effect, first suspected by Landau in 1934, takes place in any case of degenerate electronic level in non-linear molecules and complexes. Through the years, after his work a lot of paper has been published about potential energy surface and splitting of energy levels. Potential energy surfaces may be approximately obtained by the perturbation theory and the extremal points on the potential energy surface can be predicted by epikernel principle.

The JT interaction matrices have been constructed by using tensorial method or Clebsch-Gordon coefficients. In both cases one meets some mathematical difficulties. In order to overcome the mathematical difficulties, one can ask a question "is there any other simple method to calculate JT interaction matrices and to obtain PES (potential energy surfaces). During our work, thanks to symmetry, it has been shown that breaking symmetries of parent group into its little group, simplifies the problem and one can obtain PES. We have also concentrated our works on the construction of JT interaction matrices and developed a new method for this purpose. It has been shown that it is also possible to construct higher order JT interaction matrices by using the method given in this work

CHAPTER 2

LITERATURE SURVEY

The story of the discovery of C_{60}, Buckminsterfullerene and birth of Fullerene Science consists of several disparate strands which come together over ten days in September 1985. During this period of fewerish activity, working with Jim Heath, Sean O'Brien, Yuan Liu, Bob Curl and Rick Smalley at Rice University in Texas, evidence was found that C_{60} molecule was self-assembled spontaneously from a hot nucleating carbon plasma [1]. The molecule had however prehistory: The earliest paper [2] which describes C_{60} molecule to be found in Kagaku, where Eiji Osawa in 1970 suggested it should be stable [3], and following year discussed its aromatic properties and suggested that properties detail in a book with Yoshida [4]. Bochvar and Gal'pern published a theoretical study in 1972 [5], and also Stankevch et al.[6].

General information about fullerenes was reported as review papers by M.S Dresselhaus et al. [7], and Leonard Degiorgi [8]. Production of solid form of C_{60} was made by Donald R. Huffman [9]. Mitsutaka Fujita et al. proposed a projection method for describing fullerenes on a honeycomb lattice or a graphene sheet, thereby providing a geometrical understanding of the formation of general fullerenes [10]. Methods have been developed for producing bulk quantities of C_{60} and other fullerenes by Wolfang Kratschmer [11].

Another review about the discovering of the fullerenes was made by Harold Kroto [12], Robert F. Curl [13] and Richard E.Smalley [14].

The recent discovery of C_{60} molecules, with their fascinating structure, followed by the success in synthesising C_{60} crystals [1,15] and doping them, has opened an area of research that is certain to attract the interest of many. In particular, the fact that

such crystals, when doped with alkali metals, exhibit superconductivity at temperatures over 30 K offers another class of materials that might be candidates for high temperature superconductivity [16-18]. The understanding of the vibrational modes, the electronic states of C_{60} molecule, and how they are affected by doping are thus extremely important.

Several calculations of the molecular vibrations or normal modes C_{60} have been published [19-22]. A group theoretical analysis relevant to the interpretation of recent experimental observations of Raman-scattering spectroscopy in C_{60} and alkali metal doped C_{60} was made by G Dresselhaus, M.S Dresselhaus, and P.C Eklund [23]. In that paper, authors emphasized that highest symmetry space group which is appropriate for C_{60} and M_x C_{60}, even though it is only for the low temperature phase of C_{60} that the space group Th^6 (tetrahedral) has been positively identified.

Study of vibrations of icosahedral C_{60} using first principles quantum molecular dynamics method was made by G.B. Adams et al. [24]. They focused in that paper on the 14 modes, which are either first order Raman active, or infrared active.

Another model for determining the vibrational modes of C_{60} was studied by R.A. Jishi, R.M. Mirie, and M.S Dresselhaus [25]. It is generally the case in the force constant models considered so far that in addition to angle bending force constants, only bond stretching force constants for bonds connecting nearest-neighbour atoms have been considered. Such models could not reproduce even the two A_g Raman-active modes with any reasonable accuracy. In this study, calculation of vibrational modes in C_{60} has been carried out by considering interaction up to third-nearest neighbours.

J.L Feldman et al. also used intramolecular force constant model for C_{60} that includes valance-force-field (vff) parameter and keating parameter [26]. In this work, interactions were restricted to be between an atom and its three nearest neighbours.

Andrew A. Quong et al. present a first principles study of interatomic force constants in the isolated fullerene molecule [27], using the localized basis set in the local

density approximation (LDA). One of the motivations of this study was to determine the range and nature of the forces.

Qing Juang et al. used the recursion method to calculate vibrational density of states (VDOS) [28]. The Born potential is adopted for calculating the dynamic matrix. In this work, four force constants used to model the carbon bond. Two of the four force constants were used to model stretching of pentagonal and hexagonal bonds, and remaining two force constants were used to model the bending of pentagonal and hexagonal bonds. Only interaction between nearest-neighbour atoms was taken into account to write Born potential energy.

The study of the vibrational modes in crystalline C_{60} has attracted experimental interest for the past several years [29-37]. Raman scattering method is a very useful technique for investigation of physical properties, doping dynamics, and chemical modifications of the doped and undoped C_{60}..

Hans Kuzmany et al. summarized the results from Raman experiments on crystalline C_{60} in several laboratories in the last two years [38]. The first part of review concentrates on the undoped systems (fullerenes) and the second on the alkali metal doped systems (fullerides). As a conclusion, it is seen that Raman scattering is a very powerful tool for investigation of C_{60} materials. This is mainly because of chromophoric character of the fullerenes, the sensitivity of line positions and line patterns to any charge on the molecule, and the sensitivity of Raman technique to symmetry breaking effects on the molecule.

Experimental results on the Raman scattering spectra of C_{60} and M_6C_{60} taken at room temperature were presented and discussed by Ping Zhou et al. [39]. The spectra for M_6C_{60} compounds are all quite similar, and show only weak dependence on the alkali-metal mass or radius. Several of the fivefold degenerate H_g symmetry of C_{60} lines were observed to split upon doping.

The potassium doping of C_{60} to K_x C_{60} with $0 \leq x \leq 6$ was studied by Raman spectroscopy at temperatures slightly above room temperature by J.Winter and H. Kuzmany [40]. It is reported that a detailed Raman analysis of thin films which show

that for the K-doped systems besides the well-known structures with x=0,3,6, other, well-characterized phases exist at slightly elevated temperatures.

The temperature dependence of the IR active modes of undoped C_{60} films was presented at high resolution by L.R. Narasimhan et al. [41]. One of the IR absorptions at 1183 cm^{-1} narrows and shifts slightly toward higher energies while the other mode at 1429 cm^{-1} splits at approximately 245 K. Infrared absorption spectra of C_{60} films were recorded between 800 and 3000 cm^{-1}.

Temperature dependent Raman scattering from C_{60}^{-3} intramolecular modes and simultaneous electrical resistivity measurements made on Rb_3 C_{60} films by Ping Zhou et al. [59]exhibited a superconducting transition temperature T_c=28 K. The Raman spectra were found to be insensitive the particular alkali-metal dopant indicating that complete charge transfer has occurred. The electron-phonon coupling constant has been invoked to explain the broadening of the $H_g(2)$-$H_g(8)$ and $A_g(2)$ modes relative to their value in pristine C_{60} films.

Another study of the Raman spectra of undoped and doped single crystal C_{60} was made by J.Winter et al. [42]. A symmetry analysis for C_{60} crystal reveals that the $2A_g$ and $8H_g$ modes must split due to symmetry lowering. Above 260 K order-disorder transition [43] the H_g modes split into E_g and T_g components while A_g modes remain unchanged. The doping of the single crystals with potassium was performed at temperatures slightly above room temperature and doping process was studied by using Raman spectroscopy.

A high resolution Raman scattering study of intramolecular phonons of crystalline C_{60} was presented by P.J. Horoyski [44]. Many of the Raman active vibrations are richly structured, revealing crystal field splitting both above and below the orientational ordering transition at 260 K.

Raman spectra for oxygen free solid C_{60} films were obtained at T=20 K and 523 K by Zheng Hong Dong et al. using higher laser intensity at temperatures where photopolymerization is not important, over Raman lines modes [45].

Infrared and Raman studies of pressure polymerized C_{60} were discussed at different temperatures [46,47].

Today a number of theoretical methods have been applied for calculations of the electronic structure of carbon clusters. Some of the first calculations were performed by Pitzer and Clementi [48] and Hoffmann [49] who predicted a linear geometry of clusters smaller than n=10 and stability of C_2 and C_3. A review application of different theoretical methods for carbon species can be found in the work of Weltner et al. [50].

The discovery of the special C_{60} clusters has also initiated a number of semi-emprical and first principle calculations [51-55], including geometry optimisation [56-57], and the evaluation of ionisation energies and predictions of optical transitions [58-60].

The special character of C_{60} is now established by means of measurements of its ionization potential [61], electron affinity [62], optical transitions [63] and inertness regarding reactions with smaller molecules such as H_2, O_2, CO and N_2 [64]. The assumption of a cage structure is also supported by fragmentation studies where it was found that C_n clusters with $n<32$ lost species such as C_3, while the larger lost C_2 fragments. Proof of the icosahedral cage structures is the NMR spectra recorded by Taylor et al. [65] and by Johnson et al. [66]. Further supports have also been obtained from the studies of the ionic clusters of C_{60}, i.e., C_{60}^- and C_{60}^+ [64].

Shortly after the discovery of the C_{60} cluster, metal containing C_{60} clusters were found in mass spectra from laser vaporization of graphite containing different metal salts. To date organo-metallic clusters of the type MC_{60} have been observed where M=Li, Na, K, Rb, Cs and other elements. Many of these clusters were found to have the same stability and inertness as pure C_{60} cluster [67]. It was then proposed that the metal atom was located at the centre of the carbon cage. In an earlier study, calculations for LaC_{60} and its ions [68,69] were presented which also gave support for the hypothesis of a La atom located inside the cage.

Theoretical evidence for the stability of C_{120} and C_{60} molecules consisting of sp^2 hybridized carbon atoms was made by A.D.J Haymet [52]. Using the tight binding

method, electronic structure of $C_{60}Br_6$, $C_{60}Br_8$ and $C_{60}Br_{24}$ has been investigated by Jing-Non Liu et al.[70]. The ground state properties were calculated. Using the HMO (Hückel Molecular Orbital) theory, electronic structure and bonding in C_{60} were studied by Sashi Satpathy [54], and R.C Haddon co-workers[53].

Energetically optimized structure of C_{60}^- ion has been obtained by semi emprical MO calculation by Kazuyoshi Tamaka et al. [71]. There has long been a consensus; molecules with a high symmetry would cause a Jahn-Teller distortion when HOMO level is partially occupied due to its degeneracy and I_h geometry lowered with D_{3d} symmetry due to Jahn-Teller distortion.

Richiro Saito et al. made study about ground states for large icosahedral fullerenes and for C_{60}^n molecular ions ($-7<n<1$) [72]. Treating the icosahedral symmetry as a subgroup of full rotational group, the icosahedral symmetry of these molecular states was introduced. A method to calculate the electronic structure for the icosahedral molecules and ions was formulated for large fullerenes using a spherical harmonic expansion on a sphere.

K.Yabana and G.F. Betsch calculated the electronic structure of C_{60} molecule in a spherical representation, starting from the self-consistent solution of Kohn-Sham equation in the field of positively charged shell [73].

The traditional field of degenerate electron-phonon (electron-vibration) interactions in molecules [74,75] has drawn interest in recent years, excited by the discovery of new systems calling for a revision of a number of commonly accepted beliefs. Several molecular systems including C_{60} ions, higher fullerenes and Si clusters, derive their behaviour from the large (up to fivefold) degeneracy of electronic and vibrational states due to rich structure of the icosahedral symmetry group [76,77].

Potential energy surfaces (PES) have applications in many areas of chemistry and physics. They describe the way that the potential energy of a molecule in a particular electronic state, usually the ground state, varies with the nuclear positions [78] and the parameters of (PES) determine the normal modes. Symmetry relations between

the polynomial coefficients in the Taylor-series description of property surfaces are expressed in terms of Clebsch-Gordon (CG) series for the point group I_h by Fowler and Ceulemans[79].

In chemical applications of the JT effect, the shape of the adiabatic potential near the instability point is of primary importance. Two important features of the resulting potential energy surfaces [80] have been investigated: symmetry and stationary points. Group theoretical foundation for recently formulated [81] epikernel principle, predicts the location of extremal points on a JT surface. The linear $H\otimes(2h\oplus g)$ JT problem, relevant to the instability of icosahedral molecules in fivefold degenerate states is investigated by Ceulemans and Fowler [82]. The method of isostationary function is used to identify all the extrema of the corresponding potential energy surface.

As it is well known, the molecular symmetry reduced by Jahn-Teller (JT) is the result of distortion with the splitting of the electronic degeneracy. There is a substantial electron-phonon coupling in C_{60}, which is very important for many properties. For C^{n-}_{60} (n=1,...,5) molecules and doped C_{60} compounds (A_3C_{60}, A=K, Rb), t_{1u} level is partly occupied. This level couples to phonons of A_g and H_g symmetry. The fivefold degenerate H_g phonons split the three-fold degenerate t_{1u} level and lead to a JT effect [83]. The JT effect for positively charged fullerene ions C^{n+}_{60} have been analysed by De Los Rios, Manini, and Tosatti [84].

This literature survey addresses physicists, material scientists, chemists and broad readership in industry and the scientific community. The number of publications in this field meanwhile gains such dimensions that for nonspecialists it is very difficult to obtain a facile access to the topics of interest.

CHAPTER 3

THEORY

C_{60} is a highly symmetric molecule and all of the other molecules have less symmetric than C_{60} and their point groups do not contain 4-fold and 5-fold irreducible representations. It was produced a few years ago and scientists wonder its physical properties. This chapter covers two main topics to investigate its physical properties: mathematical tools and some standart physical models for C_{60} molecule. It is very important how these mathematical tools are applied for improving the physical standart models.

3.1. PARENT GROUP OF POINT GROUPS: SO(3)

The elements of SO(3) are formed by the orthogonal matrices of determinant +1. The closed subgroups of SO(3) are well known to physicists through their applications in crystallography and molecular physics. They are the cyclic groups C_n, dihedral groups D_n, tetrahadral group T, octahedral group O, and icosahedral group I. The normal operators of SO(3) associated with the quantum theory of angular momentum, and corresponding commutation relations become

$$[J_1, J_2] = iJ_3, [J_2, J_3] = iJ_1, [J_3, J_1] = iJ_2 \tag{3.1}$$

The well-known commutation algebra can be obtained by expressing $J_\pm$ in terms of operators J_1, J_2, and J_3 of SO(3). To obtain the standard form of the commutation relationship of SO(3) algebra, we can write

$$J_\pm = \frac{1}{\sqrt{2}}(J_1 \pm iJ_2) \tag{3.2}$$

with the relation

$$[J_3,J_3]=0,\quad [J_3,J_\pm]=\pm J_\pm,\quad [J_+,J_-]=J_3 \tag{3.3}$$

The irreducible representations of SO(3) are all real: up to equivalence, there is only one such representation for each odd dimension 2j+1, where j is the angular momentum quantum number. SO(3) is a subgroup of SU(2) and the finite subgroups of SO(3) can be generated by discrete rotations around the properly chosen two axes. An arbitrary group element of SO(3) can be written as $e^{i\vec{\omega}.\vec{J}}$ where J is the usual (2j+1)×(2j+1) matrix representations. The matrix elements of J are calculated from the relations

$$\begin{aligned} J_3|jm\rangle &= m|jm\rangle \\ J_\pm|jm\rangle &= \sqrt{(j\mp m)(j\pm m+1)}\,|j,m\pm 1\rangle \end{aligned} \tag{3.4}$$

where $|jm\rangle$ is the basic vectors of the (2j+1)-dimensional irreducible representation of SU(2), when j takes the values 0,1/2,1,3/2,1.... Integer values are valid for the SO(3) cases. $|jm\rangle$ stands for the scalar fields associated with the related irreducible representations.

3.1.1. Matrix Representations of SO(3) and its Finite Subgroups

The generation relations of finite subgroups of SU(2) and SO(3) are given by

$$A^p = B^q = C^r = Z \tag{3.5}$$

where C=AB, Z^2=1 for SU(2) and Z=1 for SO(3). The polyhedral subgroups of SO(3) are denoted by (pqr), which takes the values (nn1) for cyclic groups, (nn2) for dihedral groups, while (332), (432) and (532) stand for the tetrahedral, octahedral and icosahedral subgroups of SO(3), respectively. Here n is a positive integer. There are also two infinite subgroups of SO(3), $C_\infty \approx SO(2)$ generated by an arbitrary rotation around an axis, say third axis, $e^{i\theta J_3}$; and infinite dihedral group D_∞ whose

generators may be taken to be $e^{i\theta J_3}$ and $e^{i\pi J_1}$. In order to construct matrix generator of the subgroups of SO(3), a computer program written and is given in Appendix A. This program also compute the finite subgroups SU(2). In Table 3.1 the generators and generation relations are summarized.

Table 3.1. List of the generators and generation relations of finite subgroups of SO(3) and O(3). In the table, τ and σ are golden numbers and their values are $\frac{1}{2}(1+\sqrt{5})$ and $\frac{1}{2}(-1+\sqrt{5})$, respectively.

Finite Sub. of SO(3)	Generators	Generation relation	O(3)
C_n Cyclic	$A = \mathrm{Exp}\left[i\frac{2\pi}{n}J_3\right]$	$A^n=1$	$C_{nh}=C_n\times Z$
D_n Dihedral	$A = \mathrm{Exp}\left[i\frac{2\pi}{n}J_3\right]$, $B = \mathrm{Exp}[i\pi J_1]$	$A^n=B^2=(AB)^2=1$	$D_{nh}=D_n\times Z$
T Tetrahedral	$A=\mathrm{Exp}\left(\frac{i2\pi(J_1+J_2+J_3)}{3\sqrt{3}}\right)$ $C=\mathrm{Exp}(i\pi J_1)$	$A^3=B^3=(AB)^2=1$, $B=A^2C$	$T_h=T\times Z$
O Octahedral	$A=\mathrm{Exp}\left[\frac{i\pi J_3}{2}\right]$ $B=\mathrm{Exp}\left(\frac{i2\pi(J_1+J_2+J_3)}{3\sqrt{3}}\right)$	$A^4=B^3=(AB)^2=1$	$O_h=O\times Z$
I Icosahedral	$A=\mathrm{Exp}\left(\frac{i2\pi(\sigma J_1+J_3)}{\sqrt{2-\sigma}}\right)$ $B=\mathrm{Exp}\left(\frac{i2\pi(-\sigma J_2+\tau J_3)}{\sqrt{3}}\right)$	$A^5=B^3=(AB)^2=1$	$I_h=I\times Z$

The generators are transformed into real basis χ. Choosing the field $\chi_\ell = T_{k\ell}|jm\rangle$, we get

$$\chi_\ell = \frac{1}{\sqrt{2}}(|jm\rangle + (-1)^{j-m}|j-m\rangle) \quad \text{for odd } \ell$$
$$\chi_\ell = \frac{i}{\sqrt{2}}(|jm\rangle + (-1)^{j-m+1}|j-m\rangle) \text{ for even } \ell \qquad (3.6)$$
$$\chi_\ell = |j0\rangle \qquad \ell = j+1$$

In this equation ℓ =2j+1 and m=-j, -j+1,j-1, j. The matrix $T_{k\ell}$ transforms the generators of SO(3) into real basis.

3.1.2. Decomposition Reducible Representations

A group has finite number of basic or fundamental representations, which are called the irreducible representations of the group. Knowledge of the properties of these irreducible representations is of paramount importance in the application of group theory to the molecular systems. Since we normally begin with a reducible representation (the representations constructed in the previous subsection are in general reducible representations) and we must also know how to decompose (reduce) such a representation into its irreducible components. Suppose it is given a representation Γ that may be reducible. If it is, then by a suitable transformation it can be reduced to the point where it can be written as a direct sum of irreducible representations of the group.

$$\Gamma = \Gamma_1 \oplus \Gamma_2 \oplus \cdots = \sum_i C_i \Gamma_i \qquad (3.7)$$

where C_i tells us how many times Γ_i occurs in (the transformed) Γ. Although the above equation is symbolic sum, an equation for the character of a particular element s can be written in the form of algebraic relation

$$\chi(s) = \sum_i C_i \chi^i(s) \qquad (3.8)$$

Given now the characters of the various irreducible representations of the group G, we can determine C_i by multiplying $\chi(s)$ by $\chi^i(s)$ and summing over the group

elements 's'. The character orthogonality relation gives us:

$$C_i = \frac{1}{g}\sum_j k_j \chi_j^{(i)*} \chi_j \qquad (3.9)$$

where g is the order of the group and k_j is the number of element in the j^{th} class. $\chi_j^{(i)*}$ and χ_j correspond to the characters of the reducible and irreducible representations, respectively. This technique provides decomposition of reducible representation in terms of irreducible representations. The normal modes of the vibrations and electronic energy levels of the molecule are classified in this way.

3.1.3. Little Group

It will be shown that during the study of JT effect, the potential energy surface may be identified by breaking symmetries of corresponding parent group into its maximal little group. In general, a detailed analysis of the PES has been done by breaking symmetry of parent group into its all little groups. In this section, we briefly introduce a method to determine the little groups. In a real representation of any subgroup $S \subset G$, the degree of subduction can be computed by the relation

$$C_\ell(S) = \frac{1}{S}\sum_{p \in S} \chi_t(p) \qquad (3.10)$$

where $\chi_t(p)$ is the character of the representation p. In a t^{th} representation of finite group, if all subgroups $S' > S$ and $C_\ell(S') < C_\ell(S)$ then S is little group of G. For finite groups converse of this definition is also true. If the little group is a maximal subgroup then it is said to be maximal little group.

3.1.4. Construction of Projection Operators

The frequently used method for establishing permissible quantum states for a molecule involves use of projection operators. Their use frequently enables one to employ the molecular symmetry to obtain state functions of the proper symmetry by beginning with an unsymmetrized set of functions. If one has a set of basis functions

for the i^{th} irreducible representation of the group, projection operators based on the group representations are often used for formulating appropriate linear combinations of a set of basis functions.

The details regarding the formulation of projection operators from group theoretical principles can be found in most current textbooks on group theory. Only the final form of these operators will be presented. The projection operator for the α^{th} irreducible representation of dimension n_α belonging to a group of order g is defined as

$$P_{ij}^{\alpha} = \frac{n_\alpha}{g} \sum_R \Gamma_\alpha(R)_{ij} \qquad (3.11)$$

where Γ_α is an irreducible representation, R is the generic operation of the group. It is to be noted that the sum is over all individual operations and not just over classes. The character table is not enough to form the projection operators, and that a knowledge of matrices of representations is needed. This difficulty, however, does not exist for unidimensional representations, where matrices and characters coincide.

3.2. PYHSICAL PROPERTIES OF POLYATOMIC MOLECULES

The total energy of a molecule is composed of contributions due to the electronic configuration, vibration, rotation, translation, and various electron-electron, nuclear-nuclear, and nuclear-electron interactions. For real molecules it is not possible to view these contributing factors as being totally independent of each other. However, in practice these various interactions are often considered separately to provide simpler introduction to phenomenon.

First part of this section includes the Hückel method based on concepts of molecular orbital (MO) theory to obtain the electronic energy levels. From the viewpoint of spectroscopist, who is generally familiar with the concept of atomic wavefunctions, the molecular orbital method is preferable.

In the second part of this section, general information about the infrared and Raman spectrum due to vibrations in molecules is given. In this part also shows how group theory can be applied to find for any given molecule exactly how many normal modes there are belonging to each irreducible representations of the group and to find the exact form of each of the normal modes.

Third part covers the theoretical background of Jahn-Teller effect due to electron-vibron interactions.

3.2.1. Electronic Energy Levels of Polyatomic Molecules

Although an exact calculation requires solution of the many electrons Schrödinger equation for each different molecule, the qualitative description of the electronic structure of polyatomic homonuclear molecules can be understood by application of the Molecular Orbital (MO) method.

3.2.1a. Molecular Orbital Theory

The electronic structure of molecules or solids is usually described as a series of molecular orbitals. Molecular orbital theory builds on the electron wavefunctions of quantum mechanics to describe chemical bonding. MO theory treats orbital which are in general spread over the entirely of molecule. Considerations of molecular symmetry properties are extremely useful in this theory. Molecular orbitals are represented by the method of linear combination of atomic orbitals (LCAO). When atomic orbitals are combined to give molecular orbitals, the number of molecular orbitals formed equals to the number of atomic orbitals.

Hydrogen molecule H_2 is the prototype for the molecular orbital theory. If two waves of same wavelength and amplitude are combined and are in phase, they reinforce each other. If two waves are out of phase, they cancel each other. The molecular orbitals of H_2 molecule can be imagined to result from the overlap of 1s atomic orbital of two hydrogen atoms. If the overlap results in wave reinforcement, electron density between nuclei is high. The attraction of the nuclei for this extra electronic charge holds the molecule together. The molecular orbital is called σ bonding orbital.

The other molecular orbital results from the out of phase combination of waves. The electron density in region between the nuclei is low. In this case, the nuclei repel each other, since the low charge density between the nuclei does to little counteract this repulsion. This orbital is called a sigma-antibonding orbital. The energy of the σ orbital is lower than energy of the σ antibonding orbital .

There are three types of molecular orbital that are relevant in chemistry; the σ orbitals, the π orbitals and the δ orbitals. The σ orbitals do not have any nodal plane containing the internuclear axis. The π orbitals have one nodal plane containing the internuclear axis and δ orbitals have two nodal planes containing the internuclear axis.

In general, bond is formed by overlapping of two atomic orbitals that have the same symmetry with respect to internuclear axis. The σ bond, which is symmetric for rotation about the internuclear axis, can be produced by overlapping of s-s, s-d_z^2, s-p_z^2, and pz-p_z. π bonds have nodal plane containing the internuclear axis and they can be produced by overlapping of orbitals like p_x-p_x, p_y-p_y, p_z-p_z. δ bond has nodal planes containing the internuclear axis and d_{xy}-d_{xy}, $d_{x^2-y^2}$-$d_{x^2-y^2}$.

3.2.1b. The LCAO Approximation

The usual method for constructing MOs is the linear combinations of atomic orbitals (LCAO). Each atom in the molecular system is considered to attribute at least one atomic orbital to the MO system. Thus each MO is written as

$$\psi_i = \sum c_{ij}\phi_j \qquad (3.12)$$

The ϕ_j's are a basis set, and it is convenient to choose or adjust them so that they are normalized. This property, which we shall henceforth take for granted is defined by the equation

$$\int \phi_j \phi_j d\tau = 1 \qquad (3.13)$$

Using the definition the wave function, for corresponding energy can be calculated from the usual energy expression:

$$E_i = \frac{\int \psi_i H \psi_i d\tau}{\int \psi_i \psi_i d\tau} \tag{3.14}$$

The whole problem of determination of the energy E_i and the c_{ij}, the linear coefficients, may be treated under the variational principle: the best estimate of the energy is obtained when the energy E_i is minimized with respect to the coefficients c_{ij}.

Substitute the expression for the LCAO MOs into the energy expression

$$E_i = \frac{\sum_k \sum_j c_{ik} c_{ij} \int \phi_k H \phi_j d\tau}{\sum_k \sum_j c_{ik} c_{ij} \int \phi_k \phi_j d\tau} \tag{3.15}$$

Let

$$H_{kj} = \int \phi_k H \phi_j d\tau \tag{3.16}$$

and

$$S_{kj} = \int \phi_k \phi_j d\tau \tag{3.17}$$

Then

$$E_i = \frac{\sum_k \sum_j c_{ik} c_{ij} H_{kj}}{\sum_k \sum_j c_{ik} c_{ij} S_{kj}} \tag{3.18}$$

Upon rearranging we find

$$\sum_k \sum_j c_{ik} c_{ij} (H_{kj} - E_i S_{kj}) = 0 \tag{3.19}$$

Now we apply the variational principle, i.e., minimize the energy with respect to c_{kj}. The result is

$$\sum_j c_{ij} (H_{kj} - E_i S_{kj}) = 0 \tag{3.20}$$

The only nontrivial solution to this system of homogeneous equations requires the determinant of the coefficients vanish:

$$\left|H_{ij} - E_i S_{ij}\right| = 0 \qquad (3.21)$$

Eqn.(3.20) and Eqn.(3.21) are a statement of the eigenvalue problem. Although there are standard methods for the solution of such problems, unless the above array is fairly simple, the amount of labor necessary to obtain the solution by hand is prohibitive.

The coefficients (eigenvectors) can be solved, under the constraint that the sum of the squares of the coefficients in each molecular orbital is unity (the wavefunctions are normalized). Coefficients of molecular orbital wavefunction for large molecular systems are easily calculated using symmetry properties of the molecule with the aid of group theory. To determine these coefficients, projector operators of the molecular symmetry group should be calculated and used for making symmetry adapted linear combinations of atomic orbitals (SALC) on different atoms. This topic will be discussed in detail, later.

3.2.1c. Hückel Approximation

The Hückel method is a means of finding approximate solutions to the Schrödinger equation by making several simplifying assumptions for large carbon systems. The first assumption is that the σ and π frameworks are totally separate, that the σ bonds are localized, and that the system is delocalized over all the atoms in the molecule. Thus only π electrons are considered.

The LCAO-MO approach just outlined is in itself an approximation. Even, so, if no further approximations are made, the evaluation of the integrals of the Eqn.(3.16) and Eqn.(3.17) can be time consuming. Some simplifications and further approximations are often made, the most drastic of which are, as a group, called the Hückel approximation. The Hückel approximation assumes that all $S_{ij}=0$ and that all $H_{ij}=0$ unless the i^{th} and j^{th} orbitals are non adjacent atoms. The setting of all $S_{ij}=0$ means

that the normalizing factors for LCAO's are obtained very simply. If the molecular orbital is given as

$$\psi_i = N_i \sum_j c_{ij}\phi_j \tag{3.22}$$

and it is required that

$$\int \psi_i \psi_i d\tau = 1 \tag{3.23}$$

It is obtained from the normalization

$$\begin{aligned} \frac{1}{N_i^2} &= \int (\sum_j c_{ij}\phi_j)^2 d\tau \\ &= \sum_j c_{ij}^{\ 2} \int \phi_j \phi_j d\tau + \sum_{j,k} c_{ij} c_{ik} \int \phi_j \phi_k d\tau \end{aligned} \tag{3.24}$$

The second sum in Eqn.(3.24) is equal to zero because overlap is assumed to be zero. The first sum is just equal to $\sum_j c_{ij}^2$, since the ϕ_j's are assumed to be normalized.

Thus

$$\frac{1}{N_i^2} = \sum_j c_{ij}^2 \tag{3.25}$$

The Hückel approximation comprehends some assumptions regarding the evaluation of energies of molecular orbitals. For a given molecular orbitals given in section 3.2.1 b, its energy eigenvalues are obtained from the expression given as

$$\begin{aligned} E_i &= \int \psi_i H \psi_i d\tau \\ E_i &= N_i^{\ 2} \left\{ \sum_j c_{ij}^{\ 2} \int \phi_j H \phi_j d\tau + \sum_{j,k} c_{ij} c_{ik} \int \phi_j H \phi_k d\tau \right\} \\ E_i &= \alpha + N_i^{\ 2} \sum_{j,k} c_{ij} c_{ik} \int \phi_j H \phi_k d\tau \end{aligned} \tag{3.26}$$

where $\alpha = \int \phi_j H \phi_j d\tau$ and is assumed that the energies of individual atomic orbitals ϕ_j's are all equal. According to the Hückel approximation, in evaluating E_i, any integral form of $\int \phi_j H \phi_k d\tau$ can be neglected if ϕ_j and ϕ_k refer to nonadjacent atoms. Let us write for adjacent atoms as

$$\int \phi_j H \phi_k d\tau = \beta . \tag{3.27}$$

It can be shown that β is negative. Also, Eqn.(3.26) can be written as

$$E_i = \alpha + 2N_i^2 \sum_{j,k} c_{ij} c_{ik} \beta \tag{3.28}$$

The Hückel method further makes the following simplifying assumptions for large carbon systems. The Hückel approximation is applied most often to the π orbitals in which case the following abbreviations are conventional:

$\alpha = H_{jj}$, the coulomb integral, represents the energy of an electron in a $p\pi$ atomic orbital in the absence of any interaction with its neighbours, and is the same for all i since all $p\pi$ orbitals are the same.

$\beta = H_{jk}$, the resonance integral, represents the interaction energy of an electron in $p\pi$ orbital j with one in $p\pi$ orbital k. It is assumed to be zero except for pairs of $p\pi$ orbitals on adjacent carbons. All H_{jk} for bonded pairs are assumed to have the same value.

The appearance of the secular equations can be simplified if α is taken as the zero of energy and β taken as the unit of energy. It can be shown that β is inherently a negative quantity. Thus an MO whose energy is positive in units of β has an absolute energy that is negative. An electron in such an MO is therefore more stable than an electron in an isolated $p\pi$ orbital. The generalized secular determinant can then be reduced to

$$\begin{vmatrix} \alpha - E & * & * & \cdots & * \\ * & \alpha - E & * & \cdots & * \\ * & * & \alpha - E & \cdots & \vdots \\ \vdots & \vdots & \vdots & \ddots & \vdots \\ * & * & \cdots & \cdots & \alpha - E \end{vmatrix} = 0 \qquad (3.29)$$

where *=β for j and i bonded, 0 for all others. This leads to the following important conclusions:

1. N molecular orbitals can be constructed from a basis set of N atomic orbitals.
2. By solving the Schrödinger equation, it is possible to arrive at solutions that model the molecular orbitals formed by the atomic orbitals.
3. Areas of constructive interference lead to overlap of the atomic orbitals due to accumulated electron density. This results in a bonding molecular orbital that is low in energy and contributes to keeping the molecules together.
4. Areas of destructive interference lead to non-overlap of the atomic orbitals due to reduction of electron density. This results in an anti-bonding molecular orbital that is high in energy and tends to tear apart the molecule.
5. They are of reduced electron density resulting in a node where there is considered to be no electron density.
6. In a bonding molecular orbital, the probability of finding the electrons on one, both or between the atoms is quite high.
7. In an anti-bonding orbital, the probability of finding an electron in between the atoms is 0, and 1 for on one or the other atom.

So using the above assumptions and points, it will be possible to describe the molecular orbitals for metals, semiconductors, semi-metals and insulators.

3.2.2. Vibrational Modes of Polyatomic Molecules

It is ordinarily possible to deduce the number and kinds of vibrations in simple diatomic and triatomic molecules and whether the vibrations will lead to absorption. Complex molecules may contain several types of atoms as well as bonds, for these multitude of vibrations give rise to infrared absorption spectra. Additionally, Raman

scattering shows the phenomenon results from the same type of quantized vibrational changes that are associated with infrared absorption.

In defining the motion of a molecule, it should be considered: (1) the motion of the entire molecule through space (that is the translational motion of its center of gravity); (2) the rotational motion of the entire molecule around its center of gravity; and (3) the motion of each of its atoms relative to the other atoms (in other words, its individual vibrations). Definition of translational motion requires three coordinates and uses up three degrees of freedom. Another three degrees of freedom are needed to describe the rotation of molecule as a whole. The remaining (3N-6) degrees of freedom involve interatomic motion, and hence represent the number of possible vibrations with in the molecule. Each of the (3N-6) vibrations is called normal mode.

3.2.2a. Types of Molecular Vibrations

The relative positions of atoms in a molecule are not exactly fixed but instead fluctuate continuously as a consequence of multitude of different types of vibrations. For a simple diatomic or triatomic molecule, it is easy to define the number and nature of such vibrations and relate these to energies of absorption.

Vibrations fall into the basic categories of stretching and bending. A stretching vibration involves a continuous change in the interatomic distance along the axis of the bond between two atoms. Bending vibrations are characterized by a change in the angle between the two bonds and are of four types: scissoring, rocking, wagging, and twisting. The various types of vibrations are shown schematically, in Figure 3.1.

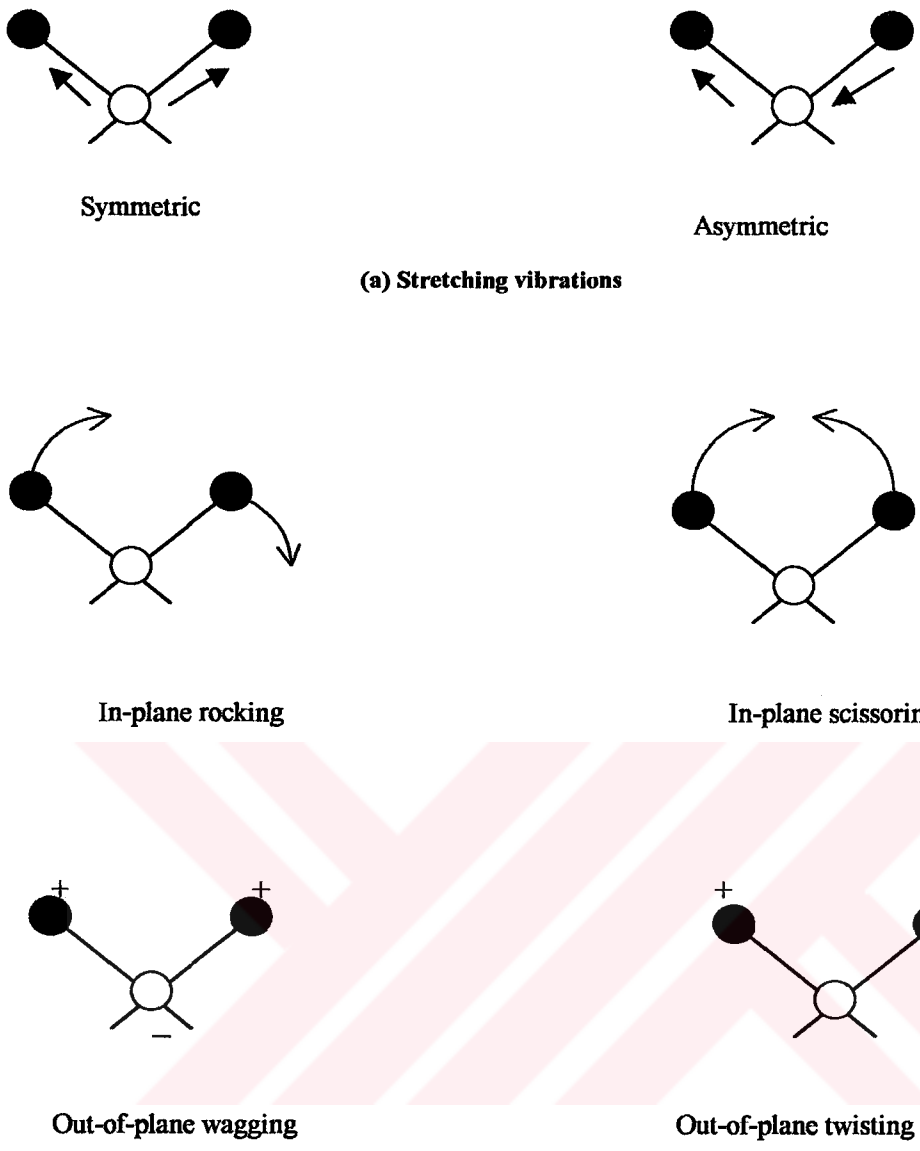

Figure 3.1. Types of molecular vibrations. Note: + indicates motion from page toward the reader; - indicates motion away from the reader.

3.2.2b. Vibrational Coupling

The energy of vibration, and thus the wavelength of its absorption peak, may be influenced (or coupled) by other vibrators in the molecule. A number of factors that influence the extent of such coupling can be identified. Strong coupling between stretching vibrations occurs only when there is an atom common to the vibrations.

1. Interaction between bending vibrations requires a common bond between the vibrating groups.
2. Coupling between a stretching and a bending vibration can occur if the stretching bond forms one side of the angle that varies in the bending vibration.
3. Interaction is greatest when the couple groups have individual energies that are approximately equal.
4. Little or no interaction is observed between groups separated by two or more bonds.
5. Coupling requires that the vibrations be of the same symmetry species.

As an example, carbon dioxide is a linear molecule and has four normal modes (3x3-5). Two stretching vibrations are possible; furthermore interaction between the two can occur since the bonds involved are associated with a common carbon atom. One of the coupled vibrations symmetric and the other asymmetric. The symmetric vibration causes no change in dipole, since the two oxygen atoms simultaneously move away from or toward the central carbon atom. Thus, the symmetric vibration is infrared inactive. One oxygen approaches the carbon atom as the other moves away during asymmetric vibration. As a consequence, a net change in charge distribution occurs periodically and this vibration is infrared active.

The remaining two vibrational modes of carbon dioxide involve scissoring. The two bending vibrations are resolved to components (at 90 degree to one another) of the bending motion in all possible of planes around the bond axis. These two vibrations are identical in energy and thus produce one peak (degenerate modes).

3.2.2c. Infrared Absorption Mechanism

Electronic transitions require energies in the ultraviolet or visible regions; absorption of infrared radiation is thus confined largely to molecular species for which small energy difference exist between various vibrational and rotational states.

In order to absorb infrared radiation, a molecule must undergo a net change in dipole moment as a consequence of its vibrational or rotational motion. Only under these circumstances can the alternating electric field of the radiation interact with the

molecule and cause changes in the amplitude of one of its motions. For example, the charge distribution around a molecule such as a hydrogen chloride is not symmetric, the chlorine having a higher electron density than the hydrogen. Thus, hydrogen chloride has significant dipole moment and is said to be polar. The dipole moment is determined by the magnitude of the charge difference and the distance between the two centres of charge. As a hydrogen chloride molecule vibrates longitudinally, a regular fluctuation in dipole moment occurs, and a field is established which can interact with radiation. If the frequency of radiation matches a natural vibrational frequency of the molecule, there occurs a net transfer of energy that results in a change in the amplitude of the molecular vibration; absorption of the radiation is the consequence. Similarly, the rotation of symmetric molecules around their centres of mass results in a periodic dipole fluctuation; again, interaction with radiation is possible.

No net change in dipole moment occurs during the vibration or rotation of homonuclear species such as O_2, N_2 or Cl_2; consequently, such compounds cannot absorb in the infrared. With the exception of this type, all molecular species exhibit infrared absorption.

3.2.2d. Mechanism of Raman Scattering

When a photon collides with a molecule, several things can happen. If the photon's frequency corresponds to a difference between energy levels of the system, the photon may be absorbed. If the photon's frequency does not correspond to such an energy difference, it may be scattered. Of the scattered photons, most will have undergone no change in frequency (Rayleigh scattering); however, during the time the photon's energy can be transferred to the molecule. This then leads to change in frequency of the scattered photon known as the Raman effect. The change in frequency of the scattered photon must correspond to a difference between two energy levels of the molecule doing scattering.

3.2.2e. Comparison of Raman and Infrared Spectrum

The differences between Raman and an infrared spectrum are not surprising when it is considered that the basic mechanisms, although dependent upon the same vibrational modes, arise from processes that are mechanistically different. Infrared absorption requires that a vibrational mode of the molecule have a change in dipole or charge distribution associated with it. Only then can radiation of the same frequency interact with the molecule and promote it to an excited vibrational state. In contrast, scattering involves momentary distortion of the electrons distributed around a bond in a molecule, followed by reemission of the radiation in all directions as the bond returns to its normal state. In its distorted form, the molecule is temporarily polarized; that is, it develops momentarily an induced dipole, which disappears upon relaxation and reemission. The effectiveness of a bond toward scattering thus depends directly upon the ease with which the electrons of the bond can be distorted from their normal positions (that is the polarizability of the bonds); polarizability decreases with increasing electron density, increasing bond strength, and decreasing bond length. The Raman shift in scattered radiation, then requires that there must be a change in polarizability rather than a change in dipole associated with the vibrational mode of the molecule; as a consequence, the Raman activity of a given mode may differ markedly, from its infrared activity. For example, a homonuclear molecule such as hydrogen nitrogen has no dipole moment either in its equilibrium position or when a stretching vibration causes a change in the distance between the two nuclei. Thus, absorption of radiation of the vibration frequency cannot occur. On the other hand, the polarizability of the bond between the two atoms of such a molecule varies periodically in phase with the stretching vibrations, reaching a maximum at the greatest separation and a minimum at the closest approach. A Raman shift corresponding in frequency to that of the vibrational mode results.

3.2.2f. Vibrational Modes of Molecular Motion: The General Dynamical Problem

The internal oscillations of any physical system have the advantage that they may be treated adequately within the framework of classical mechanics. This is because the motions are resolvable into combinations of simple harmonic oscillations whose frequencies can be determined from classical considerations. Specifically quantum mechanical effects can be incorporated subsequently.

Whether one prefers to approach the problem of analysing the motion of vibrating system by writing down Newton's second law of motion for each of particles in the system or by writing down Lagrange's equation of motion for the system one comes to conclusion that, except for the very simplest systems, it is easier to consider the normal modes of the system than to work in terms of the motions of the individual particles. The determination of the normal modes of a system and their frequencies of vibration is very often a tedious process. Group theory can be used to enable some simplification in the finding normal modes of a vibrating system to be achieved.

Consider a molecule consisting of N atoms (regarded as point masses) oscillating about equilibrium. We can describe the atomic positions in terms of cartesian coordinates: $x_1, y_1, z_1; x_2, y_2, z_2$. Let us, however, use coordinates, which describe the displacements of the atoms from their equilibrium positions: $\Delta x_1, \Delta x_2, \Delta x_3; \Delta x_4, \Delta x_5, \Delta x_6$. The kinetic energy is written as

$$T = \sum_{i=1}^{N} \frac{1}{2} m(\Delta \dot{x})^2 \qquad (3.30)$$

or

$$2T = \sum_{i=1}^{N} m_i(\Delta \dot{x})^2 \qquad (3.31)$$

where $m_1=m_2=m_3$, etc.

If Δx_i is written as vectors and the masses as a matrix M, T can be written as follows;

$$2T = \Delta \dot{x} M \Delta \dot{x} \qquad (3.32)$$

where it can seen that M is diagonal. T can be shown to be diagonal under a transformation to mass-weighted coordinates. Let;

$$q_i = \sqrt{m_i}\Delta x_i \tag{3.33}$$

then

$$2T = \sum_{i=1}^{3N} \dot{q}_i^2 \tag{3.34}$$

The kinetic energy is diagonal, however, only in cartesian-type coordinate systems. Consider the potential function for the system $V=V(q_i)$. In general the functional relationship is not known. So that in order to continue the treatment of molecular vibrations, we must produce an approximation of V. The usual procedure is to expand V in a Taylor's series about equilibrium position.

$$V = V_o + \left(\sum_{i=1}^{N} \frac{\partial V}{\partial q_i}\right)_0 q_i + \frac{1}{2}\left(\sum_{i=1}^{N}\sum_{j=1}^{N} \frac{\partial^2 V}{\partial q_i \partial q_j}\right)_0 q_i q_j + \cdots \tag{3.35}$$

The term V_0 is the potential of the system with all atoms in their equilibrium positions, and is a constant. Since the zero potential can be arbitrarily chosen, we can set $V_0=0$. Since the potential is always a minimum at the equilibrium positions, all of the $\frac{\partial V}{\partial q_i} = 0$. Thus we are left with only the second-derivative terms.

$$V = \frac{1}{2}\left(\sum_{i=1}^{N}\sum_{j=1}^{N} \frac{\partial^2 V}{\partial q_i \partial q_j}\right)_0 q_i q_j \tag{3.36}$$

Note that the array of second derivatives is symmetric with respect to interchange of i and j. Thus, a matrix constructed for V from the terminated Taylor's series produces a real symmetric (hermitian) matrix. In order to solve the vibrational problem use the Euler-Lagrange equations:

$$\frac{d}{dt}\frac{\partial L}{\partial \dot{q}_i} - \frac{\partial L}{\partial q_i} = 0 \tag{3.37}$$

The Lagrangian L is defined as L=T-V. In our case L is written in terms of the q_i.

$$L = \frac{1}{2}\sum_{i=1}^{N}\dot{q}_i^2 - \frac{1}{2}\sum_{i=1}^{N}\sum_{j=1}^{N} f_{ij}q_i q_j \tag{3.38}$$

Thus f_{ij} are the various second derivatives in the Taylor's series.

$$f_{ij} = \frac{\partial^2 V}{\partial q_i \partial q_j} \tag{3.39}$$

Note that V may be written in a bilinear form of $2V = \tilde{q}Fq$. The solution to the Euler-Lagrange equations is a set of 3N linear homogeneous coupled equations

$$\ddot{q}_i + \sum_{j=1}^{N} f_{ij}q_j = 0 \quad (i = 1,2,\cdots,3N) \tag{3.40}$$

These constitute a set of second-order differential equations. The general solutions will substitute

$$q_{i=}A_{ik}e^{i\omega t} \quad (i = 1,2,\ldots,3N) \tag{3.41}$$

Taking the second derivatives with respect to time, $\ddot{q}_i = -\omega^2 q_i = -\lambda q_i$ and substituting these back into the differential equations, Eqn(3.40) gives a set of secular equations

$$\sum_{j=1}^{N} f_{ij}A_{jk} - \lambda A_{ik} \quad (i = 1,2,\ldots,3N) \tag{3.42}$$

which may be written in the matrix form named as force matrix. The necessary and sufficient condition for the existence of a nontrivial set of solutions for these equations is that determinant of the matrix vanish

$$\begin{vmatrix} f_{11}-\lambda_k & f_{12} & \cdots & f_{1,3N} \\ f_{12} & f_{22}-\lambda_k & \cdots & f_{2,3N} \\ f_{3n,1} & f_{3n,2} & \cdots & f_{3N,3N}-\lambda_k \end{vmatrix} = \left| f_{ij} - \lambda_k \delta_{ij} \right| = 0 \tag{3.43}$$

Eigenvalues of this determinant give the normal mode frequencies of the vibrations. To find the eigenvalues of this force matrix is very difficult for large molecules. Group theoretical considerations can be used to exploit these mathematical difficulties in such a way partial diagonalization of force matrix is obtained. To block diagonalize this matrix normal (symmetry) coordinates of this matrix must be known. This is also very hard. Therefore; some models are improved.

3.2.2g. Symmetry of Normal Modes

In order to determine the symmetries of the normal modes of the vibration, we consider a representation for the molecule in question. Using a basis system for the representation, the character system is determined and put into its totally reduced form by the standard reduction formula. The most easily handled basis set for this case is a set of N cartesian coordinate systems, one cartesian systems for each atom. Each cartesian coordinate system is centred on an atom, so that all the x_i axes are parallel. The dimension of this representation is 3N×3N.

As an example, let us analyse the normal modes of H_2O molecule. It is known that symmetry group H_2O is C_{2v} and character table is given in Table 1. As seen from the character table this group has four symmetry operations named as E, C_2, σ_v, σ'_v.

Table 3.2. Character table for C_{2v}.

C_{2v}	E	C_2	σ_v	σ'_v	
A_1	1	1	1	1	z
A_2	1	1	-1	-1	R_z
B_1	1	-1	1	-1	x, R_y
B_2	1	-1	-1	1	y, R_x
Γ_{cart}	9	-1	1	3	

It is easy to construct the four 9×9 (3N×3N) matrices based on the N set of cartesian coordinates for H_2O as shown in Figure 3.2. Left side and right side hydrogen atoms are numbered as first and second, respectively. Oxygen atom is numbered as third atom.

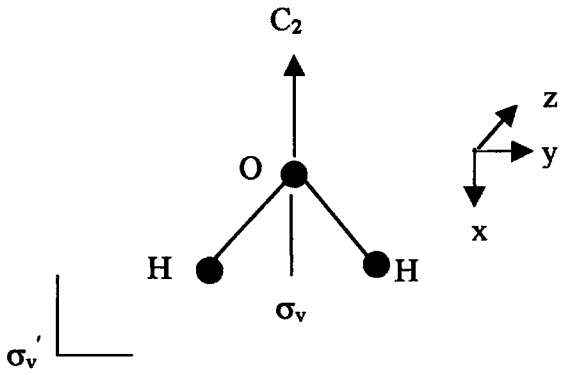

Figure 3.2. The geometry of the H_2O molecule. The three symmetry elements of point group C_{2v} are also shown.

For C_2

$$\begin{bmatrix} x_1' \\ y_1' \\ z_1' \\ x_2' \\ y_2' \\ z_2' \\ x_3' \\ y_3' \\ z_3' \end{bmatrix} = \begin{bmatrix} 0 & 0 & 0 & 1 & 0 & 0 & 0 & 0 & 0 \\ 0 & 0 & 0 & 0 & -1 & 0 & 0 & 0 & 0 \\ 0 & 0 & 0 & 0 & 0 & -1 & 0 & 0 & 0 \\ 1 & 0 & 0 & 0 & 0 & 0 & 0 & 0 & 0 \\ 0 & -1 & 0 & 0 & 0 & 0 & 0 & 0 & 0 \\ 0 & 0 & -1 & 0 & 0 & 0 & 0 & 0 & 0 \\ 0 & 0 & 0 & 0 & 0 & 0 & 1 & 0 & 0 \\ 0 & 0 & 0 & 0 & 0 & 0 & 0 & -1 & 0 \\ 0 & 0 & 0 & 0 & 0 & 0 & 0 & 0 & -1 \end{bmatrix} \begin{bmatrix} x_1' \\ y_1 \\ z_1 \\ x_2 \\ y_2 \\ z_2 \\ x_3 \\ y_3 \\ z_3 \end{bmatrix} \qquad (3.44)$$

The sum of the diagonal elements or characters is $\chi^{(C_2)}=-1$. This procedure can be repeated for the other three symmetry operations and in analogous manner the characters are found and given in Table 3.2. The direct sum for Γ_{cart} is obtained by using standard reduction formula given in Eqn(3.9). So that

$$\Gamma_{cart}=3A_1+A_2+2B_1+3B_2 \qquad (3.45)$$

From the character table we can determine the symmetries of the extra translational and rotational degrees of freedom.

Translation	Rotation
x (B_1)	R_x (B_2)
y (B_2)	R_y (B_1)
z (A_1)	R_z (A_2)

So that

$$\Gamma_{rot,trans}=A_1+A_2+2B_1+2B_2 \tag{3.46}$$

Therefore the direct sum for the vibrational degrees of freedom is

$$\Gamma_{vib}=\Gamma_{cart}-\Gamma_{rot,trans}=2A_1+B_2 \tag{3.47}$$

3.2.3. Stability of Symmetrical Configurations of the Molecule (Jahn Teller Effect)

The quantum chemistry of the electron-vibron (e-v) coupled systems has been studied throughout the century, since the early days of quantum mechanics. After the fundamental work by Jahn-Teller, effects of e-v distortion have been discovered in hundreds of molecules, ions, complexes, where degenerate electronic states are filled only partially. This tendency to shell closing through molecular distortion, generally is called Jahn-Teller effect. For this reason, the coupling of electronic and vibrational degrees of freedom is still boosting in the scientific community large interest for promising physical features in new materials.

For a symmetrical position of nuclei, an electron term of the molecule may be degenerate, if there are among the irreducible representations of the symmetry group one or more whose dimensions exceed unity. In this case, a displacement of nuclei, which destroys the symmetry of the molecule generally, results in a splitting of the term. If the configuration in question is stable, the energy of the molecule as a function of the distances between the nuclei must be a minimum for the given

position of the nuclei. This means that the change in energy due to small displacement of the nuclei must contain no terms linear in the displacements.

In other words, let D^{ℓ} be the irreducible representation which electron transforms wavefunction of the polyatomic molecule. If the symmetric product $[D^{\ell} \otimes D^{\ell}]$ does not contain any (except unit representation) of the irreducible representations of symmetric group of the molecule, a symmetrical configuration is stable. Otherwise, it is unstable.

This result constitutes a general rule, the Jahn-Teller (JT) theorem: any polyatomic molecule with the exception of linear molecule is stable only when its ground state is orbitally nondegenerate. Generally, according to the JT, the totally symmetric nuclear configuration of an electronic state of molecule which orbitally degenerate is unstable.

For stabilization to occur a descent in symmetry must take place until the degeneracy of the ground term is completely lifted. This can result either from a transition of the system to a nuclear orientation in the sense of static reduction of the symmetry, or the molecule can exist several equivalent-limiting forms, which can be easily transformed into one another by vibrations.

In order to understand the superconducting properties of any material, much work has been made about the significance of the JT effect (electron-phonon) interaction.

CHAPTER 4

MOLECULAR ENERGY LEVELS OF C_{60}

Today a number of theoretical methods has been applied for the calculations of the electronic structure of carbon clusters. A review of applications of different theoretical methods for carbon species can be found in the work of Whelther [50]. A number of semi-emprical and first principle calculations [51-55], including geometry optimization, ionization energies and predictions of optical transitions and vibrational frequencies was investigated. Studies of the literature shortly after the discovery of C_{60}, also showed that the spherical structure of carbon cluster had been postulated independently by several workers in their discussions of hollow carbon molecules. Some workers used the Hückel method to predict the eigenvalues of C_{60}.

In this section, we calculate the electronic energy levels and molecular orbitals. Such a study is necessary for understanding of any physical and chemical properties of the cluster that might exhibit.

4.1. ANALYTICAL FORMATION OF MOLECULAR ORBITALS AND GEOMETRICAL STRUCTURE OF C_{60}

The shape of the C_{60} molecule is that of a truncated icosahedron. The 20 hexagonal faces of the intact icosahedron and the 12 pentagonal faces result from the truncation perpendicular to the fivefold axes. The isolated C_{60} molecule has icosahedral symmetry, and we will assume that the same holds for each molecule in the solids. The icosahedral point group has 120 elements containing 12 fivefold axes (C_5) through pentagon centers, 20 threefold axes through the hexagon centers (C_3), 15 twofold axes through the centers of the hexagon-hexagon edges(C_2), and a center of

inversion (i). In the work of N.Laoinini, molecular orbitals of T_1 and H states were calculated by using an analytical method. In the following subsection we will give an useful method to calculate molecular orbitals of all states of icosahedral group.

4.1.1. Group Theoretical Concepts for C_{60}

In the previous section general methods have been given to find the generators of a group. Matrix generators of closed subgroups of SO(3) are found developing a computer program given in Appendix A. In order to determine the position of the atoms, the group should be constructed by using the generators which are given in Appendix B. Since 3 dimensional irreducible representations of group I project the position vectors of atoms in C_{60}, by choosing an appropriate position vector, it is possible to determine the position of 60 atoms in C_{60} molecule. All of the group elements of icosahedral complex have been computed and classified by the help of computer program given in Appendix C, and its characters are shown in Table 4.1.

Table 4.1. Character table for the full icosahedral group I_h. The last row demonstrates the characters of site symmetry matrices

I_h	E	$12C_5$	$12C_5^2$	$20C_3$	$15C_2$	I	$12S_{10}$	$12S_{10}^3$	$20S_6$	15σ	
A_g	1	1	1	1	1	1	1	1	1	1	
T_{1g}	3	τ	$-\sigma$	0	-1	3	$-\sigma$	τ	0	-1	R_x,R_y,R_z
T_{2g}	3	$-\sigma$	τ	0	-1	3	τ	$-\sigma$	0	-1	
G_g	4	-1	-1	1	0	4	-1	-1	1	0	
H_g	5	0	0	-1	1	5	0	0	-1	1	
A_u	1	1	1	1	1	-1	-1	-1	-1	-1	
T_{1u}	3	τ	$-\sigma$	0	-1	-3	σ	$-\tau$	0	1	x,y,z
T_{2u}	3	$-\sigma$	τ	0	-1	-3	$-\tau$	σ	0	1	
G_u	4	-1	-1	1	0	-4	1	1	-1	0	
H_u	5	0	0	-1	1	-5	0	0	1	-1	
χ_{sit}	60	0	0	0	0	0	0	0	0	4	

We denote the local coordinates (xyz) and choose an appropriate position vector that determines that position of the 1st atom in the site.

$$\vec{r}_1 = \frac{b}{2}(3\tau\hat{i} + \hat{j}) \tag{4.1a}$$

where b is a constant and $\tau = \frac{1}{2}(1+\sqrt{5})$ as given in Chapter 3 named as golden number.

It is obvious that position of all other atoms can be found by projecting with the vector using the generators of the group I. Position vectors of each atom in a molecule are given in Table 4.2. For simplicity the length of the edge between a hexagon and pentagon (single bond) and the length of the edge between two hexagon (double bond) have been considered equal. Geometrical optimization calculations and experiments show that the bond alternation for pure C_{60} is, ξ =0.015. This means that the position vector should be chosen

$$\vec{r}_1 = \frac{b}{2}(3\tau\hat{i} + (1-2\xi)\hat{j}) \tag{4.1b}$$

Table 4.2a. The position vectors $\frac{2\vec{r}_i}{b}$ of atoms in C_{60} site. These are obtained by projection r_1 with the generators of the T_1 representation in the class C_3.

$\frac{2x}{b}$	$\frac{2y}{b}$	$\frac{2z}{b}$
$\frac{1}{6}(-\sqrt{15}-9\tau)$	$\frac{1}{6}(1+3\sqrt{15}\,\tau)$	$\frac{1}{3}(\sqrt{5}-3\sqrt{3}\,\tau)$
$\frac{1}{6}(\sqrt{15}-9\tau)$	$\frac{1}{6}(1-3\sqrt{15}\,\tau)$	$\frac{\sqrt{5}}{3}+\sqrt{3}\,\tau$
$\frac{1}{4}(-3-2\sqrt{3}-3\sqrt{5})$	$\frac{1}{2}(-1+3\sqrt{3}\,\tau)$	0
$\frac{1}{4}(-3+2\sqrt{3}-3\sqrt{5})$	$\frac{1}{2}(-1-3\sqrt{3}\,\tau)$	0
$-\frac{\tau}{\sqrt{3}}$	$-\frac{1}{3}+\sqrt{3}$	$\frac{\sigma^2}{3}+\sqrt{3}\,\tau^2$
$-\frac{\tau}{\sqrt{3}}$	$\frac{1}{3}-\sqrt{3}$	$\frac{1}{6}(-3-9\sqrt{3}+\sqrt{5}-3\sqrt{15})$
$\frac{\sigma}{\sqrt{3}}$	$\frac{1}{6}(-2-9\sqrt{3}-3\sqrt{15})$	$-\frac{1}{2}+\sqrt{3}-\frac{\sqrt{5}}{6}$
$\frac{\sigma}{\sqrt{3}}$	$\frac{1}{6}(2+9\sqrt{3}+3\sqrt{15})$	$\frac{1}{3}(-3\sqrt{3}+\tau^2)$
$\frac{1}{6}(\sqrt{3}-\sqrt{15})$	$\frac{1}{6}(2-9\sqrt{3}-3\sqrt{15})$	$\sqrt{3}+\frac{\tau^2}{3}$
$\frac{1}{6}(\sqrt{3}-\sqrt{15})$	$\frac{1}{6}(-2+9\sqrt{3}+3\sqrt{15})$	$\frac{1}{6}(-3-6\sqrt{3}-\sqrt{5})$
$\frac{1}{6}(\sqrt{3}+\sqrt{15})$	$\frac{1}{3}+\sqrt{3}$	$\frac{1}{6}(-3+9\sqrt{3}+\sqrt{5}+3\sqrt{15})$
$\frac{1}{6}(\sqrt{3}+\sqrt{15})$	$-\frac{1}{3}-\sqrt{3}$	$\frac{1}{3}(\sigma^2-3\sqrt{3}\,\tau^2)$
$\frac{1}{12}(-18-\sqrt{3}+\sqrt{15})$	$\frac{1}{12}+\sqrt{3}+\frac{\sqrt{5}}{4}+\frac{\sqrt{15}}{2}$	$-\frac{\sqrt{5}}{3}+\sqrt{3}\,\tau$
$\frac{1}{12}(-18+\sqrt{3}-\sqrt{15})$	$\frac{1}{12}(1-12\sqrt{3}+3\sqrt{5}-6\sqrt{15})$	$-\frac{\sqrt{5}}{3}-\sqrt{3}\,\tau$
$\frac{1}{12}(-\sqrt{15}-3(6+\sqrt{3}))$	$\frac{1}{12}(1-6\sqrt{3}+3\sqrt{5})$	$\frac{1}{6}(-3+9\sqrt{3}+\sqrt{5}+3\sqrt{15})$
$\frac{1}{12}(-18+3\sqrt{3}+\sqrt{15})$	$\frac{1}{12}(1+6\sqrt{3}+3\sqrt{5})$	$\frac{1}{6}(-3-9\sqrt{3}+\sqrt{5}-3\sqrt{15})$
$\frac{1}{12}(27-\sqrt{3}+9\sqrt{5}-\sqrt{15})$	$\frac{1}{12}(1-3\sqrt{3}+3\sqrt{5}(-1+\sqrt{3}))$	$-\frac{\sqrt{5}}{3}-\sqrt{3}\,\tau$
$\frac{1}{12}(27+\sqrt{3}+9\sqrt{5}+\sqrt{15})$	$\frac{1}{12}(1+3\sqrt{3}-3\sqrt{5}(1+\sqrt{3}))$	$-\frac{\sqrt{5}}{3}+\sqrt{3}\,\tau$
$\frac{1}{12}(27-3\sqrt{3}+9\sqrt{5}+\sqrt{15})$	$\frac{1}{12}(1+9\sqrt{3}+3\sqrt{5}(-1+\sqrt{3}))$	$\sqrt{3}+\frac{\tau^2}{3}$
$\frac{1}{12}(27+3\sqrt{3}+9\sqrt{5}-\sqrt{15})$	$\frac{1}{12}(1-9\sqrt{3}-3\sqrt{5}(1+\sqrt{3}))$	$\frac{1}{3}(-3\sqrt{3}+\tau^2)$

Table 4.2b. Position vectors of 12 atoms obtained by using the generators C_5 in terms of Cartesian coordinate (x,y,z).

$\frac{2x}{b}$	$\frac{2y}{b}$	$\frac{2z}{b}$
$\frac{1}{6}(-\sqrt{15}+9\tau)$	$-\frac{\sqrt{5}}{6}-\frac{3\sqrt{3}\,\tau}{2}$	$-\frac{2}{3}$
$\frac{1}{6}(\sqrt{15}+9\tau)$	$-\frac{\sqrt{5}}{6}+\frac{3\sqrt{3}\,\tau}{2}$	$-\frac{2}{3}$
$\frac{1}{4}(3-2\sqrt{3}+3\sqrt{5})$	$-\frac{1}{12}\sqrt{5}\,(2+3\sqrt{3}+3\sqrt{15})$	$\frac{1}{3}+\sqrt{3}\,\tau$
$\frac{1}{4}(3+2\sqrt{3}+3\sqrt{5})$	$\frac{1}{6}\sqrt{5}\,(-1+3\sqrt{3}\,\tau)$	$\frac{1}{3}-\sqrt{3}\,\tau$
$\frac{1}{12}(-27-\sqrt{3}-\sqrt{5}\,(9+\sqrt{3}))$	$\frac{1}{12}(5+9\sqrt{3}+3\sqrt{5}\,(-1+\sqrt{3}))$	$-\frac{1}{2}+\sqrt{3}-\frac{\sqrt{5}}{6}$
$\frac{1}{12}(-27+\sqrt{3}-9\sqrt{5}+\sqrt{15})$	$\frac{1}{12}(5-9\sqrt{3}-3\sqrt{5}\,(1+\sqrt{3}))$	$\frac{1}{6}(-3-6\sqrt{3}-\sqrt{5})$
$\frac{1}{12}(-27-3\sqrt{3}-9\sqrt{5}+\sqrt{15})$	$\frac{1}{12}(9-3\sqrt{3}+\sqrt{5}+3\sqrt{15})$	$\frac{1}{3}-\sqrt{3}\,\tau$
$\frac{1}{4}(-9+\sqrt{3})-\frac{1}{12}\sqrt{5}\,(9+\sqrt{3})$	$\frac{1}{12}(9+3\sqrt{3}+\sqrt{5}-3\sqrt{15})$	$\frac{1}{3}+\sqrt{3}\,\tau$
$\frac{1}{12}(-18-\sqrt{3}+\sqrt{15})$	$\frac{1}{12}(-1-12\sqrt{3}-3\sqrt{5}-6\sqrt{15})$	$\frac{1}{3}(\sqrt{5}-3\sqrt{3}\,\tau)$
$\frac{1}{12}(-18+\sqrt{3}-\sqrt{15})$	$-\frac{1}{12}+\sqrt{3}-\frac{\sqrt{5}}{4}+\frac{\sqrt{15}}{2}$	$\frac{\sqrt{5}}{3}+\sqrt{3}\,\tau$
$\frac{1}{12}(-\sqrt{15}-3\,(6+\sqrt{3}))$	$\frac{1}{12}(-1+6\sqrt{3}-3\sqrt{5})$	$\frac{1}{3}(\sigma^2-3\sqrt{3}\,\tau^2)$
$\frac{1}{12}(-18+3\sqrt{3}+\sqrt{15})$	$\frac{1}{12}(-1-6\sqrt{3}-3\sqrt{5})$	$\frac{\sigma^2}{3}+\sqrt{3}\,\tau^2$

Table 4.2c. Position vectors 12 of atoms obtained by using the generators C_5^2.

$\frac{2x}{b}$	$\frac{2y}{b}$	$\frac{2z}{b}$
$\frac{1}{6}(-\sqrt{15}+9\tau)$	$\frac{1}{6}(\sqrt{5}+9\sqrt{3}\,\tau)$	$\frac{2}{3}$
$\frac{1}{6}(\sqrt{15}+9\tau)$	$\frac{1}{6}(\sqrt{5}-9\sqrt{3}\,\tau)$	$\frac{2}{3}$
$\frac{1}{4}(3-2\sqrt{3}+3\sqrt{5})$	$\frac{1}{6}\sqrt{5}\,(1+3\sqrt{3}\,\tau)$	$-\frac{1}{3}-\sqrt{3}\,\tau$
$\frac{1}{4}(3+2\sqrt{3}+3\sqrt{5})$	$\frac{1}{6}\sqrt{5}\,(1-3\sqrt{3}\,\tau)$	$-\frac{1}{3}+\sqrt{3}\,\tau$
$\frac{1}{12}(18-\sqrt{3}+\sqrt{15})$	$\frac{1}{12}(5-6\sqrt{3}+3\sqrt{5})$	$\frac{\sigma^2}{3}+\sqrt{3}\,\tau^2$
$\frac{1}{12}(18+\sqrt{3}-\sqrt{15})$	$\frac{1}{12}(5+6\sqrt{3}+3\sqrt{5})$	$\frac{1}{3}(\sigma^2-3\sqrt{3}\,\tau^2)$
$\frac{1}{12}(18-3\sqrt{3}-\sqrt{15})$	$\frac{3}{4}+\sqrt{3}-\frac{\sqrt{5}}{12}+\frac{\sqrt{15}}{2}$	$-\frac{1}{3}+\sqrt{3}\,\tau$
$\frac{1}{12}(18+3\sqrt{3}+\sqrt{15})$	$\frac{1}{12}(9-12\sqrt{3}-\sqrt{5}-6\sqrt{15})$	$-\frac{1}{3}-\sqrt{3}\,\tau$
$\frac{1}{12}(27-\sqrt{3}+9\sqrt{5}-\sqrt{15})$	$\frac{1}{12}(-1+3\sqrt{3}+3\sqrt{5}-3\sqrt{15})$	$\frac{\sqrt{5}}{3}+\sqrt{3}\,\tau$
$\frac{1}{12}(27+\sqrt{3}+9\sqrt{5}+\sqrt{15})$	$\frac{1}{12}(-1-3\sqrt{3}+3\sqrt{5}\,(1+\sqrt{3}))$	$\frac{1}{3}(\sqrt{5}-3\sqrt{3}\,\tau)$
$\frac{1}{12}(27-3\sqrt{3}+9\sqrt{5}+\sqrt{15})$	$\frac{1}{12}(-1-9\sqrt{3}+3\sqrt{5}-3\sqrt{15})$	$\frac{1}{6}(-3-6\sqrt{3}-\sqrt{5})$
$\frac{1}{12}(27+3\sqrt{3}+9\sqrt{5}-\sqrt{15})$	$\frac{1}{12}(-1+9\sqrt{3}+3\sqrt{5}\,(1+\sqrt{3}))$	$-\frac{1}{2}+\sqrt{3}-\frac{\sqrt{5}}{6}$

Table 4.2d. Position vectors of 15 atoms obtained by using the generators C_2.

$\frac{2x}{b}$	$\frac{2y}{b}$	$\frac{2z}{b}$
-3τ	$-\frac{\sqrt{5}}{3}$	$\frac{2}{3}$
-3τ	$\frac{\sqrt{5}}{3}$	$-\frac{2}{3}$
$\frac{1}{6}(-\sqrt{15}-9\tau)$	$\frac{1}{6}(-1-3\sqrt{15}\,\tau)$	$-\frac{\sqrt{5}}{3}+\sqrt{3}\,\tau$
$\frac{1}{6}(\sqrt{15}-9\tau)$	$\frac{1}{6}(-1+3\sqrt{15}\,\tau)$	$-\frac{\sqrt{5}}{3}-\sqrt{3}\,\tau$
$\frac{1}{4}(-3-2\sqrt{3}-3\sqrt{5})$	$\frac{1}{2}(1-3\sqrt{3}\,\tau)$	0
$\frac{1}{4}(-3+2\sqrt{3}-3\sqrt{5})$	$\frac{1}{2}(1+3\sqrt{3}\,\tau)$	0
3τ	-1	0
$\frac{1}{12}(-27-\sqrt{3}-\sqrt{5}\,(9+\sqrt{3}))$	$\frac{1}{12}(-5-9\sqrt{3}+3\sqrt{5}-3\sqrt{15})$	$\frac{1}{3}(-3\sqrt{3}+\tau^2)$
$\frac{1}{12}(-27+\sqrt{3}-9\sqrt{5}+\sqrt{15})$	$\frac{1}{12}(-5+9\sqrt{3}+3\sqrt{5}\,(1+\sqrt{3}))$	$\sqrt{3}+\frac{\tau^2}{3}$
$\frac{1}{12}(-27-3\sqrt{3}-9\sqrt{5}+\sqrt{15})$	$\frac{1}{12}(-9+3\sqrt{3}-\sqrt{5}-3\sqrt{15})$	$-\frac{1}{3}+\sqrt{3}\,\tau$
$\frac{1}{4}(-9+\sqrt{3})-\frac{1}{12}\sqrt{5}\,(9+\sqrt{3})$	$\frac{1}{12}(-3\,(3+\sqrt{3})+\sqrt{5}\,(-1+3\sqrt{3}))$	$-\frac{1}{3}-\sqrt{3}\,\tau$
$\frac{1}{12}(18-\sqrt{3}+\sqrt{15})$	$\frac{1}{12}(-5+6\sqrt{3}-3\sqrt{5})$	$\frac{1}{6}(-3-9\sqrt{3}+\sqrt{5}-3\sqrt{15})$
$\frac{1}{12}(18+\sqrt{3}-\sqrt{15})$	$\frac{1}{12}(-5-6\sqrt{3}-3\sqrt{5})$	$\frac{1}{6}(-3+9\sqrt{3}+\sqrt{5}+3\sqrt{15})$
$\frac{1}{12}(18-3\sqrt{3}-\sqrt{15})$	$\frac{1}{12}(-9-12\sqrt{3}+\sqrt{5}-6\sqrt{15})$	$\frac{1}{3}-\sqrt{3}\,\tau$
$\frac{1}{12}(18+3\sqrt{3}+\sqrt{15})$	$\frac{1}{12}(-9+12\sqrt{3}+\sqrt{5}+6\sqrt{15})$	$\frac{1}{3}+\sqrt{3}\,\tau$

Since molecular orbitals of the C_{60} molecule has p_z character, where p_z is a 2p orbital pointing radially out of the spherical molecule from the atom where it is centered, the molecular orbital calculations are independent from ξ. It is observed that ξ affects the Hückel energy levels. It will be chosen that ξ is taken into consideration during the construction of Hückel Hamiltonian. The placements of the 60 atoms in the site are given in Table 4.3.

Table 4.3. Nearest-neighbours atoms in C_{60} molecule. (D) indicates double bond between atoms and (S) indicates single bond between two atoms.

Atom In a site	Nearest-neighbour three atoms	Atom in a site	Nearest-neighbour three atoms	Atom in a site	Nearest-neighbour three atoms
1	12(D), 57(S), 58(S)	21	33(D), 28(S), 43(S)	41	35(D), 8(S), 24(S)
2	16(D), 45(S), 46(S)	22	44(D), 24(S), 47(S)	42	55(D), 37(S), 57(S)
3	52(D), 48(S), 38(S)	23	27(D), 17(S), 48(S)	43	31(D), 7(S), 21(S)
4	53(D) ,32(S), 26(S)	24	26(D), 22(S), 41(S)	44	22(D), 6(S), 20(S)
5	51(D), 34(S), 33(S)	25	36(D), 13(S), 55(S)	45	7(D), 2(S), 18(S)
6	56(D),44 (S), 39(S)	26	24(D), 4(S), 56(S)	46	19(D), 2(S), 8(S)
7	45(D),43 (S),40 (S)	27	23(D), 20(S), 39(S)	47	10(D), 8(S), 22(S)
8	46(D), 41(S),47 (S)	28	38(D), 20(S), 40(S)	48	50(D), 3(S), 23(S)
9	40(D), 15(S), 16(S)	29	60(D), 12(S), 50(S)	49	37(D), 36(S), 53(S)
10	47(D), 14(S),16(S)	30	59(D), 50(S), 59(S)	50	48(D), 30(S), 54(S)
11	19(D), 35(S), 36(S)	31	43(D), 13(S), 51(S)	51	5(D), 31(S), 55(S)
12	1(D), 29(S), 30(S)	32	58(D), 4(S), 60(S)	52	3(D), 33(S), 59(S)
13	18(D), 25(S), 31(S)	33	21(D), 5(S), 52(S)	53	4(D), 35(S), 49(S)
14	20(D), 10(S), 15(S)	34	57(D), 5(S), 59(S)	54	39(D), 29(S), 50(S)
15	17(D), 9(S), 17(S)	35	41(D), 11(S), 53(S)	55	42(D), 25(S), 51(S)
16	2(D), 9(S), 10(S)	36	25(D), 11(S), 49(S)	56	6(D), 26(S), 60(S)
17	15(D), 23(S), 38(S)	37	49(D), 42(S), 58(S)	57	34(D), 1(S), 42(S)
18	13(D),19 (S), 45(S)	38	28(D), 3(S), 17(S)	58	32(D), 1(S), 37(S)
19	11(D), 18(S), 46(S)	39	54(D), 27(S), 56(S)	59	30(D), 34(S), 52(S)
20	14(D), 27(S), 44(S)	40	9(D), 7(S), 28(S)	60	29(D), 32(S), 56(S)

4.1.2 Projection Operators and Molecular Orbitals

It is known that the molecular orbitals can be constructed by the use of projection operators. The simplest form of the projection operator is given by

$$P_{ij} = \frac{1}{N}\sum_{i,j}^{n} D_{ij}^{\alpha} \tag{4.2}$$

where N is normalization constant and n is the dimension of irreducible representation. D^{α} is the matrix elements of the irreducible representation α. As pointed out in previous chapter the character table is not enough to form projection operators and that a knowledge of the matrices of the representations is needed. The 60 dimensional matrix generators found from the relation

$$B_{ij} = D^{3}\vec{r}_i = \vec{r}_j \quad (i,j=1,2,\ldots,60) \tag{4.3}$$

Eqn(4.3) is read as follows. The 3-D irreducible representation is applied on to position vector $\vec{r}_i$ and it projects the vector $\vec{r}_j$. If D^3 projects the vector into itself B_{ij} takes the value one otherwise its value is zero.

In this work the projection operators are derived for icosahedral group which is useful to construct molecular orbitals. In constructing the molecular orbitals projection operators are applied on atomic orbitals. It is easy to compute the atomic orbitals by using the relation given Eqn.(4.3). Let us calculate atomic orbital $\psi(\Gamma_i)$ which transform according to the irreducible representation Γ_i, then the relation

$$\psi(\Gamma_i) = P_{ij}^{n}\phi_1 \tag{4.4}$$

gives us molecular orbitals.

4.2. CONSTRUCTION OF HUCKEL HAMILTONIAN

It is well known that, each carbon atom is bonded to three neighbour atom with two single and one double bond. To construct the Hückel Hamiltonian matrix, coulomb interactions of one atom with other two neighbour bonded atoms are only considered. Interactions between unbonded atoms are negligibly small and they are taken into account as zero.

Before we begin to build up Hückel Hamiltonian, energy level must be classified. Decomposition of the characters of 60 dimensional site matrices B classifies the energy values. The character of 60 dimensional site matrices and character table of icosahedral group are given in Table 4.1. Decomposition of χ_{site} in terms of irreducible representations are given as

$$\chi_{site} = A_g + (T_{1g} + 2T_{1u}) + (T_{2g} + 2T_{2u}) + (2G_g + 2G_u) + (3H_g + 2H_u) \qquad (4.5)$$

The last equation shows that C_{60} molecule has 16 different energy states.

The Hückel Hamiltonian can be constructed by using molecular orbitals $\psi(\Gamma_i)$, using the relation

$$(H_{Hückel})_{ij} = \langle \psi(\Gamma_i) | H | \psi(\Gamma_j) \rangle \quad (i,j=1,\ldots,16) \qquad (4.6)$$

It is obvious that Hückel Hamiltonian is in the block diagonal form:

$$16 = 1+3+3'+4+5 \qquad (4.7)$$

Computer program to find the projection operator is given in Appendix C and computed results are in Appendix D.

4.3. MOLECULAR ENERGY LEVEL OF C_{60} MOLECULE

It is known that energy expectation value of i^{th} state of a molecule is given by

$$\begin{aligned} E_i &= \langle \psi_i | H | \psi_i \rangle \\ &= N_i^2 \left[c_i^2 \langle \phi_j | H | \phi_j \rangle + c_{ij} c_{ik} \langle \phi_j | H | \phi_k \rangle \right] \\ &= \alpha + 2N_i^2 c_{ij} c_{ik} \langle \phi_j | H | \phi_k \rangle \end{aligned} \tag{4.8}$$

where $\alpha = \langle \phi_j | H | \phi_j \rangle$ and N_i, c_{ij} are scalar coefficients. According to the Hückel approximation, in evaluating E_i any integral form $\langle \phi_j | H | \phi_k \rangle$ in Eqn(4.8) can be neglected, if ϕ_j and ϕ_k refer to non-adjacent atoms. As mentioned above, for C_{60} molecule each atom is bonded to three-neighbourhood atom with two single bonds and one double bond. Length of the edge between two hexagon (double bond) is approximately r_1= 1.391 A, and length of edge between a hexagon and pentagon (single bond) is r_2=1.455 A [57]. In this case, the interaction between further atoms is neglected ,so that

$$\langle \phi_j | H | \phi_k \rangle = \begin{cases} \gamma \text{ for double bond} \\ \beta \text{ for sin gle bond} \end{cases} \tag{4.9}$$

where β and γ are the strength of interaction between single and double bonded atoms. We assume that β and γ are related by

$$\gamma = (1+\xi)\beta \tag{4.10}$$

The matrix elements of the Hückel Hamiltonian computed by using Eqn.(4.9) should be blockdiagonal form as we mentioned before. For singlet level energy value is found as

$$E_{A_g} = -3\beta . \tag{4.11}$$

The matrices of each block and corresponding eigenvalues, which give energy levels, are as follows:

$$H_{T_1}=\beta\begin{pmatrix}\frac{1}{2}(3+\sqrt{5}) & \frac{1}{\sqrt{3}} & \frac{-3+\sqrt{5}}{2\sqrt{3}}\\ \frac{1}{\sqrt{3}} & \frac{1}{6}(-7+3\sqrt{5}) & \frac{1}{6}(-3+\sqrt{5})\\ \frac{-3+\sqrt{5}}{2\sqrt{3}} & \frac{1}{6}(-3+\sqrt{5}) & -\frac{1}{3}\end{pmatrix} \qquad (4.12)$$

$$\begin{aligned}E_{T_{1g'}} &= \frac{1}{2}(3-\sqrt{5})\beta\\ E_{T_{1u'}} &= \frac{1}{4}(3-\sqrt{5}+\sqrt{38+2\sqrt{5}})\beta\\ E_{T_{1u}} &= \frac{1}{4}(3+\sqrt{5}-\sqrt{38+2\sqrt{5}})\beta\end{aligned} \qquad (4.13)$$

.

$$H_{T_2}=\beta\begin{pmatrix}\frac{1}{2}(3-\sqrt{5}) & \frac{-3+\sqrt{5}}{4\sqrt{3}} & -\frac{2}{\sqrt{3}}\\ \frac{-3+\sqrt{5}}{4\sqrt{3}} & \frac{1}{12}(-7-3\sqrt{5}) & \frac{1}{3}(3+\sqrt{5})\\ -\frac{2}{\sqrt{3}} & \frac{1}{3}(3+\sqrt{5}) & \frac{1}{3}\end{pmatrix} \qquad (4.14)$$

$$\begin{aligned}E_{T_{2g'}} &= \frac{1}{2}(3+\sqrt{5})\beta\\ E_{T_{2u'}} &= \frac{1}{4}(3+\sqrt{5}+\sqrt{38+2\sqrt{5}})\beta\\ E_{T_{2u}} &= \frac{1}{2}(+3+\sqrt{5}-\sqrt{38+2\sqrt{5}})\beta\end{aligned} \qquad (4.15)$$

.

$$H_G=\beta\begin{pmatrix}\frac{4}{3} & -\frac{1}{2}\sqrt{\frac{5}{3}} & \frac{\sqrt{5}}{6} & 0\\ -\frac{1}{2}\sqrt{\frac{5}{3}} & -2 & -\frac{1}{\sqrt{3}} & \frac{1}{2}\\ -\frac{\sqrt{5}}{6} & -\frac{1}{\sqrt{3}} & \frac{2}{3} & -\frac{\sqrt{3}}{2}\\ 0 & \frac{1}{2} & -\frac{\sqrt{3}}{2} & -2\end{pmatrix} \qquad (4.16)$$

$$
\begin{aligned}
E_{G_{g'}} &= 2\beta \\
E_{G_g} &= -\beta \\
E_{G_{u'}} &= \frac{1}{2}(1+\sqrt{17})\beta \\
E_{G_u} &= \frac{1}{2}(1-\sqrt{17})\beta
\end{aligned}
\tag{4.17}
$$

.

$$
H_H = \beta \begin{pmatrix}
\frac{1}{18}(23+3\sqrt{5}) & \frac{1}{3\sqrt{3}} & -\frac{1}{3}\sqrt{\frac{5}{3}} & \frac{1}{9}(-3+2\sqrt{5}) & -\frac{1+3\sqrt{5}}{6\sqrt{3}} \\
\frac{1}{18}(23+3\sqrt{5}) & \frac{1}{6}(-3+\sqrt{5}) & -\frac{1}{3} & -\frac{1}{3}\sqrt{\frac{5}{3}} & \frac{1}{6}(-3-\sqrt{5}) \\
-\frac{1}{3}\sqrt{\frac{5}{3}} & -\frac{1}{3} & \frac{1}{6}(-3-\sqrt{5}) & \frac{5}{3\sqrt{3}} & \frac{1}{6}(-3+\sqrt{5}) \\
\frac{1}{9}(-3+2\sqrt{5}) & -\frac{1}{3}\sqrt{\frac{5}{3}} & \frac{5}{3\sqrt{3}} & \frac{1}{18}(7-3\sqrt{5}) & \frac{-3+\sqrt{5}}{6\sqrt{3}} \\
\frac{1+3\sqrt{5}}{6\sqrt{3}} & \frac{1}{6}(-3-\sqrt{5}) & \frac{1}{6}(-3+\sqrt{5}) & \frac{-3+\sqrt{5}}{6\sqrt{3}} & \frac{1}{3}
\end{pmatrix}
\tag{4.18}
$$

$$
\begin{aligned}
E_{H_u} &= \frac{1}{2}(1-\sqrt{5})\beta \\
E_{H_{u'}} &= \frac{1}{2}(1+\sqrt{5})\beta \\
E_{H_{g1}} &= -\beta \\
E_{H_{g'}} &= \frac{1}{2}(-1+\sqrt{13})\beta \\
E_{H_{g_2}} &= \frac{1}{2}(-1-\sqrt{13})\beta
\end{aligned}
\tag{4.19}
$$

.

As we mentioned before, in order to investigate the effect of ξ we will build up the Hückel Hamiltonian in a different way. The block matrices for in terms of γ and β are given in Appendix E. The fitting procedure shows that ξ has a range between 1/100 and 1/50. The energies are measured here in units of given β, the usual nearest-neighbour orbital overlap parameter, and are given for each ξ value in Table 4.4.

Table 4.4. The energy values for different ξ values. (') indicates the antibonding energy levels

$\xi=0$	$\xi=\frac{1}{50}$	$\xi=\frac{1}{75}$	$\xi=\frac{1}{100}$
$E_{A_g}=-3\beta$	$E_{A_g}=-3.04\beta$	$E_{A_g}=-3.026\beta$	$E_{A_g}=-3.02\beta$
$E_{T_{1g}}=0.381\beta$ $E_{T_{1u}}=0.138\beta$ $E_{T_{1u}}=-2.618\beta$	$E_{T_{1g}}=0.394\beta$ $E_{T_{1u}}=0.153\beta$ $E_{T_{1u}}=-2.719\beta$	$E_{T_{1g}}=0.390\beta$ $E_{T_{1u}}=0.148\beta$ $E_{T_{1u}}=-2.731\beta$	$E_{T_{1g}}=0.388\beta$ $E_{T_{1u}}=0.146\beta$ $E_{T_{1u}}=-2.738\beta$
$E_{T_{2g}}=2.618\beta$ $E_{T_{2u}}=-1.820\beta$ $E_{T_{2u}}=1.438\beta$	$E_{T_{2g}}=2.585\beta$ $E_{T_{2u}}=-1.786\beta$ $E_{T_{2u}}=1.411\beta$	$E_{T_{2g}}=2.596\beta$ $E_{T_{2u}}=-1.797\beta$ $E_{T_{2u}}=1.420\beta$	$E_{T_{2g}}=2.601\beta$ $E_{T_{2u}}=-1.803\beta$ $E_{T_{2u}}=1.425\beta$
$E_{G_g}=2\beta$ $E_{G_g}=-\beta$ $E_{G_u}=2.561\beta$ $E_{G_u}=-1.561\beta$	$E_{G_g}=1.973\beta$ $E_{G_g}=-0.993\beta$ $E_{G_u}=2.529\beta$ $E_{G_u}=-1.549\beta$	$E_{G_g}=1.982\beta$ $E_{G_g}=-0.995\beta$ $E_{G_u}=2.540\beta$ $E_{G_u}=-1.553\beta$	$E_{G_g}=1.986\beta$ $E_{G_g}=-0.996\beta$ $E_{G_u}=2.545\beta$ $E_{G_u}=-1.555\beta$
$E_{H_g}=1.302\beta$ $E_{H_{g1}}=-\beta$ $E_{H_u}=1.618\beta$ $E_{H_{g2}}=-0.618\beta$ $E_{H_u}=-2.302\beta$	$E_{H_g}=1.277\beta$ $E_{H_{g1}}=-0.986\beta$ $E_{H_u}=1.594\beta$ $E_{H_{g2}}=-0.614\beta$ $E_{H_u}=-2.270\beta$	$E_{H_g}=1.285\beta$ $E_{H_{g1}}=-0.991\beta$ $E_{H_u}=1.602\beta$ $E_{H_{g2}}=-0.615\beta$ $E_{H_u}=-2.281\beta$	$E_{H_g}=1.290\beta$ $E_{H_{g1}}=-0.993\beta$ $E_{H_u}=1.606\beta$ $E_{H_{g2}}=-0.616\beta$ $E_{H_u}=-2.286\beta$

Molecular energy level diagram for $\xi=0$ is shown in Figure 4.1. The change in the molecular energy level diagram with respect to ξ is given in Figure 4.2.

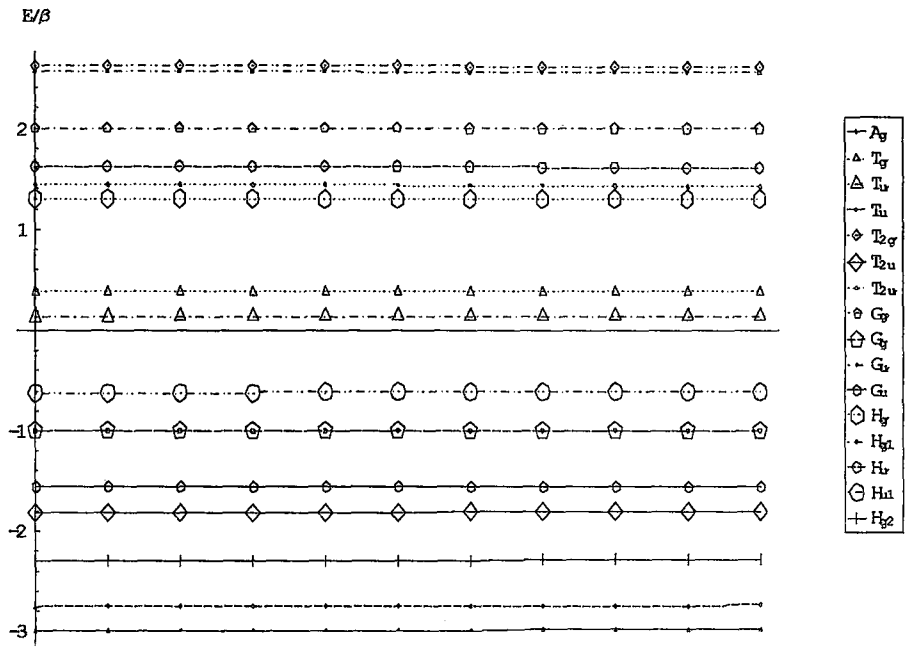

Figure 4.1. Molecular energy level diagram of C_{60} molecule.

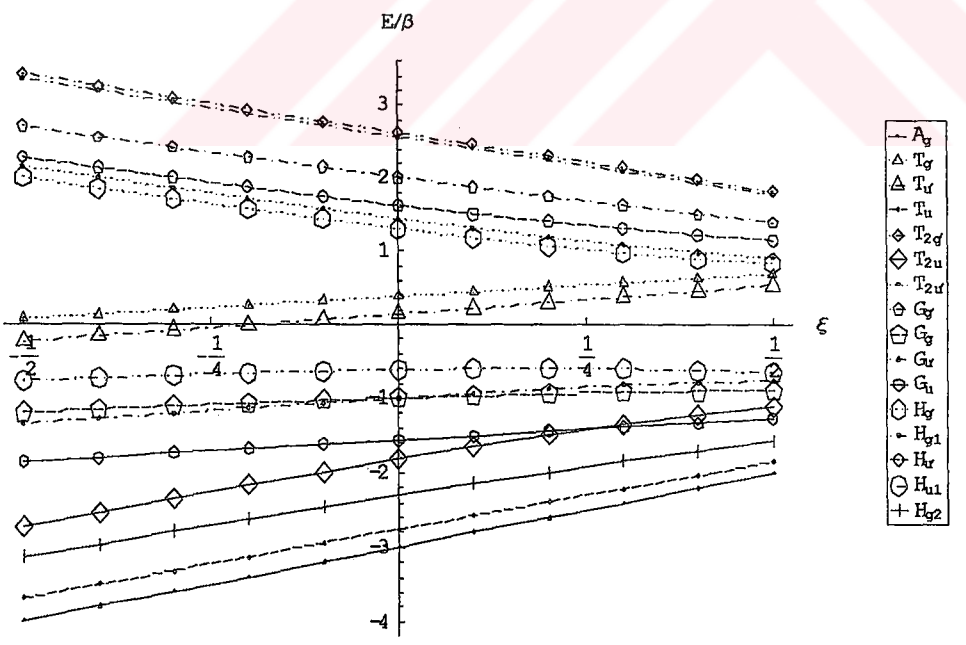

Figure 4.2. Deviation of molecular energy level with respect to ξ.

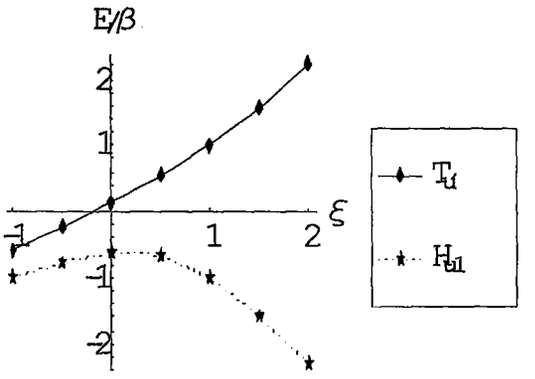

Figure 4.3. Energy gap between E_{T_u} (LUMO) level and $E_{H_{u1}}$ (HOMO) level.

The energy gap between highest occupied molecular orbital (HOMO) and lowest unoccupied molecular orbital is found approximately to be 0.8 E/β (see Figure 4.3).

4.4. CONCLUDING REMARKS

A Hückel molecular orbital model for the electronic states of C_{60} might provide a better starting point than does the band model for discussing the optical properties of C_{60}. According to the molecular approach, many electron-orbitals for the valence and conduction electron states are constructed for the π electrons on the C_{60} molecule. The lower lying σ orbitals are filled and are not generally probed by optical experiments. In relating the icosahedral levels to those of full rotational symmetry, we note that 50 π electrons fully occupy the angular momentum states through ℓ=4, and the remaining 10 electrons are available to start filling the ℓ=5 state.

In full spherical symmetry, the ℓ=5 state can accommodate 22 electrons, and the splitting of the ℓ=5 state in icosahedral symmetry is into the $H_u+T_{1u}+T_{2u}$ irreducible representations. According to the Figure 4.1, energy level that is completely filled by the 10 electrons is H_u (nondegenerate). Neglecting any thermal excitation, the two threefold T_{1u} and T_{2u} are empty.

To obtain the energy levels coordinates of 60 atoms and projection operators the symmetry mechanism is used . They are not given in literature before. Projection

operators are used to blockdiagonalize the Hückel matrix. Energy values are in agreement with literature [7,53,54].

The ratio of double and single bond lengths affect the molecular energy level and it is argued that from the Figure 4.2 alternation constant must be in the range between 1/50 and 1/100. To get optimum result ξ is taken as 0.015 as also predicted from the length of each bond given above. If 60 electrons are available in complex for establishment of the bond, we can put two electrons in each molecular orbital, starting from one lower in energy.

CHAPTER 5

A FORCE CONSTANT MODEL FOR VIBRATIONAL MODES OF C_{60}

The vibrational frequencies and modes of a molecule are strictly dynamic properties. Every molecule, at all temperatures, including even the absolute zero, is continually executing vibrational motions, that is, motions in which its distances and internal angles change periodically without producing any net translation of centre of mass of the molecule or imparting any net angular momentum (rotatory motion) to the molecule. The complex, random, and seemingly a periodic internal motion of a vibrating molecule are the result of the superposition of a number of relatively simple vibratory motions known as the normal vibrations or normal modes of vibration of the molecule. Each of these has its own frequency. Naturally, then, when many of them are superposed, the resulting motion must also be periodic.

The normal modes for C_{60} can be clearly subdivided into two main categories; one has a frequency range of 25-200 meV which consists of intramolecular modes associated with the internal vibrations of C_{60} molecule and the other has a frequency range 0-25 meV which consists of librational modes with rigid rotation of C_{60} molecule and intermolecular (between C_{60}- C_{60}) vibrational modes. Theories which attribute the superconductivity to electron-phonon coupling may be classified into two groups according to which group of phonons intermolecular or intramolecular modes is regarded to be important. Even if restricting to theories in which intramolecular modes are considered to be important, there is not general agreement yet with respect to which phonons might be most important. It is well known that the coupling between intra and inter–molecular motions is rather weak so what is discovered for molecule should be approximately valid for solid.

Although there are 180 degrees of freedom (3×60) for each C_{60} molecule, the icosahedral symmetry gives rise to a number of degenerate modes, so that only 46 distinct, mode frequencies are expected for the C_{60} molecule. Experimental information on vibrational frequencies has been provided from inelastic neutron-scattering measurement and high-resolution electron-energy-loss spectroscopy [25-29]. Several calculations of vibrational frequencies for C_{60} were reported by a number of authors. Because the vibration problem requires the diagonalization of 180×180 matrix with elements which are functions of the force constants, vibrational eigenfrequencies of C_{60} have been computed only numerically for several choices of the spring constants. In many force constant models, only bond stretching force constants between nearest neighbour atoms have been considered, in addition to angle bending force constants. In such models many of the frequencies could not be reproduced with any reasonable accuracy, and different models that fit the same data give widely different values for interatomic force constants.

In this thesis, a model that includes Keating parameters and force constants between the further than nearest neighbour atoms for vibrational frequencies of isolated C_{60} is proposed. The effect of bonded and unbonded atoms to analyse the normal frequencies of C_{60} is discussed. One of the motivations for this work is to investigate the effect of the force constants between unbonded atoms in C_{60}. In many models those were not taken into consideration, many normal frequencies did not appear.

This chapter is organised as follows: In section 1, a group theoretical analysis to determine the normal modes of C_{60} are presented. In section 2, normal modes of vibration of C_{60} are calculated and listed by constructing a simple model. Finally, the effect of force constants between bonded and unbonded atoms is discussed and our results are compared with the experimental and some theoretical results.

5.1. GROUP THEORY OF THE VIBRATIONAL STRUCTURE OF C_{60}

Most molecules present a symmetry that can be described by a group G of symmetry operations. The kinetic and potential energies of the molecule should be invariant under the symmetry operation of the group G. Symmetry can frequently be used to

deduce the qualitative appearance of normal modes, without solving the vibrational secular equation. It is known that normal mode frequencies of C_{60} are qualitatively analysed by using symmetries associated with the corresponding irreducible representation of point group I_h.

Table 5.1. The characters of 180×180 matrices.

I_h	E	$12C_5$	$12C_5^2$	$20C_3$	$15C_2$	I	$12S_{10}$	$12S_{10}^3$	$20S_6$	15σ
Γ_{180}	180	0	0	0	0	0	0	0	0	4

The site symmetry for an isolated C_{60} molecule can be found in Chapter 4. We consider a radial vector r_i from the centre of C_{60} molecule to i^{th} atom in a site. The vibrational modes are qualitatively classified in a usual way such that direct product of 60×60 matrices which are obtained from site symmetry with the 3 dimensional matrix generators given in Appendix B gives 180×180 matrix generators of the group I_h. Conjugacy classes, Γ_{180}, of 180×180 reducible representations are given in the Table 5.1. Decomposition of reducible representation Γ_{180} in terms of irreducible representation specifies the vibrational modes and is found using the Eqn.(3.9), such that

$$\Gamma_{180}= 2A_g+4T_{1g}+4T_{2g}+6G_g+8H_g+A_u+5T_{1u}+5T_{2u}+6G_u+7H_u \qquad (5.1)$$

The six degrees of freedom associated with the translations, T_{1u}, and rotations, T_{1g} must be subtracted from Γ_{180} to classify the vibrational modes

$$\Gamma_{vib}= 2A_g+3T_{1g}+4T_{2g}+6G_g+8H_g+A_u+4T_{1u}+5T_{2u}+6G_u+7H_u \qquad (5.2)$$

It is shown that, there are 174 degrees of freedom for isolated C_{60} molecule; a number of them is degenerate due to high symmetry. So that 46 distinct mode frequencies are appearing for the C_{60} molecule in Eqn (5.2). The first-order Raman active modes are even under inversion and belong to the nondegenerate A_g and fivefold H_g representations, while the infrared active modes are of odd parity and belong to the threefold degenerate T_{1u} representation. For C_{60} molecule, A_g is realized twice, H_g occurs eight times, and T_{1u} occurs four times. Thus an isolated C_{60} molecule has four threefold degenerate infrared-active T_{1u} modes, two nondegenerate

first-order Raman-active A_g modes, and eight fivefold degenerate Raman-active H_g modes. The remaining thirty-two frequencies correspond to silent modes.

5.2. DESCRIPTION OF THE MODEL

It is instructive to review briefly a few models that have been applied to diamond and graphite. The models that have been constructed for diamond and graphite which are also carbon complexes, give us some information during the construction of a model for C_{60} molecule. There have been many publications on the dynamical properties of the C_{60} molecule. These include emprical, quantum chemical, and some first principles calculations[24-28]. Different models, which fit the same data reasonably well, give widely different values for the interatomic force constants. Some force constant models include only bond-stretching force constants between two bonded atoms and bending force constants. But it is apparent that the interaction beyond nearest neighbours should be included to obtain the normal mode frequencies with a reasonable accuracy. It is generally the case that the force constant models considered so far that in addition to angle bending force constants for bonds connecting nearest-neighbour atoms have been considered. Such models could not produce all of the 46 modes of vibrations. The models should include further neighbour force constants than nearest-neighbour force constants. In our approach, each atom in the C_{60} is assumed to be a point mass, and they are connected with springs. To determine the dynamical matrix we start by writing the molecular energy. In the Harmonic approximation the molecular energy can be written in the form

$$V = \sum_{i=1}^{N} \sum_{j=i+1}^{N} \frac{\alpha_{ij}}{2} [(\vec{u}_i - \vec{u}_j) \cdot \hat{r}_{ij}]^2 \qquad (5.3)$$

where u_i is the small displacement of i^{th} carbon atom about its equilibrium position along the x_i, y_i, and z_i directions, $\hat{r}_{ij}$ is the unit vector of $\hat{r}_i - \hat{r}_j$ and α_{ij} is the force constant between i^{th} and j^{th} atoms in a C_{60} molecule. The potential of Keating type employed for the C_{60} molecule can be written in the form

$$V=\sum_{i=1}^{N}\sum_{j=i+1}^{N}\frac{\alpha_{ij}}{2}[(\vec{u}_i-\vec{u}_j)\cdot\hat{r}_{ij}]^2+\frac{\beta}{2}\sum_{i=1}^{N}\sum_{j=i+1}^{N}\sum_{k=j+1}^{N}[(\vec{u}_i-\vec{u}_j).\hat{r}_{ik}+(\vec{u}_k-\vec{u}_i)\cdot\hat{r}_{jk}]^2 \quad (5.4)$$

where β can be considered as the angle bending force constant. In Eqn.(5.4) the summations are taken over all neighbour pairs, so that the value of N is 60. It is obvious that the potential equation includes 60 single bonds and 30 double bonds and 1770 different force constants α_{ij}, except that angle bending force constant β. We have carried out a calculation of the vibrational modes for C_{60} considering the effects of the interactions up to ten neighbours. It is observed that the Harmonic approximation does not produce all vibrational modes. Our model consists of the Keating type potential in addition to Harmonic potential. If any two or more atoms are interchanged by carrying out a symmetry operation on the system, the energy of the system must be unchanged. A symmetry operation carries the system into an equivalent configuration, which is by definition, physically indistinguishable from the original configuration. Since the potential energy and kinetic energy of the C_{60} are separately invariant under symmetry operation, then we can write

$$R_{ij}V=V \quad (5.5)$$

where R_{ij}'s are the 180×180 reducible matrix generators (symmetry operator) of the I_h group. The potential energy can be simplified and number of force constants can be determined from the symmetry operation in Eqn.(5.5). After performing a few calculations, we obtain only 23 different radial force constants of which two of bonded and the remaining 21 are unbonded force constants. Dynamical matrix is obtained from the potential energy given in Eqn.(5.4), such as

$$\Phi(ij)=\frac{\partial^2 V}{\partial u_i \partial u_j} \qquad (i=1,2.....180) \text{ and } (j=1,2...180) \quad (5.6)$$

The force constants we use in these calculations are described as follows: each atom is assumed to be point mass and to be connected by springs. As we mentioned before two springs, with spring constants α_1 and α_2, are used to model the stretching of the pentagonal and hexagonal covalent bonds, respectively. The bending of the angles between the spring connecting an atom to its first nearest neighbour is modelled by

spring constants β. The force constants of the springs connecting an atom to its tenth nearest neighbours are taken into consideration.

Table 5.2. Symmetry vectors associated to the irreducible representations A_g and A_u.

Γ	Symmetry Vector ($x_1,y_1,z_1,;x_2,y_2,z_2$.....x_{60},y_{60},z_{60})
A_g	{0,0,4; τ,-σ,-2; 0,0,-4; τ,-σ,2; -τ,-σ,2; 2,-τ, σ; -τ,-σ,-2; -τ,σ,2; -2,-τ, -σ; -τ,σ,-2; τ,σ,-2; 2,-τ, -σ; τ,-σ,2; -2,τ, -σ; -2,-τ, σ; -σ,-2,τ; 2,τ, σ; -σ,-2,-τ; σ,-2,-τ; -2,τ, σ; σ,-2,τ; -σ,2,-τ; 2,τ, -σ; 0,-4,0; -σ,2,τ; σ,2,τ; 0,-4,0; -4,0,0; -σ,2,-τ; -4,0,0; 4,0,0; σ,-2,-τ; 4,0,0; 0,4,0; -σ,-2,τ; σ,-2,-τ; 0,4,0; -2,-τ,-σ; -σ,-2,-τ; -σ,2,τ; 2,-τ, σ; -σ,2,τ; σ,2,-τ; -2,-τ, σ; σ,2,τ; 2,τ, σ; 2,-τ, -σ; -τ,-σ,2; -2,τ, -σ; -τ,-σ,-2; τ,-σ,-2; 2,τ, -σ; 2,τ,-σ; τ,-σ,2; τ,σ,-2; -2,τ, σ; τ,σ,2; 0,0,-4; -τ,σ,-2; 0,0,4}/8√15 {0,-4,0; -2,-τ,-σ; 0,-4,0; -2,-τ,σ; 2,-τ,σ; -σ,-2,-τ; 2,-τ,-σ; -2,-τ,-σ; σ-2,τ; -2,-τ,σ; 2,-τ,σ; -σ,2,τ; 2,-τ, σ; -σ,-2,-τ; σ,-2,-τ; -τ,-σ,-2; σ,-2,τ; -τ,-σ,2; ,τ,-σ,2; -σ,-2,τ; τ,-σ,-2; -τ, -σ,-2; σ,-2,-τ; -4,0,0; τ,-σ,2; -τ,-σ,2; 4,0,0; 0,0,-4; τ,-σ,2; 0,0,4; 0,0,4; -τ,σ,-2; 0,0,-4; -4,0,0; τ,σ,2; -τ,σ,2; 4,0,0; -σ,2,-τ; τ,σ,-2; -τ,σ,-2; σ,2,τ; -τ,σ,2; τ,σ,2; -σ,2,τ; τ, σ,-2; -σ,2,-τ; σ,2,-τ; -2,τ, -σ; σ,2,τ; -2,τ,σ; 2,τ,σ; -σ,2,τ; 2,τ,-σ; -2,τ,-σ; σ,2,-τ; -2,-τ,σ; 0,4,0; 2,τ,-σ; 0,4,0}/8√15
A_u	{4,0,0; -σ,2-τ; -4,0,0; σ,-2,-τ; σ,2,τ,; τ, σ,-2; -σ,-2,τ; σ,-2,τ; -τ, σ,2; -σ,2,τ; -σ,-2,-τ; -τ, -σ,-2; σ,2,-τ; -τ, -σ,2; τ,- σ,2; 2,-τ,-σ; τ,- σ;-2; -2,τ, -σ; -2,-τ, σ; τ, σ,2; 2,τ; σ; -2,τ σ; -τ, σ,-2; 0,0,-4; 2,τ,- σ; 2,-τ, σ; 0,0,4; 0,-4,0; -2,-τ, -σ; 0,4,0; 0,-4,0; 2,τ, -σ; 0,4,0; 0,0,4; -2,τ, σ; -2,-τ,- σ; 0,0,-4; τ,-σ,-2; 2,-τ, σ; -2,-τ, σ; -τ,- σ,2; 2,τ, σ; 2,-τ,- σ; -τ, σ,-2; -2,τ,- σ; -τ, σ,2; τ, σ,2; - σ, -2,-τ; τ, σ,-2; σ,2,-τ; σ,-2,τ; τ, -σ,2; - σ,2,τ; σ,2,τ; -τ,-σ,-2; - σ,-2,τ; σ,2,-τ; 4,0,0; σ,-2,-τ,σ; -4,0,0}/8√15

Eigenvalues of the dynamical matrix Φ of size 180×180 corresponds to the vibrational frequencies $m\omega^2$ of the C_{60}. The matrix Φ is block-diagonalized by using symmetry vectors. Eigenvalues of each block matrix gives vibrational eigenvalues for corresponding irreducible representation. The symmetry vectors belonging to the i^{th} irreducible representation can be obtained by the projection method. In this work, calculations of the symmetry vectors have been carried out symbolically by Mathematica, developing a simple method. The symmetry vectors for A_g and A_u representations are listed in Table 5.2.

Table 5.3. Calculated, experimental and other theoretical values for the vibrational modes of the C_{60} in cm^{-1}. Experimental data are taken from Refs. [27, 28] and theoretical results are from [25, 26, 27]. The experimental data indicated by symbol (*) were measured by neutron inelastic scattering and high-resolution electron-energy-loss spectroscopy [26].

Rep.	Expt.	Prese.	Feld.	Jishi	Quon.	Rep.	Expt.	Prese.	Feldm	Jishi	Quon.
A_g	496	493	496	492	478	A_u		883	1012	1142	850
	1470	1501	1470	1468	1499						
						T_{1u}	527	541	527	505	547
T_{1g}		558	584	501	580		577	565	578	589	570
	970*	959	879	981	788		1183	1025	1208	1208	1176
	1369	1303	1297	1346	1252		1428	1447	1445	1450	1461
T_{2g}	560*	507	573	541	547	T_{2u}	355*	335	377	367	342
		731	888	847	610		680*	779	705	677	738
	870*	785	957	931	770			995	1014	1025	962
	1360	1346	1433	1351	1316			1167	1274	1212	1185
								1548	1564	1575	1539
G_g		439	449	498	486						
		633	612	626	571	G_u	403*	341	346	385	356
		775	840	805	759		760*	669	829	789	683
	1065	987	1153	1056	1087			739	931	929	742
	1360	1173	1396	1375	1296		1065	937	994	961	957
		1408	1534	1521	1505		1310	1286	1425	1327	1298
							1440	1378	1451	1413	1440
H_g	273	258	268	269	258						
	437	428	438	439	439	H_u	355*	358	387	361	404
	710	769	692	708	727		560*	523	521	543	539
	774	806	782	788	767			583	667	700	657
	1099	1075	1094	1102	1093			625	814	801	737
	1250	1234	1226	1217	1244			1159	1141	1129	1205
	1428	1372	1431	1401	1443			1361	1358	1385	1320
	1575	1579	1568	1575	1576		1555	1541	1558	1552	1565

We have computed the eigenvalues of block diagonalized matrix Φ, by considering interaction up to ten-neighbours. The calculated 46 distinct vibrational frequencies are listed in Table 5.3. The values of the bond stretching and angle bending force constants that we have used to obtain the results are given in Table 5.4.

Table 5.4. Force constants α and distances d between atoms in mdyn/cm and Angstrom, respectively.

α_1=4.56	d_1=1.40	α_2=2.48	d_2=1.47	α_3=1.28	d_3=2.38	α_4=1.06	d_4=2.49
α_5=-0.98	d_5=2.83	α_6=0.032	d_6=3.62	α_7=0.04	d_7=3.74	α_8=0.39	d_8=4.16
α_9=0.012	d_9=4.57	α_{10}=0.02	d_{10}=4.66	β=0.196			

5.3. DISCUSSION AND CONCLUSION

So far, we have obtained dynamical matrix Φ that is involving interactions among an atom with its ten neighbouring atoms. In Table 5.3, the 46 distinct vibrational frequencies are listed. For comparison, we have also listed the 14 optically observed Raman and infrared active modes, the modes measured by neutron inelastic scattering and high-resolution electron-energy-loss spectroscopy, and some recent calculations. It can be shown that, with a few exceptions, all computed modes are in agreement with experimental results. These comparisons give us confidence that our model should be useful for interpretation of experimental data. This model should serve as the starting point for determination of the electron-phonon coupling strength and vibrational frequencies in doped C_{60}.

We also investigated that the effect of the bond-stretching force constants α_1, α_2, α_3 and α_4 on the vibrational modes. It turns out that A_u mode, lowest A_g mode, first lowest T_{1g}, T_{2g}, T_{1u} and T_{2u} modes and first three lowest G_g, G_u, H_g and H_u modes were not dependent on the values of α_1, α_2 and α_3. Therefore any force constant model should include force between four or five shells of atoms. For the model of ref.[28] at least a large radial forth and fifth nearest neighbour force constant was needed whereas the model did not include a radial force constant between further than nearest neighbours. For the ref. [26], although the distance between the

reference atom and third nearest neighbour atom is approximately equal to the distance between reference atoms and fourth nearest atom, their force constants are found much differently, from each other. In fact, the force constants α_3 and α_4 should be nearly equal to each other. The results demonstrate that our method is a useful to study the electron-phonon interactions between vibrational levels.

CHAPTER 6

JAHN-TELLER EFFECT FOR C_{60} MOLECULE

Except at absolute zero in temperature, all atoms and molecules have energy and vibrate. The electrons in C_{60} molecule will be sensitive to these vibrations. It is believed that this vibronic coupling plays an important role in determining the behaviour of C_{60} molecules and related fullerene compounds.

Icosahedral symmetry is extremely rare in nature and vibronic coupling effects have not been investigated in this symmetry until very recently. Many interesting effects due to vibronic coupling are possible from a theoretical point of view due to quantum-mechanical four and five-fold degenerate states. The ground state of pure C_{60} molecule is singlet A_g state, so is not very sensitive to JT effect. However, the ground state of C_{60}^{+} and C_{60}^{-} states do potentially strong effects. The highest occupied molecular orbital (HOMO), H_u orbital, is fivefold degenerate, and the lowest unoccupied orbital (LUMO), T_{1u} orbital, is threefold degenerate. When ionising this molecule, either by taking one electron to obtain C_{60}^{+}, or by adding one electron C_{60}^{-}, JT active state is created. This means that there will be a nuclear distortion, and the symmetry will be lowered. Also the electronic states will alter. Since the most of the chemical and physical properties of a molecule depend on its electronic states an investigation of JT effect is necessary to understand and to explain the properties of C_{60}.

JT effect is also important from experimental point of view. Most workers agree that electron-vibron interactions are very important for many properties of fullerenes and may explain superconductivity. It is known that origin of superconducting pairing in

C_{60} compounds is due to the interaction of the electrons with vibronic modes of C_{60} molecule.

In this part, a group theoretical treatment of JT distortion in general case of a fivefold degenerate state of I_h molecule is provided. The JT surface energies have been obtained by breaking symmetries of I_h group into its maximal little group. This is never done before. This chapter includes the treatment of the JT interaction matrices for threefold and fourfold degenerate coupling systems.

6.1. POTENTIAL ENERGY SURFACES (PES) FOR H⊗(2h⊕g) SYSTEM

In the general formalism of the JT effect, a degenerate electronic state corresponding to a representation of D of symmetry group G of the molecule can interact with the vibrational modes corresponding to representations contained in the symmetric part of the direct product $D \otimes D$ (excluding the identical representation which is trivial). As it is well known, the molecular symmetry is reduced by the JT distortion with splitting of the electronic-state degeneracy. The distorting forces acting along a certain non-totally vibrational modes carry the nuclei over into distorted configurations. Distorted configuration of a molecule can be characterised by subgroup symmetries of parent molecular group.

In general, a physical system may pass from a symmetric to less symmetric state, during its evolution. This symmetry transition is known as spontaneously symmetry breaking [85,86]. The process of symmetry breaking applies to all domains described by expectation values of operators. This common mathematical technique can be applied successfully to different domains of physics because they all share in the occurrence of broken symmetry.

In order to study the JT structure of A_x C_{60} and/or $C^{\pm n}$ various theoretical approaches have been used. Ceulemans has proposed an analytical treatment of JT distortion in the general case of a fivefold degenerate state of an I_h molecule. The extreme points were identified by using the isostationary function and epikernel methods [80,82]. First order JT interaction and its continuous group invariance were

discussed and the energies were found for JT coupling with and without splitting [87]. The ground state Berry phase of some JT systems were calculated in the five dimensional rotation group SO(5) [88]. Classical and semi-classical models were introduced about JT manifold for electron vibron interactions, by Auerback, Manini and Tosatti [89]. The H⊗(h⊕g) problem is investigated analytically using a unitary transformation by C.P Moate,J.L Dunn et al.[90].

6.1.1. Symmetry Aspects and Coupling of States

In this section, we start by describing the Hamiltonian that generates $D^{\ell}\otimes D^{\ell}$ surface where D^{ℓ} denotes the irreducible representation. The standard Hamiltonian may be written in the form

$$\begin{aligned} H &= H_o + H_{JT} \\ H_o &= \frac{1}{2}\hbar\omega\sum_i (P_i^2 + Q_i^2) \end{aligned} \tag{6.1}$$

where H_o describes free (uncoupled) electrons/holes and vibrations and Q_i is the distortion coordinate and P_i is the conjugate momentum. In general, H_{JT} introduces a rotationally invariant linear coupling between the electronic state and the vibrational mode. It is known that the Hamiltonian for a linear JT coupling of H⊗(2h⊕g) system is invariant under the rotational operations of SO(3) group. If either the restriction of linear coupling or harmonic forces is relaxed, the symmetry of Hamiltonian is reduces to point group G

As we have mentioned above, totally symmetric part of direct product of an irreducible representation of a finite group, which describes the properties of JT surfaces, is written in the form of

$$[D^{\ell}\otimes D^{\ell}] = D^{\ell 1}\oplus D^{\ell 2}\oplus\ldots\oplus D^{\ell n} \tag{6.2}$$

where ℓ is the angular momentum quantum number. Decomposition of $[D^{\ell}\otimes D^{\ell}]$ implies that the JT Hamiltonian can be written in the following way

$$H_{JT} = H^{\ell_1} + H^{\ell_2} + \cdots + H^{\ell_n} \tag{6.3}$$

where H^{ℓ} is the JT Hamiltonian and it is invariant under the symmetry operations of corresponding finite group, for the $2\ell+1$ dimensional representation. A hole in the HOMO interacts with the vibrational modes. We focus on modes, which couple linearly with the hole density fluctuations. Hence the icosahedral symmetry of the molecule restricts the linearly coupled modes to those of the same symmetry as the irreducible representations of the group (I_h) contained in the symmetric part of a hole representation with itself:

$$[H_u \otimes H_u] = [H_u^2] = [H_g^2] = A_g \oplus H_g \oplus (G_g \oplus H_g) \tag{6.4}$$

where A_g, G_g and H_g are one, four and five dimensional irreducible representations of I_h, respectively. Since the I_h group is a subgroup of O(3), decomposition of coupling of two states should be written in the form

$$[D^2 \otimes D^2] = D^0 \oplus D^2 \oplus D^4 \tag{6.5}$$

In order to take advantage of spherical symmetry, and as a simplifying approximation at this initial state, we neglect the icosahedral details of the molecular shape so that we study the problem of D^2 holes coupled to D^0, D^2 and D^4 vibrations. The decomposition of direct product of $[H_u \otimes H_u]$ coupling in O(3) is found using the Table 6.1. The Hamiltonian we consider has the following structure:

$$H_{JT} = H^0 + H^2 + H^4 \tag{6.6}$$

where the superscripts 2 and 4 are ℓ values. The symmetric part contains the totally symmetric representation $H^0=A_g$ that is trivial polaronic problem [77,84] and it can be solved, exactly. The H^0 vibration shifts energies but it does not cause splitting. Remaining vibrations subtend the configuration space, which contains all distorted configurations, may be reached by JT active coordinates. As seen from Table 6.1, the

Hamiltonian H^2 corresponds five dimensional representations H_g and H^4 corresponds to the direct sum of $G_g \oplus H_g$ vibrational levels.

Table 6.1. The representations of the O(3) group with $\ell<14$ are splitted by the icosahedral point group.

ℓ	I_h	ℓ	I_h
0	A_g	7	$T_{1u}+T_{2u}+G_u+H_u$
1	T_{1u}	8	$T_{2g}+G_g+H_g+H_g$
2	H_g	9	$T_{1u}+T_{2u}+G_u+G_u+H_u$
3	G_u+T_{2u}	10	$A_g+T_{1g}+T_{2g}+G_g+2H_g$
4	G_g+H_g	11	$2T_{1u}+T_{2u}+G_u+2H_u$
5	$T_{1u}+T_{2u}+H_u$	12	$A_g+T_{1g}+T_{2g}+2G_g+2H_g$
6	$A_g+T_{1g}+G_g+H_g$	13	$T_{1u}+2T_{2u}+2G_u+2H_u$

6.1.2. Determination of Stationary Points on JT Surface Using Little Groups of Icosahedral

The second important aspect of invariant polynomial functions, in addition to linear Jahn-Teller matrices, concerns the extremum points on JT surface. Since our interest are the minimal points and the saddle points, the present section is devoted to the determining of extremum points on JT surface by breaking symmetries of icosahedral group into its maximal little groups. The problem has been studied by Ceulemans with method of epikernel principle [82].

The little group is the new symmetry group of distorted molecule as a result of coupling and its definition is given in Chapter 3. In order to simplify the notation, we shall switch from O(3) to the SO(3) notation, omitting therefore the g/u symbol for inversion. Then, the electronic–vibrational coupling is symbolized as $H\otimes(2h\oplus g)$ where capital letter shows electronic and small letters show the vibrational levels. Without loss of generality the problem for I_h group can be treated equally well in the subgroup of proper rotations of group I. The maximal little subgroups of I group have been computed by using Eqn.(3.10) and are given in Table 6.2. As seen from

Table 6.2, the maximal little groups predict the existence of dihedral groups D_5, D_3, and D_2 minima on the icosahedral molecular cage. In the coordinate space the distortion that is the result of JT instability should conserve all maximal little group symmetries.

Table 6.2. Maximal Little groups of H and G representations. Decomposition implies that T is not maximal little group of H state, and D_5 is not maximal little group for G state.

	D_2	D_3	D_5	T
H	$2A+B_1+B_2+B_3$	A_1+2E	$A_1+E_1+E_2$	$E+T_2$
G	$A+B_1+B_2+B_3$	A_1+A_2+E	E_1+E_2	$2A+E$
H⊕G	$3A+2B_1+2B_2+2B_3$	$2A_1+A_2+3E$	$A_1+2E_1+2E_2$	$2A+2E+T_2$

In our perspective the structure of Jahn-Teller surfaces have been identified by the symmetry breaking of the continuous symmetry to the true finite point group of the representation space and its maximal little groups. This may be represented as follows

$$I \rightarrow S' \tag{6.7}$$

where S' are little groups of I group given in Table 6.2.

6.1.3. Group Invariance of JT Systems for H⊗(2h⊕g) Coupling and JT Matrices

As we stated in the previous section, the Hamiltonian of H⊗(2h⊕g) coupling has three parts H^0, H^2 and H^4, which must be separately invariant under I symmetry. In this section, we want to construct a polynomial function in electronic and nuclear configuration space, to examine symmetry properties of potential energy surface. A polynomial function, which has been produced for this purpose, is in the form

$$U_{\ell m}(X,Q) = \sum_{i,j=1}^{2\ell+12m+1} \sum_{k=1} F_{ijk} X_i X_j Q_k \tag{6.8}$$

In this expression X_i and X_j correspond to electronic coordinates and Q_k corresponds to nuclear(active) coordinates. The force elements or coupling coefficients should be chosen appropriately for each H⊗h and H⊗(h⊕g) coupling. In the Eqn.(6.8) the indices $2\ell+1$ and $2m+1$ stand for dimensions electronic and active coordinates, respectively. For H⊗h coupling ℓ and m take value 2 and for H⊗(h⊕g) case ℓ and m take values 2 and 4, respectively.

We will focus our treatment for the computation of invariant polynomials for H⊗h and H⊗(h⊕g) problems. The invariant polynomial function for ℓ=2, in real basis, has been computed by using the matrix representations of H state. The 5×5 generators transform electronic coordinates X_i (i=1...5) and nuclear coordinates $Q_{i..}$ It can be written in the form

$$\sum_{i,j=1}^{5}\sum_{k=1}^{5} F_{ijk} X_i X_j Q_k = \sum_{i,j=1}^{5}\sum_{k=1}^{5} F_{ijk} X'_i X'_j Q'_k \qquad (6.9)$$

In this equation, $X'_i = \sum_{n=1}^{5} \Gamma^r_{in} X_n$ and $Q'_k = \sum_{n=1}^{5} \Gamma^r_{in} Q_n$. Γ^r_{in} is the matrix elements of 5×5 generators of I. The Eqn(6.9) has been solved for F_{ijk} and two linearly independent polynomial function have been obtained. One of our main goal is that the first order JT interaction matrices can be derived by working out invariant polynomial function. The double differentiation of $U_{22}(X,Q)$ with respect to electronic coordinates X_i and X_j produce linear JT interaction matrix. In general, we can write

$$(B_m)_{ij} = \frac{\partial^2 U_{2m}}{\partial X_i \partial X_j}, \quad (i,j = 1,2\cdots 5) \qquad (6.10)$$

The JT interaction matrix for H⊗h coupling is

$$B_2 = F_1 \begin{pmatrix} 2Q_5 & 0 & -\sqrt{3}Q_3 & \sqrt{3}Q_4 & 2Q_1 \\ 0 & 2Q_5 & -\sqrt{3}Q_4 & -\sqrt{3}Q_3 & 2Q_2 \\ -\sqrt{3}Q_3 & -\sqrt{3}Q_4 & -\sqrt{3}Q_1 - Q_5 & -\sqrt{3}Q_2 & -Q_3 \\ \sqrt{3}Q_4 & -\sqrt{3}Q_3 & -\sqrt{3}Q_2 & \sqrt{3}Q_1 - Q_5 & -Q_4 \\ 2Q_1 & 2Q_2 & -Q_3 & -Q_4 & -2Q_5 \end{pmatrix} +$$

$$F_2 \begin{pmatrix} \sqrt{15}Q_1 - \frac{\sqrt{3}}{2}Q_4 + \frac{\sqrt{5}}{2}Q_5 & -\sqrt{15}Q_2 + \frac{\sqrt{3}}{2}Q_3 & \frac{\sqrt{3}}{2}Q_2 & -\frac{\sqrt{3}}{2}Q_1 - 3Q_5 & \frac{\sqrt{5}}{2}Q_1 - 3Q_4 \\ -\sqrt{15}Q_2 + \frac{\sqrt{3}}{2}Q_3 & -\sqrt{15}Q_1 + \frac{\sqrt{3}}{2}Q_4 + \frac{\sqrt{5}}{2}Q_5 & \frac{\sqrt{3}}{2}Q_1 - 3Q_5 & \frac{\sqrt{3}}{2}Q_2 & \frac{\sqrt{5}}{2}Q_2 - 3Q_3 \\ \frac{\sqrt{3}}{2}Q_2 & \frac{\sqrt{3}}{2}Q_1 - 3Q_5 & -2\sqrt{3}Q_4 - \sqrt{5}Q_5 & -2\sqrt{3}Q_3 & -3Q_2 - \sqrt{5}Q_3 \\ -\frac{\sqrt{3}}{2}Q_1 - 3Q_5 & \frac{\sqrt{3}}{2}Q_2 & -2\sqrt{3}Q_3 & 2\sqrt{3}Q_4 - \sqrt{5}Q_5 & -3Q_1 - \sqrt{5}Q_4 \\ \frac{\sqrt{5}}{2}Q_1 - 3Q_4 & \frac{\sqrt{5}}{2}Q_2 - 3Q_3 & -3Q_2 - \sqrt{5}Q_3 & -3Q_1 - \sqrt{5}Q_4 & \sqrt{5}Q_5 \end{pmatrix} \tag{6.11}$$

The force elements F_1 and F_2 are given by

$$F_1 = \frac{1}{135\sqrt{3}}(-13\sqrt{5}F_{H1} + 15F_{H2})$$
$$F_2 = \frac{1}{27\sqrt{15}}(\sqrt{5}F_{H1} + 3F_{H2}) \tag{6.12}$$

In this equation, F_{H1} and F_{H2} are coupling parameters of H mode. The invariant polynomial function is derived for H⊗(h⊕g) as in the same way done for H⊗h. In this case Eqn.(6.9) takes form

$$\sum_{i,j=1}^{5}\sum_{k=1}^{9} F_{ijk} X_i X_j Q_k = \sum_{i,j=1}^{5}\sum_{k=1}^{9} F_{ijk} X'_i X'_j Q'_k \tag{6.13}$$

Nine dimensional H⊗(h⊕g) state consists of one H mode with components {Q_1, Q_2, Q_3, Q_4, Q_5} and G mode with components {Q_6, Q_7, Q_8, Q_9}. The icosahedral generators transform the electronic and nuclear coordinates. The transformation of X'_i and X'_j are the same as given in Eqn.(6.9). The nuclear coordinates Q'_k is transformed as $Q'_k = \sum_{n=1}^{9} \Lambda^{\ell}_{in} Q_n$ where Λ^{ℓ} is the direct sum of 5 and 4 dimensional irreducible matrix generators. Solution of the Eqn.(6.13) for coefficients F_{ijk} gives

three linearly independent functions. In Ceulemans's paper [82], relations between the polynomial coefficients F_{ijk} in Eqn.(6.9) and Eqn.(6.13) are expressed in terms of Clebsch Gordon series for the icosahedral point group [79]. The linear JT interaction matrices for this coupling are derived from the relation (6.10). The two of them are the same with matrices of H⊗h coupling and third one is

$$B_4=F_3\begin{pmatrix} -Q_6-2\sqrt{5}Q_8 & 2\sqrt{5}Q_7 & \frac{5}{4}Q_7-\frac{9\sqrt{5}}{4}Q_9 & -\frac{5\sqrt{5}}{4}Q_6-\frac{5}{4}Q_8 & \frac{\sqrt{15}}{2}Q_8 \\ 2\sqrt{5}Q_7 & -Q_6+2\sqrt{5}Q_8 & -\frac{5\sqrt{5}}{4}Q_6+\frac{5}{4}Q_8 & \frac{5}{4}Q_7+\frac{9\sqrt{5}}{4}Q_9 & \frac{\sqrt{15}}{2}Q_7 \\ \frac{5}{4}Q_7-\frac{9\sqrt{5}}{4}Q_9 & -\frac{5\sqrt{5}}{4}Q_6+\frac{5}{4}Q_8 & 4Q_6+\sqrt{5}Q_8 & \sqrt{5}Q_7 & -\frac{5\sqrt{3}}{2}Q_7 \\ -\frac{5\sqrt{5}}{4}Q_6-\frac{5}{4}Q_8 & \frac{5}{4}Q_7+\frac{9\sqrt{5}}{4}Q_9 & \sqrt{5}Q_7 & 4Q_6-\sqrt{5}Q_8 & -\frac{5\sqrt{3}}{2}Q_8 \\ \frac{\sqrt{15}}{2}Q_8 & \frac{\sqrt{15}}{2}Q_7 & -\frac{5\sqrt{3}}{2}Q_7 & -\frac{5\sqrt{3}}{2}Q_8 & -6Q_6 \end{pmatrix} \quad (6.14)$$

The sum of the B_2 given in Eqn.(6.11) and JT interaction matrix given in Eqn.(6.14) corresponds to the first order JT interaction matrix (B_4) for H⊗(h⊕g) coupling. It is obvious that the interaction matrix is also obtained by considering only H⊗g coupling. Force element F_3 is related by coupling parameter of G mode and is given by $F_3=F_G/9$. The first order linear JT interaction matrices for H state have been found in [82,91] and are in agreement with our results. We guess that the higher order JT interaction matrices may be obtained by constructing higher order icosahedral invariant polynomials. Program that computes JT interaction matrices is given in Appendix F.

6.1.4. Transitions Associated With H⊗h and H⊗(h⊕g) Couplings

In this section, symmetry of icosahedral is broken into its little groups for H⊗h and H⊗(h⊕g) cases. Combination of eigenvalues of the B_m with harmonic potential energy, in terms of little groups yields JT surface energy.

The five dimensional irreducible representation of I group has three maximal little groups named; D_2, D_3 and D_5. In order to break symmetry of a parent group into its little groups, one should assign an appropriate Q_i which can be computed by constructing set of equations such that

$$Q_i = \sum_{j=1}^{2\ell+1} \Gamma_{ij} Q_j \qquad (6.15)$$

where Γ_{ij}'s are the matrix elements of little group generator which are given in Appendix B. The method of symmetry breaking predicts the existence of saddle points, trigonal and pentagonal turning points on JT surfaces associated with D_2, D_3 and D_5 groups. From the solution of Eqn.(6.15) two H type coordinates Q_{H1}, Q_{H2} and one G type coordinate Q_G are found. The H and G type coordinates are constrained to $Q_4 = -\tau Q_{H1}$, $Q_5 = -\frac{\sqrt{15}}{2} Q_{H2}$, $Q_6 = Q_G$, where $\tau = \frac{1}{2}(1+\sqrt{5})$ under the given conditions; the energy eigenvalues of each little group are computed by developing a computer program in Mathematica given in Appendix G.

6.1.4a. D_2 Transition

Decomposition of five dimensional representations in D_2 group is $2A+B_1+B_2+B_3$. The symmetry of the icosahedral group is broken into D_2, assigning as $Q_1 \to \sqrt{5}Q_4 - \sqrt{3}Q_5$, $Q_2 \to 0$, $Q_3 \to 0$, $Q_4 \to Q_4$, $Q_5 \to Q_5$, using the Eqn.(6.15). After substituting values of Q_i into B_2, the eigenvalues of B_2 are found. Combinations of eigenvalues of B_2 with harmonic restoring potentials for the distortional coordinates Q_{H1}, and Q_{H2} give JT surface energy expressions.

$$\begin{aligned}
E(A) &= \pm\frac{1}{2\sqrt{10}}\left[(3F_{H1}^2 + F_{H2}^2)(2\tau^2 Q_{H1}^2 - 5\tau Q_{H1}Q_{H2} + 5Q_{H2}^2)\right]^{\frac{1}{2}} + \frac{1}{2}K_H(Q_{H1}^2 + Q_{H2}^2) \\
E(B_1) &= \frac{1}{4\sqrt{5}}(F_{H1} + F_{H2})(4\tau Q_{H1} - 5Q_{H2}) + (F_{H1} - 3F_{H2})\sqrt{5}Q_{H2} + \frac{1}{2}K_H(Q_{H1}^2 + Q_{H2}^2) \\
E(B_2) &= \frac{1}{4\sqrt{5}}(F_{H2} - F_{H1})(4\tau Q_{H1} - 5Q_{H2}) + (F_{H1} + 3F_{H2})\sqrt{5}Q_{H2} + \frac{1}{2}K_H(Q_{H1}^2 + Q_{H2}^2) \\
E(B_3) &= -\frac{1}{\sqrt{5}}(2\tau F_{H1}Q_{H1} - \frac{1}{2}(F_{H1} - \sqrt{5}F_{H2})Q_{H2} + \frac{1}{2}K_H(Q_{H1}^2 + Q_{H2}^2)
\end{aligned} \qquad (6.16)$$

In this equation, K_H is the harmonic force constant. The energy values of E(A) predicts the existence of saddle points.

The direct sum of g and h states consists of both G-type and H-type nuclear coordinates. For this reason, computations are more complicated than the h state. In this case, there are three distortional coordinates that are invariant under D_2. In

Eqn.(6.15) nine dimensional matrix generators which have been obtained by taking direct sum of five and four dimensional representations are used to assign Q_i values. It is found that,

$Q_1 \to \sqrt{5}Q_4 - \sqrt{3}Q_5, Q_2 \to 0, Q_3 \to 0, Q_4 \to Q_4, Q_5 \to Q_5, Q_6 \to Q_6, Q_7 \to 0, Q_8 \to \sqrt{5}Q_6, Q_9 \to 0$. In this basis, combination of eigenvalues of B_4 with harmonic potential gives us PES as

$$
\begin{aligned}
E(A) &= \pm\frac{1}{2\sqrt{10}}\left[(3F_{H1}^2 + F_{H2}^2)(2\tau^2 Q_{H1}^2 - 5\tau Q_{H1}Q_{H2} + 5Q_{H2}^2)\right]^{\frac{1}{2}} + \frac{3}{8}F_G Q_G + \\
&\quad \frac{1}{2}K_G Q_G^2 + \frac{1}{2}K_H(Q_{H1}^2 + Q_{H2}^2) \\
E(B_1) &= \frac{1}{4\sqrt{5}}(F_{H1} + F_{H2})(4\tau Q_{H1} - 5Q_{H2}) + (F_{H1} - 3F_{H2})\sqrt{5}Q_{H2} - \frac{1}{4}F_G Q_G + \\
&\quad \frac{1}{2}K_G Q_G^2 + \frac{1}{2}K_H(Q_{H1}^2 + Q_{H2}^2) \\
E(B_2) &= \frac{1}{4\sqrt{5}}(F_{H2} - F_{H1})(4\tau Q_{H1} - 5Q_{H2}) + (F_{H1} + 3F_{H2})\sqrt{5}Q_{H2} - \frac{1}{4}F_G Q_G + \\
&\quad \frac{1}{2}K_G Q_G^2 + \frac{1}{2}K_H(Q_{H1}^2 + Q_{H2}^2) \\
E(B_3) &= -\frac{1}{\sqrt{5}}(F_{H1}22Q_{H1} - \frac{1}{2}(F_{H1} - \sqrt{5}F_{H2})Q_{H2} - \frac{1}{4}F_G Q_G + \frac{1}{2}K_G Q_G^2 + \\
&\quad \frac{1}{2}K_H(Q_{H1}^2 + Q_{H2}^2)
\end{aligned}
\qquad (6.17)
$$

K_G in the Eqn.(6.17) is the harmonic force constant of G mode. It is obvious that the magnitude of splitting of energy values is increasing in h⊕g state compared to h state.

6.1.4b. D_3 Transition

In this case, decomposition of H representation of irreducible representations of D_3 is $A_1 + 2E$ in D_3. Following the same procedure given in 6.1.4, symmetry of I group can be broken into D_3, in the directions, $Q_1 \to 0$, $Q_2 \to 0$, $Q_3 \to 0$, $Q_4 \to 0$, $Q_5 \to Q_5$. The computed energy values are given as

$$
\begin{aligned}
E(A_1) &= -\frac{2}{3}F_{H1}Q_{H2} + \frac{1}{2}K_H Q_{H2}^2 \\
E_{\mp}(E) &= \frac{1}{6}F_{H1}Q_{H2} \mp \sqrt{\left(\frac{F_{H1}}{3}\right)^2 + \left(\frac{F_{H2}}{2}\right)^2}\,Q_{H2} + \frac{1}{2}K_H Q_{H2}^2
\end{aligned}
\qquad (6.18)
$$

Transformation of nuclear coordinates for h⊕g state gives that $Q_1 \to 0, Q_2 \to 0, Q_3 \to 0, Q_4 \to 0, Q_5 \to Q_5, Q_6 \to Q_6, Q_7 \to 0, Q_8 \to 0, Q_9 \to 0$. The energy values consists of the two distortional coordinates, and therefore

$$E(A_1) = -\frac{2}{3}(F_G Q_G + F_{H1} Q_{H2}) + \frac{1}{2} K_G Q_G^2 + \frac{1}{2} K_H Q_{H2}^2$$

$$E_{\mp}(E) = \frac{1}{6}(F_G Q_G + F_{H1} Q_{H2}) \mp \left[\left(\frac{1}{3} F_{H1} Q_{H2} - \frac{5}{12} F_G Q_G\right)^2 + \frac{1}{4} F_{H2}^2 Q_{H2}^2\right]^{\frac{1}{2}} + \quad (6.19)$$

$$\frac{1}{2} K_G Q_G^2 + \frac{1}{2} K_H Q_{H2}^2 .$$

These energy values are in agreement with the energy values given in [82].

6.1.4c. D_5 Transition

In D_5 the quintet irreducible representation state reduces to $A_1+E_1+E_2$. Applying the same procedure as in the previous section, Q_i values are found as $Q_1 \to -\frac{Q_4}{\tau^2}$, $Q_2 \to 0$, $Q_3 \to 0$, $Q_4 \to 0$, $Q_5 \to \frac{\sqrt{3}}{2\tau} Q_4$. The corresponding energies are obtained as

$$E(A_1) = -\frac{2}{\sqrt{5}} F_{H2} Q_{H1} + \frac{1}{2} K_H Q_{H1}^2$$

$$E(E_1) = \frac{1}{2}\left(-F_{H1} + \frac{1}{\sqrt{5}} F_{H2}\right) Q_{H1} + \frac{1}{2} K_H Q_{H1}^2 \quad (6.20)$$

$$E(E_2) = \frac{1}{2}\left(F_{H1} + \frac{1}{\sqrt{5}} F_{H2}\right) Q_{H1} + \frac{1}{2} K_H Q_{H1}^2 .$$

The calculations have been carried out for H⊗(h⊕g) coupling and the same results have been obtained as expected.

Tetrahedral group (T) is also maximal little group of G representation of I group. In H⊗(h⊕g) coupling some energy values have been expected. (Since T is not little group of H representation. Thus in H⊗h coupling energy eigenvalues of B_2 is zero.) Decomposition of H state in T group is E+T, and symmetry is broken according to

the directions $Q_9 \to -\sqrt{\frac{5}{3}}Q_6$, $Q_i \to 0, (i=1,\ldots 8)$. The corresponding eigenvalues of B_4 are $F_G Q_G$ and $-\frac{2}{3}F_G Q_G$, for E and T, respectively.

In general, minimal energy values for each little group can be obtained from the given energy expressions.

6.2. JAHN-TELLER INTERACTION MATRICES FOR T⊗h SYSTEM

For C_{60}^{n-} molecules and doped C_{60} compounds (A_3C_{60}), the T level is partly occupied. This level couples to phonons of one dimensional (A) or five dimensional (H) representation. Coupling to the unit representation does not lower icosahedral symmetry and is irrelevant to the JT distortion. Then problem is designated to T⊗h. Due to this coupling, molecule is expected to undergo a JT distortion. In this section, electron-vibron interaction matrices, which are used to get potential energy term for the new symmetries (D3 and D5), have been obtained for T_1⊗h and T_2⊗h systems.

Firstly, we consider threefold electronic states belonging to T=T_1or T_2. Symmetric part of the three dimensional direct product for I_h group can be written as

$$[T\otimes T]=A\oplus H \tag{6.21}$$

JT Hamiltonian can be written in the following way

$$H_{JT} = H^0 + H^2 \tag{6.22}$$

where the superscripts 0 and 2 are ℓ values. Hamiltonian of T⊗h coupling has one part H^2 that must be separately invariant under I symmetry (H^0 is again polaronic problem). As in the previous section, we want to construct a polynomial function in electronic and nuclear configuration space. The invariant polynomial function for ℓ=1, in real basis has been computed by using the matrix representations of T state which are given in Appendix B. The 3×3 generators transform electronic coordinates X_i (i=1…3) and nuclear coordinates Q_i. It can be written in the form

$$\sum_{i,j=1}^{3}\sum_{k=1}^{5}F_{ijk}X_iX_jQ_k=\sum_{i,j=1}^{3}\sum_{k=1}^{5}F_{ijk}X'_iX'_jQ'_k\ . \qquad (6.23)$$

In this equation, $X'_i=\sum_{n=1}^{3}\Gamma^r_{in}X_n$ and $Q'_k=\sum_{n=1}^{5}\Gamma^r_{in}Q_n$. Γ^r_{in} represents the matrix elements of 3×3 generators of I. The Eqn.(6.23) is solved for F_{ijk}. One of our main goal is that the first order JT interaction matrices can be derived by working out invariant polynomial function. The double differentiation of $U_{12}(X,Q)$ with respect to electronic coordinates X_i and X_j gives linear JT interaction matrix for $T_1\otimes h$ coupling as in the form

$$B_1=\frac{F}{2}\begin{pmatrix} Q_1-\sqrt{3}Q_4 & -\sqrt{3}Q_3 & -\sqrt{3}Q_2 \\ -\sqrt{3}Q_3 & Q_1+\sqrt{3}Q_4 & -\sqrt{3}Q_5 \\ -\sqrt{3}Q_2 & -\sqrt{3}Q_5 & -2Q_1 \end{pmatrix}. \qquad (6.24)$$

For $T_2\otimes h$, it is equal to

$$B'_1=\frac{F}{2}\begin{pmatrix} Q_1-\sqrt{3}Q_2 & \sqrt{3}Q_5 & \sqrt{3}Q_4 \\ \sqrt{3}Q_5 & Q_1+\sqrt{3}Q_2 & \sqrt{3}Q_3 \\ \sqrt{3}Q_4 & \sqrt{3}Q_3 & -2Q_1 \end{pmatrix} \qquad (6.25)$$

where F is the coupling parameter. This interaction matrices will warp to produce well of either D_3 or D_5 symmetry, depending on the strengths of coupling.

6.3. JAHN-TELLER INTERACTION MATRICES FOR G⊗h AND G⊗g SYSTEMS

JT interaction matrices for fourfold G⊗G coupling system requires the inclusion in the theory of spin-orbit interaction between states. Symmetric part of the direct product of fourfold degenerate states is in the form

$$[G\otimes G]=A\oplus G\oplus H \tag{6.26}$$

Then, JT interaction matrices can be found in two forms of G⊗h and G⊗g separately. Using the same procedure outlined in section 6.2, we get JT interaction matrices for G⊗h

$$\begin{pmatrix} 2Q_2-\sqrt{3}Q_1 & 2Q_5 & Q_2-Q_4 & Q_3-Q_5 \\ 2Q_5 & -\sqrt{3}Q_1-2Q_2 & -Q_3-Q_5 & Q_2-Q_4 \\ Q_2-Q_4 & -Q_3-Q_5 & \sqrt{3}Q_1-2Q_4 & -2Q_3 \\ Q_3-Q_5 & -Q_2-Q_4 & -2Q_3 & \sqrt{3}Q_1+2Q_4 \end{pmatrix} \tag{6.27}$$

and for G⊗g is

$$\begin{pmatrix} -Q_8 & -Q_9 & -Q_6+Q_8 & -Q_7-Q_9 \\ -Q_9 & Q_7 & Q_7-Q_9 & -Q_6-Q_8 \\ -Q_6+Q_8 & Q_7-Q_9 & Q_6 & -Q_7 \\ -Q_7-Q_9 & -Q_6-Q_8 & -Q_2 & -Q_6 \end{pmatrix}. \tag{6.28}$$

6.4. SUMMARY AND CONCLUSION

It is now well known that electron (hole)-vibron coupling and hence Jahn-Teller (JT) effect is important in understanding the properties of C_{60} and related molecules. In this chapter, H⊗(2h⊕g) coupling case has been studied to find the potential energy surfaces for the positively charged C_{60} molecule. The H⊗(2h⊕g) Jahn-Teller systems are of particular importance as this will be the JT effect displayed by C_{60}^{+} molecules removed with an electron. C_{60}^{+} is obtained by removing one electron from fivefold degenerate H_u highest occupied molecular orbital (HOMO) and a hole in LUMO interacts with the vibrational modes of C_{60} and symmetry is broken. The method of symmetry breaking mechanism is applied to obtain expressions for the states associated with minima on the potential energy surface.

In summary, we have shown how the symmetry breaking method is applied for the determination of the potential energies of the H⊗(2h⊕g) surface. In Ceulemans' paper [82], these energies were found by using the method of isostationary function and potential energies of D_3 and D_5 groups were investigated. In our work, all maximal little groups of icosahedral group are studied for the H⊗(h⊕g) and H⊗h states. Splitting of the energy levels of icosahedral system due to distortion is analysed and amazingly interesting that, there is a proper contribution on the connection between our method and method of isostationary function. This method can also be used for other distorted systems.

An epikernel is an intermediate subgroup in the decomposition scheme of a given point group. The epikernels are uniquely defined by the irreducible representations of the symmetry lowering process. In the case of a JT distortion along modes of G and H symmetry, the maximal epikernels correspond [80] to maximal subgroups T, D_5, and D_3. According to the epikernel principle, stable minima on the JT surface are found with structures of the maximal epikernel symmetries. The T epikernel is forbidden, since it splits the electronic manifold into two degenerate components, $E+T_2$, which remain JT active. The remaining D_5 and D_3 epikernels are indeed found to characterize the minima of the JT surface, in agreement with the general principle.

Jahn-Teller interaction matrices for T⊗h, G⊗g and G⊗h coupling systems have been obtained by using our new method and compared with literature [91] and seen that our work gives good results.

CHAPTER 7

CONCLUSIONS AND FURTHER STUDIES

A great deal of interest has recently been generated by C_{60} molecules due to their unique symmetry and special properties. The understanding of the electronic states, the vibrational normal modes in C_{60} molecule, and how they are affected by doping or ionising are extremely important.

The purpose of this work is to clarify molecular structure of C_{60}, to develop a new method, and to improve the current methods. In summary, we have focused on the investigation of electronic and vibrational properties of C_{60} including vibronic coupling. They have also important applications particularly in relation of formation of solid C_{60} and hence superconductivity.

Geometrical optimisation calculations and analysis of molecular energy level using the Hückel method give good insight to predict the energy gap of molecule in terms of Hückel parameters γ and β. In many models the relation between single and double bond is not taken into consideration. In our study, how this relation affects the molecular energy level was emphasized.

C_{60} has 174 vibrational degrees of freedom, but thanks to symmetry-induced degeneracy, the vibron spectra shows relatively few peaks, and nowadays there is general agreement on their identification. The relative cleanness of the observed vibrational spectra pays the price of leaving most vibrational modes inaccessible to direct infrared and Raman spectroscopy. In particularly, $4T_{1u}$ dipolar modes are seen infrared and $2A_g$ and $8H_g$ modes have the correct symmetry for Raman scattering.

Neutron experiments are sensitive to all modes, but with very low resolution. Computations are therefore useful for getting a global view of the vibrational spectrum. The agreement among different computations, unfortunately, is rather poor: typical discrepancies on the order of meV are well above nowadays' experimental resolution. In conclusion, we have presented a model that includes Keating type potential in addition to Harmonic potential. This model is also satisfactory for all molecular and crystal systems. As a future study, investigation of the vibrational states of polyatomic molecules can also be made by using algebraic methods.

The linear $H\otimes(2h\oplus g)$ for positively charged C_{60} JT problem, relevant to instability of icosahedral molecules in fivefold degenerate states has been analysed by improving new model. This model can be applied for other symmetry groups and make easy the computational difficulties compared to other methods [80-82]. In this method JT interaction matrices have been found with the help of the symmetry and prediction of new symmetry due to distortion was obtained using the definition of little group. In fact, two methods have been improved to obtain PES of new symmetry groups. Former one includes computation of JT interaction matrices and latter one is symmetry breaking mechanism depending on the little group phenomenon. This is the first time that symmetry breaking is used to describe PES and to explain JT phenomenon.

The other linear coupling cases ($T\otimes h$, $G\otimes g$ and $G\otimes h$) which occur in icosahedral group have also been investigated. The calculated JT interaction matrices for these systems are in a good agreement with the matrices found by C.C. Chancey et. al. [91].

In all linear JT systems, studied until now, the ground state after vibronic interaction has always been the same symmetry as the original state except $H\otimes(2h\oplus g)$ system. For that reason, to see the symmetry change after the distortion, higher order JT interaction matrices should be obtained to observe symmetry breaking. If this should be done PES of new symmetry can be obtained. As a further study, our method is also applicable to get higher order (quadratic, cubic, etc) interaction matrices of the

all coupled states of icosahedral for the use of another application of JT systems to get accurate results.

Nanotubes (tubular fullerenes) produced by arc-discharge between two carbon electrodes are candidates as one-dimensional fibers. The description of the dielectric response of such materials is thus of prime interest in foreseeing future applications.

REFERENCES

[1] H.W Kroto, J.R. Heath, S.C O'Brien, R.F. Curl, and R.E. Smalley, 1985, Nature, 318, 162-163.

[2] E. Osawa, 1970, Kagaku 25, 854-863 (In Japanese).

[3] E. Osawa, 1971, Chemical Abstract 74, 75698.

[4] Z. Yoshida and E. Osawa, 1971, Aromacity, 174-178 (In Japanese).

[5] O.A. Boschvar, and E.G. Gal'pern, 1973, Dokl. Akad Nauk SSSR 209, 610-612.

[6] I.V. Stankevich, M.V. Nikerow, and D.A. Boschvar, 1984, Russian Chem. Rev., 53(7), 640-645.

[7] M.S. Dresselhaus, G. Dreseelhaus, P.C. Eklund, 1993, J.Mater.Res., Vol 8, No:8.

[8] Leonardo Degirgio, 1998, Advance in Physics, Vol 47, No:2,207-316.

[9] Donald R.Huffman, American Institute of Physics, 1991.

[10] M.Fijuta, R.Saito, G.Dresselhaus, M.S. Dresselhaus, 1992, Physical Review B, Vol 45, No:25.

[11] W. Kratschmer, 1995, Synthetic Metals, 70, 1309-1312.

[12] H.W. Kroto, 1997, Review of Modern Physics, Vol 69, No:3.

[13] R.F.Curl, R.E. Smalley, 1991, Scientific American, 1991.

[14] R.E. Smalley, 1997, Review of Modern Physics, Vol 69, No:3.

[15] W. Kratschmer, L.D. Lamb, and et al., 1990, Nature, 347-354.

[16] A.F. Hebard, M.J.Roseinsky, R.C. Haddon, D.W Murphy, and et al. 1991, Nature, 350, 600.

[17] M. J. Rosseinsky, A.P. Ramirez, S. H. Glarum, 1991, Phys. Rev. Lett., 1991, 66, 2830.

[18] K. Tanigaki, T.W. Ebbesen, et al., 1991, Nature, 352, 222.

[19] Z.C. Wu, D.A. Jelski and T.F. George, 1987, Chem. Phys.Lett., 137, 291.

[20] R.A. Stanton and M.D. Newton, 1988, J.Phys. Chem., 92.

[21] D.E Wekks and W.G. Harter, 1988,Chem. Phys. Lett., 144, 366.

[22] K. Raghavachari, and C.M. Rohfling, J.Phys. Chem.,95, 5768.

[23] G. Dresselhaus, M.S. Dreseelhaus, and P.C. Eklund, 1992, Physical Review B, Vol 45, 6923.

[24] G.B. Adams, J.B. Page, O.F. Sonkey, K.Sinha and et al., 1991, Physical Review B, Vol 44, 4052.

[25] R.A. Jishi, R.M. Mirie, and M.S. Dresselhaus, 1992, Physical Review B, Vol 45, 13685.

[26] J.L. Feldman, J.Q Broughton, and et al., 1992, Physical Review B, Vol 46, 12731.

[27] A.A Quong, M.R. Pederson, J.L. Feldman, 1993, Solid State Communications, Vol 87, No:6, 535.

[28] Q. Jiong, H.Xia and et al., 1992, Chem. Phys. Lett., Vol 192, 93.

[29] R.L. Cappeletti, et al., 1991, Phys. Rev. Lett., 66, 3261.

[30] L.Pintchovious et al., 1992, Phys. Rev. Lett., 69, 2662.

[31] P.Zhou et al., 1992, Appl. Phys. Lett., 60, 2871.

[32] V.N. Denisov, B.N. Mavrin, and et al., 1992, Sov. Phys. JETP ,75, 158.

[33] P.J. Horoyski, M.L.W Thealt, 1993, Physical Review B, Vol 48, 11446.

[34] Z.H.Dong et al., 1993, Physical Review B, Vol 48, 2862.

[35] K.A. Wong, A. M. Rao, P.C. Eklund, M.S Dresselhaus, G. Dresselhaus, 1993, Physical Review B, Vol 48, 11375.

[36] M.C. Martin et al.,1995, Physical Review B, Vol 51, 2844.

[37] P.J. Horoyski, M.L.W Thealt, and T.R. Anthony, 1995, Physical Rev. Lett.,74, 194.

[38] H.Kuzmany, M.Matus, B.Burger and J.Winter, 1994, Adv.Mater., 6, No:10.

[39] P.Zhou, K.Weng, P.C. Eklund, et al., 1993, Physical. Review B, 48, 8412.

[40] J. Winter, H.Kuzmany, 1992, Solid State Comminucations, Vol: 84, No: 10, 935-938.

[41] L.R. Narasimhan, D.N. Stoneback, et al., Physical. Review B., 1992, 46, No: 64.

[42] J.Winter, B.Burger, H.Kuzmany, 1995, Synthetic Metals, 70, 1385-1386.

[43] W.I.F David, R.M. Ibberson, J.C. Matthewman, et al., 1991, Nature, 353, 147.

[44] P.J. Horoyski, M.L.W. Thewalt, 1996, Physical Review B., 54.

[45] Z.H. Dong, P.Zhou, et al., 1993, Physical Review B., 54, 2862.

[46] V.D. Vankateswaren, D. Sanzi, et al., 1996, Physica Stat. Solidi B., 198/1, 545.

[47] A.M. Rao, P.C. Eklund et al., 1997, Physical. Review B., 55, 4766.

[48] K.S. Pitzer, E. Clementi, 1959, J. Am.Chem. Soc., 81, 4477.

[49] R. Hoffman, Tetrahedron, 1996, 22, 521.

[50] J.W. Welther, J.R. Van Zee, 1989, Chem.Rev., 89, 1713.

[51] A.D.J. Haymet, 1986, J.Am. Chem. Soc.,108, 319.

[52] A.D.J. Haymet, 1985, Chem. Phys. Lett., 122,421.

[53] R.C. Haddon, L.E. Brus, and K.Raghavachari, 1986, J. Mol. Struct., 125, 459.

[54] S. Satpathy, 1986, Chem. Phys. Lett, 130, 545.

[55] P.D. Hale, 1986, J.Am. Chem. Soc., 108, 6087.

[56] M.D. Newton, R.E. Stanton, 1986, J. Am. Chem. Soc., 108, 2469.

[57] N.Laouni, O.K. Andersen, and O.Gunnarson, 1995, Physical Review B, 51, 17446.

[58] S. Larson, A. Volgov, anmd A. Rosen, 1987, Chem. Phys. Lett., 137, 501.

[59] I. Loszlo, L. Udvardi, 1989, J. Mol. Struct., 183, 271.

[60] M. Braga, A. Rosen, and S. Larsson, 1990, Z.Phys. D., In Press.

[61] D. L. Lictenberger, K.W. Nebesny, et al.,1991, Chem. Phys. Lett., 176, 203.

[62] S.H. Yeng, C.L. Petiette, 1987, Chem. Phys. Lett., 139, 233.

[63] R.E. Stanton, M.D. Newton, 1988, J.Phys. Chem., 92, 2141.

[64] P.D. Radi, M.T. Hsu, et al., 1990, Chem. Phys. Lett., 174, 2223.

[65] R. Taylor, J.P. Hare, 1990, Chem. Soc., Chem. Commun., 1423.

[66] R.D. Johnson, G. Meijer, and D.S. Bethuna, 1990, J. Am. Chem. Soc., 112, 8983.

[67] F.D. Weiss, J.L.Elkind, and et al., 1988, J. Am. Chem. Soc., 110, 4464.

[68] A. Rosen, B. Watsberg, 1988, J. Am. Chem. Soc., 110, 870.

[69] B. Watsberg, A. Rosen, 1991, Physica Scripta, 44, 276.

[70] J.N. Liu, B.L. Gu, et al., 1993, Solid State Comminucations, 85, No:2, 89-92.

[71] K.Tanaka, M.Okada, et a., Nuclear 1,2,3, Vol:193, 1992.

[72] R. Saito, G. Dresselhaus, M.S. Dreseelhaus, 1992, Physical Review B., 46, 9906.

[73] K. Yabana, G.F. Bertsch, 1997, Physica Scripta, 48, 533-637.

[74] R.Englman, *The Jahn-Teller Effect in Molecules and Crystals,* (Wiley, London, 1972).

[75] B.Bersuker and V.Z.Polinger, *Vibronic Interactions in Molecules and Crystals* (Springer Verlag, Berlin, 1989).

[76] E.Lo and B.R. Judd, 1999, Phys.Rev. Lett. 82, 3224 .

[77] J.Ihm, 1994, Physical Review B, 49, 10726.

[78] M. Born, R. Oppenheimer, 1927, Annln Phys., 84, 57.

[79] P.W. Fowler, A. Ceulemans, 1985, Molecular Physics, 54, 767.

[80] A.Ceulemans, 1987, J.Chem. Phys. 87, 5374.

[81] A.Ceulemans, D.Beyens, and L.G. Vankickenborne, 1984, J. Am. Chem. Soc. 106, 5284.

[82] A.Ceulemans, P.W. Fowler, 1990, J. Chem. Phys. 93, 1221.

[83] O.Gunnarson, 1996, Max-Planck-Institut., 1.

[84] P.L. Rios, N. Manini, E. Tosatti, 1996, Phys.Rev.B, 54, 7157.

[85] D. R.Pooler, J.Phys.C: , 1980, Solid St.Phys. 13, 1029.

[86] S.E. Apsel, C.C. Chancey, M.C.M O'Brien, 1992, Phys. Rev. B, 45, 5251.

[87] N. Manini, E. Tosatti, A. Auerbach, 1994, Phys. Rev. B, 49, 13008.

[88] L. Michel, 1980, Rev.Mod.Phys., 52, 617.

[89] M. Koca, R. Koç, 1997, M. Al-Barwani, J.Phys.A: Math.Gen., 30, 2109.

[90] M.C.M. O'Brien, 1996, Phys.Rev.B , 53, 3775.

[91] C.P.Moate, J.L.Dunn,C.A.Bates and Y.M.Liu, 1997, Zeitschrift fur Physikalische Chemie, 200, 137.

[92] C.C. Chancey and M.C.M O'Brien, *The Jahn-Teller Effect in C_{60} and Other Icosahedral Complexes* (Princeton Press, 1997).

APPENDICES

APPENDIX A

MATHEMATICA PROGRAM TO OBTAIN MATRIX GENERATORS of CLOSED SUBGROUPS OF SO(3)

◆ This program computes the matrix generators of SO(3) and its subgroups. j is the angular momentum quantum number; JP and JM are ladder operators of J_+ and J_- respectively. J3 is angular momentum quantum orepator along the z direction.

```
j = 1; M = 2 j + 1;
JP = Table[0, {i, 1, M}, {k, 1, M}]; J3 = Table[0, {i, 1, M}, {k, 1, M}];
Do[JP[[i, i + 1]] = Sqrt[j (j + 1) - (j - i) (j - i + 1)], {i, 1, M - 1}];
Do[J3[[i, i]] = j - i + 1, {i, 1, M}]; JM = Transpose[JP]; J1 = (JP + JM)/2;
J2 = (JP - JM)/(2 I); J3;
```

Following part of the program evaluatesexponential form of the matrices into an appropriate form. For the above program aprropriate angles θ_1, θ_2, θ_3, ϕ_1, ϕ_2 and ϕ_3 are selected for Tetrehedral (T) Group

```
θ1 = 2 π/(3 Sqrt[3]); θ2 = 2 π/(3 Sqrt[3]); θ3 = 2 π/(3 Sqrt[3]); ϕ1 = π; ϕ2 = 0; ϕ3 = 0;
T1 = θ1 J1 + θ2 J2 + θ3 J3;
T2 = Simplify[ϕ1 J1 + ϕ2 J2 + ϕ3 J3];
G1 = Simplify[MatrixExp[T1 I]];
G2 = Simplify[MatrixExp[T2 I]];
```

◆ This following section of the program computes the matrices which transform G1 and G2 in to real basis

```
S =
  Table[If[i == k && k ≤ (M - 1)/2, 1/Sqrt[2], If[i + k == M + 1 && k ≤ (M - 1)/2,
      (-1)^(i+j+1)/Sqrt[2], If[i == k && i == (M + 1)/2, 1, If[i == k && k ≥ (M - 1)/2,
        I/Sqrt[2], If[i + k == M + 1 && k ≥ (M - 1)/2, I (-1)^(i+j)/Sqrt[2], 0]]]]],
    {k, 1, M}, {i, 1, M}];
R1 = FullSimplify[S . G1 . Inverse[S]];
R2 = FullSimplify[S . G2 . Inverse[S]];
```

APPENDIX B

GENERATORS OF ICOSAHEDRAL GROUP AND ITS SUBGROUPS

◆ 3, 4 and 5 dimensional irreducible representations for the icosahedral group

$$G_1[1] = \begin{pmatrix} \frac{1}{2} & -\frac{\sqrt{\frac{5}{3}}}{2} & \frac{1}{\sqrt{3}} \\ \frac{\sqrt{3}}{2} & \frac{\sqrt{5}}{6} & -\frac{1}{3} \\ 0 & \frac{2}{3} & \frac{\sqrt{5}}{3} \end{pmatrix}$$

$$G_1[2] = \begin{pmatrix} -1 & 0 & 0 \\ 0 & -\frac{\sqrt{5}}{3} & \frac{2}{3} \\ 0 & \frac{2}{3} & \frac{\sqrt{5}}{3} \end{pmatrix}$$

$$G_2[1] = \begin{pmatrix} \frac{1}{4} - \frac{\sqrt{5}}{4} & -\frac{\sqrt{\frac{5}{3}}}{4} + \frac{1}{4\sqrt{3}} & \frac{\sqrt{\frac{5}{3}}}{2} + \frac{1}{2\sqrt{3}} \\ \frac{\sqrt{\frac{5}{3}}}{4} + \frac{\sqrt{3}}{4} & -\frac{1}{12} - \frac{\sqrt{5}}{4} & \frac{1}{2} - \frac{\sqrt{5}}{6} \\ \frac{1}{\sqrt{3}} & \frac{\sqrt{5}}{3} & \frac{1}{3} \end{pmatrix}$$

$$G_2[2] = \begin{pmatrix} -\frac{1}{2} & -\frac{\sqrt{\frac{5}{3}}}{2} & \frac{1}{\sqrt{3}} \\ -\frac{\sqrt{\frac{5}{3}}}{2} & -\frac{1}{6} & -\frac{\sqrt{5}}{3} \\ \frac{1}{\sqrt{3}} & -\frac{\sqrt{5}}{3} & -\frac{1}{3} \end{pmatrix}$$

$$G_3[1] = \begin{pmatrix} -\frac{2}{3} & -\frac{\sqrt{\frac{5}{3}}}{2} & -\frac{\sqrt{5}}{6} & 0 \\ 0 & 0 & 0 & 1 \\ \frac{\sqrt{5}}{3} & -\frac{1}{\sqrt{3}} & -\frac{1}{3} & 0 \\ 0 & -\frac{1}{2} & \frac{\sqrt{3}}{2} & 0 \end{pmatrix}$$

$$G_3[2] = \begin{pmatrix} -\frac{2}{3} & 0 & \frac{\sqrt{5}}{3} & 0 \\ 0 & 0 & 0 & 1 \\ \frac{\sqrt{5}}{3} & 0 & \frac{2}{3} & 0 \\ 0 & 1 & 0 & 0 \end{pmatrix}$$

$$G_4[1] = \begin{pmatrix} -\frac{7}{18} & -\frac{\sqrt{\frac{5}{3}}}{2} & \frac{1}{\sqrt{3}} & -\frac{\sqrt{5}}{9} & \frac{1}{3\sqrt{3}} \\ \frac{7}{6\sqrt{3}} & -\frac{\sqrt{5}}{6} & \frac{1}{3} & \frac{\sqrt{\frac{5}{3}}}{3} & -\frac{1}{3} \\ \frac{\sqrt{\frac{5}{3}}}{3} & \frac{1}{3} & \frac{\sqrt{5}}{6} & -\frac{1}{6\sqrt{3}} & \frac{\sqrt{5}}{3} \\ -\frac{\sqrt{5}}{9} & \frac{1}{\sqrt{3}} & \frac{\sqrt{\frac{5}{3}}}{2} & \frac{1}{18} & -\frac{\sqrt{\frac{5}{3}}}{3} \\ -\frac{2}{3\sqrt{3}} & 0 & 0 & \frac{2\sqrt{\frac{5}{3}}}{3} & \frac{1}{3} \end{pmatrix}$$

$$G_4[2] = \begin{pmatrix} \frac{7}{9} & 0 & 0 & \frac{2\sqrt{5}}{9} & -\frac{2}{3\sqrt{3}} \\ 0 & \frac{\sqrt{5}}{3} & -\frac{2}{3} & 0 & 0 \\ 0 & -\frac{2}{3} & -\frac{\sqrt{5}}{3} & 0 & 0 \\ \frac{2\sqrt{5}}{9} & 0 & 0 & -\frac{1}{9} & \frac{2\sqrt{\frac{5}{3}}}{3} \\ -\frac{2}{3\sqrt{3}} & 0 & 0 & \frac{2\sqrt{\frac{5}{3}}}{3} & \frac{1}{3} \end{pmatrix}$$

◆ 3, 4 and 5 dimensional irreducible representations for the D_5 group

$$G_1[1] = \begin{pmatrix} \frac{1}{2} & -\frac{\sqrt{\frac{5}{3}}}{2} & \frac{1}{\sqrt{3}} \\ \frac{\sqrt{3}}{2} & \frac{\sqrt{5}}{6} & -\frac{1}{3} \\ 0 & \frac{2}{3} & \frac{\sqrt{5}}{3} \end{pmatrix}$$

$$G_1[2] = \begin{pmatrix} -1 & 0 & 0 \\ 0 & \frac{\sqrt{5}}{3} & -\frac{2}{3} \\ 0 & -\frac{2}{3} & -\frac{\sqrt{5}}{3} \end{pmatrix}$$

$$G_2[1] = \begin{pmatrix} \frac{1}{4}\frac{\sqrt{5}}{4} & -\frac{\sqrt{\frac{5}{3}}}{4} + \frac{1}{4\sqrt{3}} & \frac{\sqrt{\frac{5}{3}}}{2} + \frac{1}{2\sqrt{3}} \\ \frac{\sqrt{\frac{5}{3}}}{4} + \frac{\sqrt{3}}{4} & -\frac{1}{12} - \frac{\sqrt{5}}{4} & \frac{1}{2} - \frac{\sqrt{5}}{6} \\ \frac{1}{\sqrt{3}} & \frac{\sqrt{5}}{3} & \frac{1}{3} \end{pmatrix}$$

$$G_2[2] = \begin{pmatrix} -\frac{1}{4} + \frac{\sqrt{5}}{4} & \frac{\sqrt{\frac{5}{3}}}{4} - \frac{1}{4\sqrt{3}} & -\frac{\sqrt{\frac{5}{3}}}{2} - \frac{1}{2\sqrt{3}} \\ \frac{\sqrt{\frac{5}{3}}}{4} - \frac{1}{4\sqrt{3}} & -\frac{5}{12} - \frac{\sqrt{5}}{4} & -\frac{1}{2} + \frac{\sqrt{5}}{6} \\ -\frac{\sqrt{\frac{5}{3}}}{2} - \frac{1}{2\sqrt{3}} & -\frac{1}{2} + \frac{\sqrt{5}}{6} & -\frac{1}{3} \end{pmatrix}$$

$$G_3[1] = \begin{pmatrix} -\frac{2}{3} & -\frac{\sqrt{\frac{5}{3}}}{2} & -\frac{\sqrt{5}}{6} & 0 \\ 0 & 0 & 0 & 1 \\ \frac{\sqrt{5}}{3} & -\frac{1}{\sqrt{3}} & -\frac{1}{3} & 0 \\ 0 & -\frac{1}{2} & \frac{\sqrt{3}}{2} & 0 \end{pmatrix}$$

$$G_3[2] = \begin{pmatrix} -\frac{2}{3} & 0 & \frac{\sqrt{5}}{3} & 0 \\ 0 & 0 & 0 & -1 \\ \frac{\sqrt{5}}{3} & 0 & \frac{2}{3} & 0 \\ 0 & -1 & 0 & 0 \end{pmatrix}$$

$$G_4[1] = \begin{pmatrix} -\frac{7}{18} & -\frac{\sqrt{\frac{5}{3}}}{2} & \frac{1}{\sqrt{3}} & -\frac{\sqrt{5}}{9} & \frac{1}{3\sqrt{3}} \\ \frac{7}{6\sqrt{3}} & -\frac{\sqrt{5}}{6} & \frac{1}{3} & \frac{\sqrt{\frac{5}{3}}}{3} & -\frac{1}{3} \\ \frac{\sqrt{\frac{5}{3}}}{3} & \frac{1}{3} & \frac{\sqrt{5}}{6} & -\frac{1}{6\sqrt{3}} & \frac{\sqrt{5}}{3} \\ -\frac{\sqrt{5}}{9} & \frac{1}{\sqrt{3}} & \frac{\sqrt{\frac{5}{3}}}{2} & \frac{1}{18} & -\frac{\sqrt{\frac{5}{3}}}{3} \\ -\frac{2}{3\sqrt{3}} & 0 & 0 & \frac{2\sqrt{\frac{5}{3}}}{3} & \frac{1}{3} \end{pmatrix}$$

$$G_4[2] = \begin{pmatrix} \frac{7}{9} & 0 & 0 & \frac{2\sqrt{5}}{9} & -\frac{2}{3\sqrt{3}} \\ 0 & -\frac{\sqrt{5}}{3} & \frac{2}{3} & 0 & 0 \\ 0 & \frac{2}{3} & \frac{\sqrt{5}}{3} & 0 & 0 \\ \frac{2\sqrt{5}}{9} & 0 & 0 & -\frac{1}{9} & \frac{2\sqrt{\frac{5}{3}}}{3} \\ -\frac{2}{3\sqrt{3}} & 0 & 0 & \frac{2\sqrt{\frac{5}{3}}}{3} & \frac{1}{3} \end{pmatrix}$$

◆ 3, 4 and 5 dimensional irreducible representations for the D_2 group

$$G_1[1] = \begin{pmatrix} -1 & 0 & 0 \\ 0 & -\frac{\sqrt{5}}{3} & \frac{2}{3} \\ 0 & \frac{2}{3} & \frac{\sqrt{5}}{3} \end{pmatrix}$$

$$G_1[2] = \begin{pmatrix} -1 & 0 & 0 \\ 0 & \frac{\sqrt{5}}{3} & -\frac{2}{3} \\ 0 & -\frac{2}{3} & -\frac{\sqrt{5}}{3} \end{pmatrix}$$

$$G_2[1] = \begin{pmatrix} -\frac{1}{2} & -\frac{\sqrt{\frac{5}{3}}}{2} & \frac{1}{\sqrt{3}} \\ -\frac{\sqrt{\frac{5}{3}}}{2} & -\frac{1}{6} & -\frac{\sqrt{5}}{3} \\ \frac{1}{\sqrt{3}} & -\frac{\sqrt{5}}{3} & -\frac{1}{3} \end{pmatrix}$$

$$G_2[2] = \begin{pmatrix} -\frac{1}{4} + \frac{\sqrt{5}}{4} & \frac{\sqrt{\frac{5}{3}}}{4} - \frac{1}{4\sqrt{3}} & -\frac{\sqrt{\frac{5}{3}}}{2} - \frac{1}{2\sqrt{3}} \\ \frac{\sqrt{\frac{5}{3}}}{4} - \frac{1}{4\sqrt{3}} & -\frac{5}{12} - \frac{\sqrt{5}}{4} & -\frac{1}{2} + \frac{\sqrt{5}}{6} \\ -\frac{\sqrt{\frac{5}{3}}}{2} - \frac{1}{2\sqrt{3}} & -\frac{1}{2} + \frac{\sqrt{5}}{6} & -\frac{1}{3} \end{pmatrix}$$

$$G_3[1] = \begin{pmatrix} -\frac{2}{3} & 0 & \frac{\sqrt{5}}{3} & 0 \\ 0 & 0 & 0 & 1 \\ \frac{\sqrt{5}}{3} & 0 & \frac{2}{3} & 0 \\ 0 & 1 & 0 & 0 \end{pmatrix}$$

$$G_3[2] = \begin{pmatrix} -\frac{2}{3} & 0 & \frac{\sqrt{5}}{3} & 0 \\ 0 & 0 & 0 & -1 \\ \frac{\sqrt{5}}{3} & 0 & \frac{2}{3} & 0 \\ 0 & -1 & 0 & 0 \end{pmatrix}$$

$$G_4[1] = \begin{pmatrix} \frac{7}{9} & 0 & 0 & \frac{2\sqrt{5}}{9} & -\frac{2}{3\sqrt{\square}} \\ 0 & \frac{\sqrt{5}}{3} & -\frac{2}{3} & 0 & 0 \\ 0 & -\frac{2}{3} & -\frac{\sqrt{5}}{3} & 0 & 0 \\ \frac{2\sqrt{5}}{9} & 0 & 0 & -\frac{1}{9} & \frac{2\sqrt{\frac{5}{3}}}{3} \\ -\frac{2}{3\sqrt{3}} & 0 & 0 & \frac{2\sqrt{\frac{5}{3}}}{3} & \frac{1}{3} \end{pmatrix}$$

$$G_4[2] = \begin{pmatrix} \frac{7}{9} & 0 & 0 & \frac{2\sqrt{5}}{9} & -\frac{2}{3\sqrt{3}} \\ 0 & -\frac{\sqrt{5}}{3} & \frac{2}{3} & 0 & 0 \\ 0 & \frac{2}{3} & \frac{\sqrt{5}}{3} & 0 & 0 \\ \frac{2\sqrt{5}}{9} & 0 & 0 & -\frac{1}{9} & \frac{2\sqrt{\frac{5}{3}}}{3} \\ -\frac{2}{3\sqrt{3}} & 0 & 0 & \frac{2\sqrt{\frac{5}{3}}}{3} & \frac{1}{3} \end{pmatrix}$$

◆ 3, 4 and 5 dimensional irreducible representations for the D_3 group

$$G_1[1] = \begin{pmatrix} \frac{1}{4} + \frac{\sqrt{5}}{4} & \frac{\sqrt{\frac{5}{3}}}{4} - \frac{\sqrt{3}}{4} & \frac{1}{\sqrt{3}} \\ \frac{\sqrt{\frac{5}{3}}}{4} + \frac{1}{4\sqrt{3}} & \frac{1}{12} - \frac{\sqrt{5}}{4} & -\frac{\sqrt{5}}{3} \\ \frac{\sqrt{\frac{5}{3}}}{2} - \frac{1}{2\sqrt{3}} & \frac{1}{2} + \frac{\sqrt{5}}{6} & -\frac{1}{3} \end{pmatrix}$$

$$G_1[2] = \begin{pmatrix} -1 & 0 & 0 \\ 0 & \frac{\sqrt{5}}{3} & -\frac{2}{3} \\ 0 & -\frac{2}{3} & -\frac{\sqrt{5}}{3} \end{pmatrix}$$

$$G_2[1] = \begin{pmatrix} \frac{1}{4} - \frac{\sqrt{5}}{4} & -\frac{\sqrt{\frac{5}{3}}}{4} - \frac{\sqrt{3}}{4} & -\frac{1}{\sqrt{3}} \\ -\frac{\sqrt{\frac{5}{3}}}{4} + \frac{1}{4\sqrt{3}} & \frac{1}{12} + \frac{\sqrt{5}}{4} & -\frac{\sqrt{5}}{3} \\ \frac{\sqrt{\frac{5}{3}}}{2} + \frac{1}{2\sqrt{3}} & -\frac{1}{2} + \frac{\sqrt{5}}{6} & -\frac{1}{3} \end{pmatrix}$$

$$G_2[2] = \begin{pmatrix} -\frac{1}{4} + \frac{\sqrt{5}}{4} & \frac{\sqrt{\frac{5}{3}}}{4} - \frac{1}{4\sqrt{3}} & -\frac{\sqrt{\frac{5}{3}}}{2} - \frac{1}{2\sqrt{3}} \\ \frac{\sqrt{\frac{5}{3}}}{4} - \frac{1}{4\sqrt{3}} & -\frac{5}{12} - \frac{\sqrt{5}}{4} & -\frac{1}{2} + \frac{\sqrt{5}}{6} \\ -\frac{\sqrt{\frac{5}{3}}}{2} - \frac{1}{2\sqrt{3}} & -\frac{1}{2} + \frac{\sqrt{5}}{6} & -\frac{1}{3} \end{pmatrix}$$

$$G_3[1] = \begin{pmatrix} \frac{1}{6} & 0 & -\frac{\sqrt{5}}{3} & -\frac{\sqrt{\frac{5}{3}}}{2} \\ -\frac{\sqrt{\frac{5}{3}}}{2} & \frac{1}{2} & \frac{1}{2\sqrt{3}} & -\frac{1}{2} \\ \frac{\sqrt{5}}{6} & \frac{\sqrt{3}}{2} & -\frac{1}{6} & \frac{1}{2\sqrt{3}} \\ -\frac{\sqrt{\frac{5}{3}}}{2} & 0 & -\frac{1}{\sqrt{3}} & \frac{1}{2} \end{pmatrix}$$

$$G_3[2] = \begin{pmatrix} -\frac{2}{3} & 0 & \frac{\sqrt{5}}{3} & 0 \\ 0 & 0 & 0 & -1 \\ \frac{\sqrt{5}}{3} & 0 & \frac{2}{3} & 0 \\ 0 & -1 & 0 & 0 \end{pmatrix}$$

$$G_4[1] = \begin{pmatrix} \frac{5}{36}+\frac{\sqrt{5}}{12} & -\frac{\sqrt{\frac{5}{3}}}{12}+\frac{5}{12\sqrt{3}} & \frac{\sqrt{\frac{5}{3}}}{3}+\frac{2}{3\sqrt{3}} & -\frac{2}{3}+\frac{\sqrt{5}}{9} & -\frac{1}{3\sqrt{3}} \\ -\frac{\sqrt{\frac{5}{3}}}{12}+\frac{\sqrt{3}}{4} & -\frac{1}{4}-\frac{\sqrt{5}}{12} & -\frac{1}{3} & -\frac{1}{3\sqrt{3}} & -\frac{\sqrt{5}}{3} \\ \frac{2}{3\sqrt{3}} & \frac{2}{3} & -\frac{1}{4}+\frac{\sqrt{5}}{12} & \frac{\sqrt{\frac{5}{3}}}{12}+\frac{\sqrt{3}}{4} & -\frac{1}{3} \\ \frac{1}{3}+\frac{\sqrt{5}}{9} & \frac{\sqrt{\frac{5}{3}}}{3}-\frac{1}{3\sqrt{3}} & \frac{\sqrt{\frac{5}{3}}}{12}-\frac{11}{12\sqrt{3}} & -\frac{11}{36}-\frac{\sqrt{5}}{12} & \frac{\sqrt{\frac{5}{3}}}{3} \\ -\frac{\sqrt{\frac{5}{3}}}{2}+\frac{1}{6\sqrt{3}} & \frac{1}{6}+\frac{\sqrt{5}}{6} & \frac{1}{6}-\frac{\sqrt{5}}{6} & -\frac{\sqrt{\frac{5}{3}}}{6}-\frac{1}{2\sqrt{3}} & -\frac{1}{3} \end{pmatrix}$$

$$G_4[2] = \begin{pmatrix} \frac{7}{9} & 0 & 0 & \frac{2\sqrt{5}}{9} & -\frac{2}{3\sqrt{3}} \\ 0 & -\frac{\sqrt{5}}{3} & \frac{2}{3} & 0 & 0 \\ 0 & \frac{2}{3} & \frac{\sqrt{5}}{3} & 0 & 0 \\ \frac{2\sqrt{5}}{9} & 0 & 0 & -\frac{1}{9} & \frac{2\sqrt{\frac{5}{3}}}{3} \\ -\frac{2}{3\sqrt{3}} & 0 & 0 & \frac{2\sqrt{\frac{5}{3}}}{3} & \frac{1}{3} \end{pmatrix}$$

◆ <u>3,4 and 5 dimensional irreducible representations for the Tetrahedral (T) group</u>

$$G_1[1] = \begin{pmatrix} -\frac{1}{2} & \frac{\sqrt{3}}{2} & 0 \\ -\frac{\sqrt{3}}{2} & -\frac{1}{2} & 0 \\ 0 & 0 & 1 \end{pmatrix}$$

$$G_1[2] = \begin{pmatrix} \frac{1}{4}+\frac{\sqrt{5}}{4} & \frac{\sqrt{\frac{5}{3}}}{4}-\frac{\sqrt{3}}{4} & \frac{1}{\sqrt{3}} \\ \frac{\sqrt{\frac{5}{3}}}{4}+\frac{1}{4\sqrt{3}} & \frac{1}{12}-\frac{\sqrt{5}}{4} & -\frac{\sqrt{5}}{3} \\ \frac{\sqrt{\frac{5}{3}}}{2}-\frac{1}{2\sqrt{3}} & \frac{1}{2}+\frac{\sqrt{5}}{6} & -\frac{1}{3} \end{pmatrix}$$

$$G_2[1] = \begin{pmatrix} \frac{1}{4} + \frac{\sqrt{5}}{4} & -\frac{\sqrt{\frac{5}{3}}}{4} - \frac{1}{4\sqrt{3}} & -\frac{\sqrt{\frac{5}{3}}}{2} + \frac{1}{2\sqrt{3}} \\ -\frac{\sqrt{\frac{5}{3}}}{4} + \frac{\sqrt{3}}{4} & \frac{1}{12} - \frac{\sqrt{5}}{4} & \frac{1}{2} + \frac{\sqrt{5}}{6} \\ -\frac{1}{\sqrt{3}} & -\frac{\sqrt{5}}{3} & -\frac{1}{3} \end{pmatrix}$$

$$G_2[2] = \begin{pmatrix} \frac{1}{4} + \frac{\sqrt{5}}{4} & \frac{\sqrt{\frac{5}{3}}}{4} - \frac{\sqrt{3}}{4} & \frac{1}{\sqrt{3}} \\ \frac{\sqrt{\frac{5}{3}}}{4} + \frac{1}{4\sqrt{3}} & \frac{1}{12} - \frac{\sqrt{5}}{4} & -\frac{\sqrt{5}}{3} \\ \frac{\sqrt{\frac{5}{3}}}{2} - \frac{1}{2\sqrt{3}} & \frac{1}{2} + \frac{\sqrt{5}}{6} & -\frac{1}{3} \end{pmatrix}$$

$$G_3[1] = \begin{pmatrix} \frac{1}{6} & 0 & -\frac{\sqrt{5}}{3} & -\frac{\sqrt{\frac{5}{3}}}{2} \\ 0 & 1 & 0 & 0 \\ -\frac{\sqrt{5}}{3} & 0 & \frac{1}{3} & -\frac{1}{\sqrt{3}} \\ \frac{\sqrt{\frac{5}{3}}}{2} & 0 & \frac{1}{\sqrt{3}} & -\frac{1}{2} \end{pmatrix}$$

$$G_3[2] = \begin{pmatrix} \frac{1}{6} & 0 & -\frac{\sqrt{5}}{3} & -\frac{\sqrt{\frac{5}{3}}}{2} \\ -\frac{\sqrt{\frac{5}{3}}}{2} & \frac{1}{2} & \frac{1}{2\sqrt{3}} & -\frac{1}{2} \\ \frac{\sqrt{5}}{6} & \frac{\sqrt{3}}{2} & -\frac{1}{6} & \frac{1}{2\sqrt{3}} \\ -\frac{\sqrt{\frac{5}{3}}}{2} & 0 & -\frac{1}{\sqrt{3}} & \frac{1}{2} \end{pmatrix}$$

$$G_4[1] = \begin{pmatrix} -\frac{1}{2} & -\frac{\sqrt{3}}{2} & 0 & 0 & 0 \\ \frac{\sqrt{3}}{2} & -\frac{1}{2} & 0 & 0 & 0 \\ 0 & 0 & -\frac{1}{2} & \frac{\sqrt{3}}{2} & 0 \\ 0 & 0 & -\frac{\sqrt{3}}{2} & -\frac{1}{2} & 0 \\ 0 & 0 & 0 & 0 & 1 \end{pmatrix}$$

$$G_4[2] = \begin{pmatrix} \frac{5}{36} + \frac{\sqrt{5}}{12} & -\frac{\sqrt{\frac{5}{3}}}{12} + \frac{5}{12\sqrt{3}} & \frac{\sqrt{\frac{5}{3}}}{3} + \frac{2}{3\sqrt{3}} & -\frac{2}{3} + \frac{\sqrt{5}}{9} & -\frac{1}{3\sqrt{3}} \\ -\frac{\sqrt{\frac{5}{3}}}{12} + \frac{\sqrt{3}}{4} & -\frac{1}{4} - \frac{\sqrt{5}}{12} & -\frac{1}{3} & -\frac{1}{3\sqrt{3}} & -\frac{\sqrt{5}}{3} \\ \frac{2}{3\sqrt{3}} & \frac{2}{3} & -\frac{1}{4} + \frac{\sqrt{5}}{12} & \frac{\sqrt{\frac{5}{3}}}{12} + \frac{\sqrt{3}}{4} & -\frac{1}{3} \\ \frac{1}{3} + \frac{\sqrt{5}}{9} & \frac{\sqrt{\frac{5}{3}}}{3} - \frac{1}{3\sqrt{3}} & \frac{\sqrt{\frac{5}{3}}}{12} - \frac{11}{12\sqrt{3}} & -\frac{11}{36} - \frac{\sqrt{5}}{12} & \frac{\sqrt{\frac{5}{3}}}{3} \\ -\frac{\sqrt{\frac{5}{3}}}{2} + \frac{1}{6\sqrt{3}} & \frac{1}{6} + \frac{\sqrt{5}}{6} & \frac{1}{6} - \frac{\sqrt{5}}{6} & -\frac{\sqrt{\frac{5}{3}}}{6} - \frac{1}{2\sqrt{3}} & -\frac{1}{3} \end{pmatrix}$$

APPENDIX C

MATHEMATICA PROGRAM TO GET BLOCKDIAGONALIZED HÜCKEL HAMILTONIAN MATRICES

◆ This section evaluates all matrix elements for 3-D representation. g[1] and g[2] are the generators of Icosahedral group. kp shows number of generators, lp, mp and np matrix powers of generators. op implies dimension of the representation

```
g[1] = G2[1]; g[1] = G2[2]; mp = 5; np = 3; lp = 2; kp = 2; op = 3
Do[kp++; g[kp] = Expand[MatrixPower[g[1], j]], {j, 1, mp}
Do[kp++; g[kp] = Expand[MatrixPower[g[2], j]], {j, 1, np}
Do[kp++; g[kp] = Expand[MatrixPower[g[1].g[2], j]], {j, 1, lp}]
GT1 = Table[
        Expand[Transpose[g[i]].g[j].g[i]], {i, 1, kp}, {j, 1, kp}] // Flatten;
  GT1 = Partition[GT1, op]; GT1 = Partition[GT1, op];
  GT1 = Union[GT1]; kp = Dimensions[GT1][[1]]
GT1 = Table[{Expand[GT1[[i]].GT1[[j]]]}, {i, 1, kp}, {j, 1, kp}] // Flatten;
  GT1 = Partition[GT1, op]; GT1 = Partition[GT1, op];
  GT1 = Union[GT1]; kp = Dimensions[GT1][[1]]
```

◆ This part shows the character table in terms of each irreducible representation seperating the conjugacy classes. ct[i] represents the conjugacy classes.

```
GT2 = GT1; kz = 0; kj = kp; kk = 0; Do[kk++;
  ct[k] = Table[Expand[GT1[[j]].GT2[[1]].Transpose[GT1[[j]]]], {j, 1, kp}];
  ct[k] = Union[ct[k]]; GT2 = Complement[GT2, ct[k]];
  kz = kz + Dimensions[ct[k]][[1]]; kj = kp - kz;
  If[kz == kp, Break[], Continue[]], {k, 1, kj}]; DisplayForm[
  GridBox[Table[{Dimensions[ct[k]][[1]], Tr[ct[k][[1]]]}, {k, 1, kk}],
    RowLines → True, ColumnLines → True]];
DisplayForm[FrameBox[%]]
```

◆ This part computes the position vectors of sixty atoms using the matrix elements. GT1 is combined form of classes. R[i] is the position vectors.

```
GT1 = Join[ct[5], ct[2], ct[3], ct[4], ct[1]];
Y[1] = FullSimplify[{3 (1 + Sqrt[5]) / 2, 1, 0}];
Do[R[i] = Simplify[GT1[[i]] . Y[1]], {i, 1, kp}];
FullSimplify[Table[R[i], {i, 1, 60}]];
st = Sort[Simplify[Table[(R[1] - R[j]) . (R[1] - R[j]), {j, 2, 60}]], Greater]
```

◆ This part computes Hückel matrices and Projection operators of icosahedral symmetry. B is the matrix representations to get Hückel matrix in terms of new position vectors after operating the generators of icosahedral group seperately for each class. PT1 is the projection operators and HCK is the Hückel matrix.

```
B = Table[If[Expand[GT1[[i]] . R[j]] == Expand[R[k]], 1, 0],
    {i, 1, kp}, {k, 1, kp}, {j, 1, 1}];
B = Flatten[B]; B = Partition[B, kp];
Do[If[B[[i, k]] == 1, f[i] = k, Continue[]], {k, 1, kp}, {i, 1, kp}]; kt = 0;
Do[kt++; Do[p[kt, f[i]] = GT1[[i, j, k]], {i, 1, kp}], {j, 1, op}, {k, 1, op}]
PT1 = Table[p[i, j], {i, 1, op op}, {j, 1, kp}];
Do[PT1[[i]] = Simplify[PT1[[i]] / Sqrt[Expand[PT1[[i]] . PT1[[i]]]]], {i, 1, op op}]
PTA = Table[1, {i, 1, 60}]; PTA = Simplify[PTA / Sqrt[Expand[PTA . PTA]]];
PT1 = {PTA}; HCK = Table[If[Simplify[(R[j] - R[i]) . (R[j] - R[i])] == 4,
      β, If[Simplify[(R[j] - R[i]) . (R[j] - R[i])] ==
        1/6 (67 - 6 Sqrt[3] - 3 Sqrt[5] - 6 Sqrt[15]), γ, 0]],
    {j, 1, kp}, {i, 1, kp}];
```

◆ This part calculates the block diagonalized Hückel matrices using Projection operators. Eigenvalues of each block diagonalized Hückel matrices gives molecular energy levels.

```
HT1 = Expand[PT1 . HCK . Transpose[PT1]];
ET1 = Eigenvalues[HT1];
```

APPENDIX D

PROJECTION OPERATORS FOR ICOSAHEDRAL SYMMETRY

$$P_{T_1} = \begin{cases} \frac{1}{4\sqrt{5}}(2,-2,-\tau,-\tau,-\tau,-\tau,\sigma,\sigma,\sigma,\sigma,-1,2,-1,-1,-1,-2,-1,-1,-1,-1,0,\tau,0,0,0,0,0,\tau,-\sigma,-\sigma,\tau,-\sigma,0,-\sigma,\tau,0, \\ \quad 1,\tau,1,\sigma,\tau,1,\tau,\tau,\sigma,\sigma,\sigma,1,1,1,-\tau,-\tau,-\tau,1,1,-\tau,-\sigma,-\sigma,-\sigma,-\sigma) \\ \frac{1}{8\sqrt{15}}(0,0,-2\,\kappa,2\,\kappa,-2\,\tau,2\,\tau,2\,\nu,-2\,\sigma,2\,\sigma,-2\,\nu,6,0,-2\sqrt{5},2\sqrt{5},-6,0,6,2\sqrt{5},-6,-2\sqrt{5},4\,\sigma,-2\,\kappa,-4\,\tau, \\ \quad 4\,\sigma,4\,\tau,2-2\sqrt{5},4\,\tau,2\,\tau,-2\,\sigma,2\,\nu,2\,\kappa,-2\,\nu,2-2\sqrt{5},2\,\sigma,-2\,\tau,-4\,\tau,-2\sqrt{5},-2\,\tau,-6,-2\,\sigma,2\,\tau,6,-2\,\kappa, \\ \quad 2\,\kappa,-2\,\nu,2\,\sigma,2\,\nu2\sqrt{5},2\sqrt{5},-2\sqrt{5},2\,\tau,2\,\kappa,-2\,\kappa,6,-6,-2\,\tau,-2\,\sigma,2\,\nu,-2\,\nu,2\,\sigma) \\ \frac{1}{2\sqrt{15}}(0,0,1,-1,-\sigma,\sigma,1,\tau,-\tau,-1,0,0,1,-1,0,0,0,-1,0,1,\tau,1,\sigma,\tau,-\sigma,-\tau,-\sigma,\sigma,\tau,\ 1,-1,-1,-\tau,-\tau,-\sigma,\sigma,1, \\ \quad -\sigma,0,\tau,\sigma,0,1,-1,-1,-\tau,1,-1,-1,1,\sigma,-1,1,0,0,-\sigma,\tau,\ 1,-1,-\tau) \end{cases}$$

$$P_{T_2} = \begin{cases} \frac{1}{4\sqrt{5}}(2,-1,-1,-2,\sigma,-\tau,2,-\tau,-1,\sigma,-\tau,-\tau,\sigma,-1,-2,\sigma,\tau,0,\tau,0,-\sigma,-\sigma,0,0,\tau,-1,-\sigma,-\sigma,-1, \\ \quad 0,0,-1,\tau,0,0,-1,-\sigma,1,-\tau,1,-\sigma,-\sigma,1,-\sigma,-\tau,1,-\tau,-\tau,1,\tau,\sigma,\tau,\tau,1,\tau,\sigma,1,1,\sigma,\sigma) \\ \frac{1}{4\sqrt{15}}(0,-\sqrt{5},3,0,\nu,-\tau,0,\kappa,\sqrt{5},-\nu,-\kappa,\tau,-\sigma,-3,0,\sigma,-\tau,\ 2\,\tau,\kappa,-2\,\sigma,\nu,-\nu,-2\,\tau,-2\,\sigma,-\kappa, \\ \quad -3,\sigma,-\sigma,-\sqrt{5},2\,\tau,2\,\sigma,\sqrt{5},\tau,2\,\sigma,-2\,\tau,3,-\sigma,\sqrt{5},\kappa,-\sqrt{5},\sigma,\nu,3,-\nu,\tau,-3,-\tau,-\kappa,\sqrt{5},\kappa, \\ \quad \nu,-\kappa,-\tau,-3,\tau,-\nu,3,-\sqrt{5},-\sigma,\sigma) \\ \frac{1}{2\sqrt{15}}(0,1,0,0,1,-\sigma,0,-1,-1,-1,1,\sigma,\tau,0,0,-\tau,-\sigma,-\sigma,-1,-\tau,1,-1,\sigma,-\tau,1,0,-\tau,\tau,1,-\sigma, \\ \quad \tau,-1,\sigma,\tau,\sigma,0,\tau,-1,-1,1,-\tau,1,0,-1,\sigma,0,-\sigma,1,-1,-1,1,1,-\sigma,0,\sigma,-1,0,1,\tau,-\tau) \end{cases}$$

$$P_G = \begin{cases} \frac{1}{6\sqrt{15}}(6,-4,1,1,-4,-4,1,-4,-4,1,1,6,6,6,1,-4,1,6,1,6,1,1,1,1,1,1,1,1,1,1,1,1,1,1,1,1,\ 1,-4,1,-4,-4,\\ \quad 1,-4,1,1,1,-4,1,-4,-4,-4,-4,1,1,-4,-4,-4,1,1,1,1) \\ \frac{1}{6}(0,0,-1,1,1,-1,-1,1,-1,1,0,0,0,0,0,0,0,0,0,0,0,1,0,-1,1,1,-1,1,-1,1,0,0,0,-1,-1,1,-1,-1,1,0,1,-1,\\ \quad 0,0,0,1,-1,-1,1,1,-1,-1,1,-1,0,0,1,1,0,0,-1) \\ \frac{1}{6\sqrt{3}}(0,2,1,1,-1,-1,1,-1,-1,1,-2,0,0,0,-2,2,-2,0,-2,0,1,-2,1,1,1,1,1,1,1,-2,-2,-2,1,1,1,1,-1,1,2,\\ \quad -1,1,2,-2,-2,1,-1,1,-1,-1,-1,-1,1,1,2,2,-1,1,-2,-2,1) \\ \frac{1}{6}(0,0,-1,1,0,0,1,0,0,-1,-1,0,0,0,1,0,-1,0,1,0,1,-1,1,1,-1,-1,-1,-1,-1,1,\ 1,-1,-1,1,1,1,0,1,0,0,\\ \quad -1,0,-1,1,-1,0,1,0,0,0,0,1,-1,0,0,0,-1,1,-1,1) \end{cases}$$

$$P_H = \begin{cases} \frac{1}{36}(0,-4,2,2,\eta,\eta,2,\lambda,\lambda,2,0,0,-2,-2,0,-4,0,-2,0,-2,\eta,\eta,\lambda,\eta,\lambda,\eta,\lambda,-2,-2,\lambda,\eta,\lambda,\eta,-2,-2,\lambda,-4,-2,\\ \quad 2,\lambda,-2,2,\eta,\eta,2,\lambda,2,-4,-4,-4,\eta,2,2,2,2,\eta,-2,\lambda,\lambda,-2) \\ \frac{1}{12\sqrt{3}}(0,0,-2,2,-2\tau,2\tau,2,-2\sigma,2\sigma,-2,0,0,-2\sqrt{5},2\sqrt{5},0,0,0,2\sqrt{5},0,-2\sqrt{5},-2\tau,2\tau,2\sigma,-2\tau,\\ \quad -2\sigma,2\tau,-2\sigma,-2\sqrt{5},2\sqrt{5},2\sigma,-2\tau,-2\sigma,2\tau,-2\sqrt{5},2\sqrt{5},2\sigma,0,2\sqrt{5},2,-2\sigma,-2\sqrt{5},-2,2\tau,-2\tau,\\ \quad -2,2\sigma,2,0,0,0,2\tau,2,-2,-2,2,-2\tau,2\sqrt{5},2\sigma,-2\sigma,-2\sqrt{5}) \\ \frac{1}{6\sqrt{3}}(0,0,\sqrt{5},-\sqrt{5},\sigma,-\sigma,-\sqrt{5},-\tau,\tau,\sqrt{5},0,0,-1,1,0,0,0,1,0,-1,\sigma,-\sigma,\tau,\sigma,-\tau,-\sigma,-\tau,-1,1,\tau,\ \sigma,-\tau,\\ \quad -\sigma,-1,1,\tau,0,1,-\sqrt{5},-\tau,-1,\sqrt{5},-\sigma,\sigma,\sqrt{5},\tau,-\sqrt{5},0,0,0,-\sigma,-\sqrt{5},\sqrt{5},\sqrt{5},-\sqrt{5},\sigma,1,\ \tau,-\tau,-1) \\ \frac{1}{36}(0,4\sqrt{5},-2\sqrt{5},-2\sqrt{5},-2\upsilon,-2\upsilon,-2\sqrt{5},2\kappa,2\kappa,-2\sqrt{5},0,0,0,2\sqrt{5},2\sqrt{5},0,0,4\sqrt{5},0,0,2\sqrt{5},\ 0,\\ \quad 2\sqrt{5},-2\upsilon,-2\upsilon,2\kappa,-2\upsilon,2\kappa,-2\upsilon,2\kappa,2\sqrt{5},2\sqrt{5},2\kappa,-2\upsilon,2\kappa,-2\upsilon,2\sqrt{5},\ 2\sqrt{5},2\kappa,4\sqrt{5},2\sqrt{5},\\ \quad -2,2\kappa,2\sqrt{5},-2\sqrt{5},-2\upsilon,-2\upsilon,-2\sqrt{5},2\kappa,-2\sqrt{5},4\sqrt{5},4\sqrt{5},4\sqrt{5},-2\upsilon,-2\sqrt{5},-2\sqrt{5},-2\sqrt{5},\\ \quad -2\sqrt{5},-2\upsilon,2\sqrt{5},2\kappa,2\kappa,2\sqrt{5}) \\ \frac{1}{6\sqrt{3}}(3,1,1,1,-1,-1,1,-1,-1,1,3,3,-1,-1,3,1,3,-1,3,-1,-1,-1,-1,-1,-1,-1,-1,-1,-1,-1,-1,-1,-1,-1,-1,-1,-1,\\ \quad -1,1,-1,1,-1,-1,1,-1,-1,\ 1,-1,1,1,1,1,1,-1,1,1,1,1,1,-1,-1,-1,-1,-1) \end{cases}$$

$$\sigma=\frac{1}{2}(-1+\sqrt{5}),\ \tau=\frac{1}{2}(1+\sqrt{5}),\ \kappa=\frac{1}{2}(3-\sqrt{5}),\ \upsilon=\frac{1}{2}(3+\sqrt{5}),\ \eta=(1-3\sqrt{5}),\ \lambda=(1+3\sqrt{5})$$

APPENDIX E

HÜCKEL HAMILTONIAN MATRICES

$$H_{T1} = \begin{pmatrix} \beta + \frac{\gamma}{2} + \frac{\sqrt{5}\gamma}{2} & \frac{\gamma}{\sqrt{3}} & \frac{1}{2}\sqrt{\frac{5}{3}}\gamma - \frac{\sqrt{3}\gamma}{2} \\ \frac{\gamma}{\sqrt{3}} & -\beta - \frac{\gamma}{6} + \frac{\sqrt{5}\gamma}{2} & -\frac{\gamma}{2} + \frac{\sqrt{5}\gamma}{6} \\ \frac{1}{2}\sqrt{\frac{5}{3}}\gamma - \frac{\sqrt{3}\gamma}{2} & -\frac{\gamma}{2} + \frac{\sqrt{5}\gamma}{6} & -\beta + \frac{2\gamma}{3} \end{pmatrix}$$

$$H_{T2} = \begin{pmatrix} -\frac{\beta}{4} - \frac{\sqrt{5}\beta}{4} + \frac{\gamma}{2} - \frac{\sqrt{5}\gamma}{2} & \frac{1}{4}\sqrt{\frac{5}{3}}\beta + \frac{\beta}{4\sqrt{3}} - \frac{\gamma}{\sqrt{3}} & \frac{1}{2}\sqrt{\frac{5}{3}}\beta - \frac{\beta}{2\sqrt{3}} - \frac{1}{2}\sqrt{\frac{5}{3}}\gamma - \frac{\sqrt{3}\gamma}{2} \\ \frac{1}{4}\sqrt{\frac{5}{3}}\beta + \frac{\beta}{4\sqrt{3}} - \frac{\gamma}{\sqrt{3}} & -\frac{5\beta}{12} + \frac{\sqrt{5}\beta}{4} - \frac{\gamma}{6} - \frac{\sqrt{5}\gamma}{2} & \frac{\beta}{2} + \frac{\sqrt{5}\beta}{6} + \frac{\gamma}{2} + \frac{\sqrt{5}\gamma}{6} \\ \frac{1}{2}\sqrt{\frac{5}{3}}\beta - \frac{\beta}{2\sqrt{3}} - \frac{1}{2}\sqrt{\frac{5}{3}}\gamma - \frac{\sqrt{3}\gamma}{2} & \frac{\beta}{2} + \frac{\sqrt{5}\beta}{6} + \frac{\gamma}{2} + \frac{\sqrt{5}\gamma}{6} & -\frac{\beta}{3} + \frac{2\gamma}{3} \end{pmatrix}$$

$$H_G = \begin{pmatrix} \beta + \frac{\gamma}{3} & -\frac{1}{2}\sqrt{\frac{5}{3}}\gamma & -\frac{\sqrt{5}\gamma}{6} & 0 \\ -\frac{1}{2}\sqrt{\frac{5}{3}}\gamma & -\beta - \gamma & -\frac{\gamma}{\sqrt{3}} & \frac{\gamma}{2} \\ -\frac{\sqrt{5}\gamma}{6} & -\frac{\gamma}{\sqrt{3}} & \beta - \frac{\gamma}{3} & -\frac{\sqrt{3}\gamma}{2} \\ 0 & \frac{\gamma}{2} & -\frac{\sqrt{3}\gamma}{2} & -\beta - \gamma \end{pmatrix}$$

$$H_H = \begin{pmatrix} \beta + \frac{5\gamma}{18} + \frac{\sqrt{5}\gamma}{6} & \frac{\gamma}{3\sqrt{3}} & -\frac{1}{3}\sqrt{\frac{5}{3}}\gamma & -\frac{\gamma}{3} + \frac{2\sqrt{5}\gamma}{9} & -\frac{1}{2}\sqrt{\frac{5}{3}}\gamma - \frac{\gamma}{6\sqrt{3}} \\ \frac{\gamma}{3\sqrt{3}} & -\beta + \frac{\gamma}{2} + \frac{\sqrt{5}\gamma}{6} & -\frac{\gamma}{3} & -\frac{1}{3}\sqrt{\frac{5}{3}}\gamma & -\frac{\gamma}{6} - \frac{\sqrt{5}\gamma}{2} \\ -\frac{1}{3}\sqrt{\frac{5}{3}}\gamma & -\frac{\gamma}{3} & -\beta + \frac{\gamma}{2} - \frac{\sqrt{5}\gamma}{6} & \frac{5\gamma}{3\sqrt{3}} & -\frac{\gamma}{2} + \frac{\sqrt{5}\gamma}{6} \\ -\frac{\gamma}{3} + \frac{2\sqrt{5}\gamma}{9} & -\frac{1}{3}\sqrt{\frac{5}{3}}\gamma & \frac{5\gamma}{3\sqrt{3}} & \beta - \frac{11\gamma}{18} - \frac{\sqrt{5}\gamma}{6} & \frac{1}{6}\sqrt{\frac{5}{3}}\gamma - \frac{\gamma}{2\sqrt{3}} \\ -\frac{1}{2}\sqrt{\frac{5}{3}}\gamma - \frac{\gamma}{6\sqrt{3}} & -\frac{\gamma}{6} - \frac{\sqrt{5}\gamma}{2} & -\frac{\gamma}{2} + \frac{\sqrt{5}\gamma}{6} & \frac{1}{6}\sqrt{\frac{5}{3}}\gamma - \frac{\gamma}{2\sqrt{3}} & \beta - \frac{2\gamma}{3} \end{pmatrix}$$

APPENDIX F

MATHEMATICA PROGRAM THAT COMPUTES JT INTERACTION MATRICES

◆ JT Potential of D⊗d coupling should be in the form of $V=\sum_{i=1}^{m}\sum_{j=1}^{m}\sum_{k=1}^{n} x_i\, x_j\, Q_k$,where, m is equal to the dimension of D and n is equal to the dimension of d, While x_i is invariant under the genarators of D Q_k is invariant under the genarators of d. General potential is invariant under the generators of SO(3) and found using the generators $G_m[1]$ and $G_n[2]$ which represent appropriate generators given in Appendix 2.

```
m = 5; n = 5;
V = Sum[F[i,j,k] x[i] x[j] Q[k], {i, 1, m}, {j, 1, m}, {k, 1, n}];
SF = Table[F[i,j,k], {i, 1, m}, {j, 1, m}, {k, 1, n}] // Flatten;
ST1 = Join[
    Table[x[i] → Sum[G[m][1][[i, j]] x[j], {j, 1, m}], {i, 1, m}],
    Table[Q[i] → Sum[G[n][2][[i, j]] Q[j], {j, 1, n}], {i, 1, n}]] // Simplify;
ST2 = Join[
    Table[x[i] → Sum[G[,m][1][[i, j]] x[j], {j, 1, m}], {i, 1, m}],
    Table[Q[i] → Sum[G[n][2][[i, j]] Q[j], {j, 1, n}], {i, 1, n}]] // Simplify;
V1 = Expand[V /. ST1] - V;
SV1 = Table[D[V1, x[i], x[j], Q[k]] == 0,
    {i, 1, m}, {j, 1, m}, {k, 1, n}] // Flatten;
SL1 = Solve[SV1, SF] // Flatten; SL1 = Expand[SL1];
V = V /. SL1; V = Expand[V];
V1 = Expand[V /. ST2] - V;
SV1 = Table[D[V1, x[i], x[j], Q[k]] == 0,
    {i, 1, m}, {j, 1, m}, {k, 1, n}] // Flatten;
SL1 = Solve[SV1, SF]// Flatten; SL1 = Expand[SL1];
V = V /. SL1;
V = Expand[V];
```

◆ JT interaction matrices are found by double differentiation with respect to electronic coordinates x_i, x_j. These matrices are given in Chapter 6.

```
JTHhg = Table[D[V, x[i], x[j]], {i, 1, m}, {j, 1, m}];
```

APPENDIX G

MATHEMATICA PROGRAM FOR POTENTIAL ENERGY SURFACES OF MAXIMAL SUBGROUPS

◆ In this part, coordinates of maximal subgroups are simplified using the invariance property of group theory for five dimensional irreducible representation. n shows number of the nuclear coordinates and dimension of the matrices. $G_n[i]$ are the generator of each maximal little group. D22, D23, D25 and T little groups of five dimensonal H state.

```
n = 5; SQ = Table[Qi, {i, 1, n}];
ST1 = Join[ Table[Qi == Sum[Gn[1][[i, j]] Qj, {j, 1, n}], {i, 1, n}],
    Table[Qi == Sum[Gn[2][[i, j]] Qj, {j, 1, n}], {i, 1, n}]] // Flatten;
D22 = FullSimplify[Solve[ST1, SQ]] // Flatten
ST1 = Join[Table[Qi == Sum[Gn[3][[i, j]] Qj, {j, 1, n}], {i, 1, n}],
    Table[Qi == Sum[Gn[4][[i, j]] Qj, {j, 1, n}], {i, 1, n}]] // Flatten;
D23 = FullSimplify[Solve[ST1, SQ]] // Flatten
ST1 = Join[
    Table[Qi == Sum[Gn[5][[i, j]] Qj, {j, 1, n}], {i, 1, n}],
    Table[Qi == Sum[Gn[6][[i, j]] Qj, {j, 1, n}], {i, 1, n}]] // Flatten;
D25 = FullSimplify[Solve[ST1, SQ]] // Flatten
ST1 = Join[
    Table[Qi == Sum[Gn[7][[i, j]] Qj, {j, 1, n}], {i, 1, n}],
    Table[Qi == Sum[G[8][[i, j]] Qj, {j, 1, n}], {i, 1, n}]] // Flatten;
D2T = FullSimplify[Solve[ST1, SQ]] // Flatten
```

◆ This section makes same evalution for nine dimensional matrix representations.

```
n = 9; SQ = Table[Qi, {i, 1, n}];
ST1 = Join[ Table[Qi == Sum[Gn[1][[i, j]] Qj, {j, 1, n}], {i, 1, n}],
    Table[Qi == Sum[Gn[2][[[i, j]] Qj, {j, 1, n}], {i, 1,,n}]] // Flatten;
D42 = FullSimplify[Solve[ST1, SQ]] // FlattenST1 =
        Join[Table[Qi == Sum[Gn[3][[[i, j]] Qj, {j, 1, n}], {i, 1, n}],
    Table[Qi == Sum[Gn[4][[i, j]] Qj, {j, 1, n}], {i, 1, n}]] // Flatten;
D43 = FullSimplify[Solve[ST1, SQ]] // Flatten
ST1 = Join[
    Table[Qi == Sum[Gn[5][[i, j]] Qj, {j, 1, n}], {i, 1, n}],
    Table[Qi == Sum[Gn[6][[i, j]] Qj, {j, 1, n}], {i, 1, n}]] // Flatten;
D45 = FullSimplify[Solve[ST1, SQ]] // Flatten
ST1 = Join[
    Table[Qi == Sum[Gn[7][[i, j]] Qj, {j, 1, n}], {i, 1, n}],
    Table[Qi == Sum[G[8][[i, j]] Qj, {j, 1, n}], {i, 1, n}]] // Flatten;
D4T = FullSimplify[Solve[ST1, SQ]] // Flatten
```

This part uses the simplified set of nuclear coordinates each maximal subgrop (little group of each representation computed in above sections. JT interaction matrices in terms of these set are reorganised. Eigenvalues of this JT interaction matrices gives potential energy surfaces (PES) of each little group in terms of 5 and 9 dimensional representations.

$$F_1 = \frac{1}{135\sqrt{3}}\left(-13\sqrt{5}\,F_a + 15\,F_b\right);$$

$$F_2 = \frac{2}{27\sqrt{15}}\left(\sqrt{5}\,F_a + 3\,F_b\right);\; F_3 = F_g/9;$$

$$\text{JTHh} = \text{ExpandAll}[F_1 * m1 + F_2 * m2];$$

$$\text{JTHhg} = \text{ExpandAll}[F_1 * m1 + F_2 * m2 + F_3 * m3];$$

$$\text{D22} = \left\{Q_1 \to \sqrt{5}\,Q_4 - \sqrt{3}\,Q_5,\; Q_2 \to 0,\; Q_3 \to 0\right\};$$

$$\text{D23} = \{Q_1 \to 0,\; Q_4 \to 0,\; Q_2 \to 0,\; Q_3 \to 0\};$$

$$\text{D25} =$$

$$\left\{Q_5 \to -\frac{1}{4}\sqrt{3}\left(-1+\sqrt{5}\right)Q_4,\; Q_1 \to -\frac{1}{2}\left(-3+\sqrt{5}\right)Q_4,\; Q_2 \to 0,\; Q_3 \to 0\right\};$$

$$\text{D2T} = \{Q_1 \to 0,\; Q_2 \to 0,\; Q_3 \to 0,\; Q_4 \to 0,\; Q_5 \to 0\};$$

$$\text{D42} =$$

$$\left\{Q_6 \to \frac{Q_8}{\sqrt{5}},\; Q_1 \to \sqrt{5}\,Q_4 - \sqrt{3}\,Q_5,\; Q_7 \to 0,\; Q_9 \to 0,\; Q_2 \to 0,\; Q_3 \to 0\right\};$$

$$\text{D43} = \{Q_9 \to 0,\; Q_1 \to 0,\; Q_4 \to 0,\; Q_8 \to 0,\; Q_2 \to 0,\; Q_3 \to 0,\; Q_7 \to 0\};$$

$$\text{D45} = \left\{Q_6 \to 0,\; Q_8 \to 0,\; Q_9 \to 0,\; Q_7 \to 0,\right.$$

$$\left.Q_5 \to -\frac{1}{4}\sqrt{3}\left(-1+\sqrt{5}\right)Q_4,\; Q_1 \to -\frac{1}{2}\left(-3+\sqrt{5}\right)Q_4,\; Q_2 \to 0,\; Q_3 \to 0\right\};$$

$$\text{D4T} = \left\{Q_6 \to -\sqrt{\frac{3}{5}}\,Q_9,\; Q_7 \to 0,\right.$$

$$\left.Q_8 \to 0,\; Q_5 \to 0,\; Q_1 \to 0,\; Q_2 \to 0,\; Q_3 \to 0,\; Q_4 \to 0\right\};$$

$$\text{DS} = \left\{Q_4 \to -\frac{1}{2}\left(1+\sqrt{5}\right)Q_a,\; Q_5 \to -\frac{1}{2}\sqrt{15}\,Q_b,\; Q_8 \to -\frac{1}{4}\sqrt{5}\,Q_g,\right.$$

$$\left.Q_6 \to Q_g,\; Q_9 \to -\text{Sqrt}[5/3]\,Q_c\right\};$$

```
ex = JTHhg /. D42; ex = ex /. DS; ex = ExpandAll[ex];
e = Eigenvalues[ex];
ex = JTHhg /. D43; ex = ex /. DS; ex = ExpandAll[ex];
e = Eigenvalues[ex];
ex = JTHhg /. D45; ex = ExpandAll[ex /. DS];
e = Eigenvalues[ex];
ex = JTHhg /. D4T; ex = ExpandAll[ex /. DS];
e = Eigenvalues[ex];
ex = JTHh /. D22; ex = ExpandAll[ex /. DS];
e = Eigenvalues[ex];
ex = JTHh /. D23; ex = ExpandAll[ex /. DS];
e = Eigenvalues[ex];
ex = JTHh /. D25; ex = ExpandAll[ex /. DS];
e = Eigenvalues[ex];
ex = JTHh /. D2T; ex = ExpandAll[ex /. DS];
e = Eigenvalues[ex];
```

CURRICULUM VITAE

The author was born in Gaziantep, in June, 1965. She graduated from the primary, secondary, and high school in Gaziantep, in 1977, 1980 and 1983, respectively. She received the B.S. degree from the Middle East Technical University, Gaziantep Extension Campus, Faculty of Engineering, Deparment of Physics Engineering in 1990. She has been working as a research assistant since 1991. She received the M.S. degree from the Department of Physics, University of Gaziantep in 1994. In 1995, she was accepted to the Ph.D. program in the Deparment of Engineering Physics, University of Gaziantep.

She married in October, 1990 by Ümit and has two sons; Anıl and Berkay.